行政院國家科學委員會專題研究計畫　成果報告

（子計畫三）人類移形上皮癌之基因表現檔案－尋找與砷有關之致癌機轉及調整化學治療處方（3/3）

計畫類別：整合型計畫
計畫編號：NSC93-3112-B-002-008-
執行期間：93 年 05 月 01 日至 94 年 07 月 31 日
執行單位：國立臺灣大學醫學院泌尿科

計畫主持人：蒲永孝

計畫參與人員：李德章、侯自銓、林家齊、王壯維、官靜儀、王榮蓮

報告類型：完整報告
報告附件：出席國際會議研究心得報告及發表論文
處理方式：本計畫可公開查詢

中　華　民　國 94 年 11 月 1 日

摘要

先前二年研究當中，我們計畫以cDNA基因列陣，找出具不同化學敏感度腫瘤之特殊基因表現模式，但是由cDNA基因列陣結果挑出標的基因後，進一步以real-time PCR, Western blotting和免疫組織染色法確認，發現大部分與DNA基因列陣結果不相符合，因此我們決定直接探討蛋白質層次，以蛋白質學(Proteomics)技術，探討在不同抗藥性之膀胱癌細胞株中，有那些分子受到影響而有表現量的變化，藉以尋找膀胱癌之抗藥機轉。進而討膀胱癌細胞株其抗藥性之分子機制。我們利用先前已建立具抗藥性之五株膀胱癌細胞株，分別對臨床上常用的五種抗癌藥物：doxorubicin 、cisplatin、gemcitabine、paclitaxel (taxol)與arsenic trioxide具抗藥性。利用蛋白質體學(Proteomics)技術，探討在不同抗藥性之膀胱癌細胞株中，有那些分子受到影響而有表現量的變化，藉以尋找膀胱癌之抗藥機轉。我們找出24個有表現差異的蛋白質點，其中我們先以Rac1蛋白質做一系列研究，以Western blotting發現具paclitaxel與cisplatin抗性之細胞株其Rac1蛋白之表現量有明顯增加，其它細胞株則有被抑制現象。不過Rho家族的成員之一,RhoA和Cdc42在這些抗藥性細胞內表現量並無差異。利用lovastatin抑制細胞膜上Rac1表現實驗中發現，以Lovastatin (10 μM)加入具cisplatin抗性之細胞株，經過六小時、十二小時、二十四小時及四十八小時之後，以Western blotting分析發現在十二小時Rac1有被抑制下來，但在二十四小時及四十八小時之後，Rac1似乎有回復的現象。同時以流式細胞儀觀察lovastatin抑制細胞膜上Rac1表現時細胞週期之改變，結果發現在8小時細胞有18.8 %產生Sub-G1，另外在6、8、12小時細胞有停留在S期的現象。另外我們也發現paclitaxe(太平洋紫杉醇)處理細胞，會增加超氧化物(superoxide)、過氧化氫 、硝酸氧化物(NO), 氧化態的DNA adducts、G2-M期滯留, 和產生核碎片。這些結果建議, 活性氧及活性氮物質會牽涉到paclitaxel的細胞毒性(cytotoxicity).所以paclitaxel的化學治療敏感性可以從細胞樣本測得的總抗氧化容量來預報得知.故本研究找到這些分子表現差異的蛋白質，對解開膀胱癌抗藥性機轉有所助益，但是否能成為具抗藥性之膀胱癌診斷的分子標記則須再進一步的研究。

緒論

泌尿上皮細胞癌(urothelial cell carcinoma, UCC) 是泌尿系統最常見的惡性腫瘤。治療轉移性 UCC 是以化學治療為主(1,2)，尤其是以 cisplatin 為主的各種處方。 一般治療反應率可達 45 至 70%，但毒性不小，且必需有良好的腎功能，台灣地區約 3 成的 UCC 病人因為腎功能不全，因此必需減低化學治療劑量，使治療效果打折扣，也使病人對化學治療之忍受度降低。為了改善化學治療的成績，過去幾年來許多人作了一些努力，包括在實驗室探究 UCC 化學抗藥性的機轉，及其反制之道；將化學治療調控制應用在臨床試驗上(3)；設計低毒性化學治療處方，以符合台灣地區某些病人的特性；根據既有之經驗，開發一系列化學治療新處方，以提昇臨床療效。

自從二十世紀初化學藥物被證實可以治療惡性腫瘤那一刻起，科學家便積極參與新藥的研發。到了 1970 年代，由於 5-FU、Cisplatin 及其他 Alkylating agent 陸陸續續開發製造(4-8)，使得化學治療進入新的紀元，這些藥物不僅具有抗癌能力，而且對人體毒性也降低不少，因此不管單一或綜合使用皆有不錯的療效，成為近代抗癌治療之主流。自從八○年代 Sternberg 醫師發展出合併使用 methotrexate 、 viblastine、 doxorubicine 以及 cisplatin 等化療藥物(MVAC)，發現它對轉移性膀胱癌具有相當優異的療效以來(總反應率高達 50%以上)，MVAC 一直為美國醫師廣泛使用於轉移性泌尿道移形上皮癌之治療，且其療效已有前瞻性隨機分配臨床試驗證實較單獨使用 Cisplatin 來得優異(3)。單用化療不易將癌細胞完全消滅。有些化療藥物開始使用時療效很好，但幾個療程以後，癌細胞即產生抗藥性，使化療失效。移行上皮癌之化學治療反應率約 50%至 70%左右，但是絕大多數之病人最後仍因腫瘤出現抗藥性再發而死亡，因此如何降低毒性及提昇療效，一直是臨床腫瘤學重要之課題。

近來，抑制細胞程序性死亡被認為是重要的致癌機轉。當細胞的程序性死亡過程被抑制時，細胞有較高的機會累積各種基因的突變；同時細胞有較強的抗化學治療藥劑的能力，而不被化療藥劑毒殺。

抗藥性可分為三方面來討論：

1. 細胞抗藥性動力學：主要的原因是因為大部分腫瘤的 Growth fraction 低。
2. 化學藥物抗藥性之影響(Biochemical causes of resistance)：

特別值得一提的是，Multidrug resistance（MDR）已成為腫瘤化療中一個影響治療效果的關鍵性因素。MDR 得名的原因是腫瘤細胞在抗腫瘤藥作用一段時間後，不僅對該藥物會產生抗藥性，而且對其它許多結構差異極大的抗癌藥也會產生抗藥性。已經發現 MDR 主要與體內一大類稱作 ATP-binding Cassette (ABC) Transporters 的蛋白有關，這是一類廣泛存在於原核和真核細胞中的 Energy-Dependant Efflux Pumps，其中對 P-glycoprotein (P-gp)的研究最為深入。從稍早的研究知道，雖然僅有 20% 的 UCC 細胞株會表現 mdr-1，但 mdr-1 在次發抗藥性 (包括 doxorubicin 及 cisplatin) 之細胞株很易被誘發出來(5)。目前已有多種抑制 P-gp 作用的小分子被發現，甚至研發成對抗 MDR 的有效藥

物。也有一些小分子可以作為某種抗癌藥如 Taxol 與 P-gp 的競爭性結合劑，從而使 Taxol 不能與 P-gp 結合並被排出細胞外(5)。Combination therapy 特別是合併如 Calcium channel blockers、Antiarrhythmics 或 Cyclosporin A 等可以克服此種 MDR 之影響。

3. 藥理抗藥性(Pharmacologic causes of resistance)：藥理抗藥性的產生主要是由於化學藥物無法有效的運送到組織細胞間。

研究目的

移行上皮癌之化學治療反應率約50%至70%左右，但是絕大多數之病人最後仍因腫瘤出現抗藥性再發而死亡，因此如何降低毒性及提昇療效，一直是臨床腫瘤學重要之課題。本研究中，原本我們計畫以cDNA基因列陣，找出具不同化學敏感度腫瘤之特殊基因表現模式，建立一個以個別病人基因表現為基礎的藥物選擇機制 (drug-selecting algorithm)，以提昇治療效果。方法是，先建立一群UC細胞株 (包括敏感及抗藥株)對各種藥物之敏感度資料，再將各細胞，進行數千組基因之cDNA基因列陣之研究，找出對每種藥物敏感度有關之特殊表現基因組，再製作另一個cDNA基因列陣。此第二級基因列陣，可能包含數百個藥物敏感度相關基因，其表現可以預測對每一種藥物之敏感度或抗藥性程度。因此可以建構一個藥物選擇機制。後來因為cDNA基因列陣結果挑出標的基因後，進一步以real-time PCR, Western blotting和免疫組織染色法確認，發現大部分與DNA基因列陣結果不相符合，因此我們決定直接探討蛋白質層次，以蛋白質學(Proteomics)技術，探討在不同抗藥性之膀胱癌細胞株中，有那些分子受到影響而有表現量的變化，藉以尋找膀胱癌之抗藥機轉。

材料與方法

材料

（一）細胞株:

- 烏腳病地區之膀胱癌細胞株
  BFTCC909
- 非烏腳病地區之膀胱癌細胞株與所衍生的抗藥株
  T24
  T24 / D　　T24/Doxorubicin（0.4 μM）resistant
  NTUB1
  NTUB1/G　　NTUB1/Gemcitabine（0.3 μM）resistant
  NTUB1/T　　NTUB1/Paclitaxel（0.005 μM）resistant
  NTUB1/P　　NTUB1/Cisplatin（14 μM）resistant
  NTUB1/As　　NTUB1/Arsenic trioxide（0.5 μM）resistant

得自台大醫院泌尿科蒲永孝醫師核心實驗室(Fig 1.)。

（二）培養基：

RPMI-1640 medium：

取一包RPMI-1640 培養基粉末，加入 4.4 g的$NaHCO_3$，溶於 1000ml 之去離子水中，調pH至 7.2，過濾以確保無菌，存放於 4 ℃冰箱中。

（二）抗癌藥物（Chemotherapeutic agents）：

(1) Paclitaxel (Taxol): Bristol-Myers Squibb Co., Princeton, NJ08543, USA
(2) Gemcitabine: Lilly France,S.A.S., F-67640 Fegersheim, France
(3) Doxorubicin: Pharmacia&Upjohn S.p.A., Viadel Murillo Km, 2800 Sermoneta, Italy
(4) Arsenic trioxide: Sigma chemical Co.P.O. Box, USA
(5) Cisplatin: Bristol-Myers Squibb S.p.A., Viadel Murillo Km, 2800 Sermoneta, Italy

實驗方法

(一) 細胞培養:

人類膀胱癌細胞株 T24、T24/Doxorubicin (0.4 μM)、BFTCC909、NTUB1、NTUB1/Gemcitabine (0.3 μM)、NTUB1/Paclitaxel (0.005 μM)、NTUB1/Cisplatin (14 μM)、NTUB1/Arsenic trioxide (0.5 μM) (得自台大醫院泌尿科蒲永孝醫師核心實驗室)，分別培養於 10 %胎牛血清(Fetal bovine serum)的 RPMI-1640 的培

養基(內含 100 unit/ml Penicillin-G，100 μg/ml streptomycin 和 2 mM L-glutamine) ，上述細胞株皆培養 37℃，溼度 9.8 % 含 5 %二氧化碳之培養箱中培養。

(二) 繼代培養(Cell Culture) :

細胞長滿後，以 1X PBS 緩衝液清洗二次，加入 0.5 ml 1X Trypsin-EDTA 溶液，於 37 ℃細胞培養箱作用 2 ~ 5 分鐘，待細胞剝落後，立即加入細胞培養液，並將之吸至無菌離心管，以 1000 rpm 離心 5 分鐘，移除上層液，接著加入 10 mL 培養液，並均勻打散細胞，再取 1/4 的細胞數移至新的培養皿生長。

(三) 西方點墨法(Western blotting) :

1. 細胞溶解物之(cell lysate)之製備：

將培養皿內培養液吸走，以冰冷 1XPBS 沖洗細胞二次，再將培養皿內殘餘液吸淨，接著加入含蛋白酵素抑制劑(Protease inhibitor)的細胞溶解緩衝液(RIPA lysis buffer)約 50 μL 至培養皿中，隨即用刮勺將細胞刮下，取 Cell lysates 到 Eppendorf 中，放置冰上 30 分鐘之後，在 4 ℃下高速離心 12000 rpm，15 分鐘，吸取上清液(注意勿觸及沉澱物)到新的 eppendorf，儲存在-20 ℃冰箱中，待用。

2. 蛋白質定量(protein normalization)：

以 PIERCE 的 BCA Protein Assay Reagent Kit 來定量，拿牛血清白蛋白(Bovine serum albumin, BSA) 作標準品，波長 562 nm，於紫外光可見光光譜儀(BECKMAN)畫出標準曲線(校正係數需在 0.998 以上)，測出檢體的蛋白質吸光度，並利用內插法算出樣品的濃度。製備定量成濃度為 50 μg 的蛋白質檢體，再進行蛋白質電泳。

3. 凝膠電泳分離(SDS-PAGE)分析：

以 Sodium dodecyl sulfate-polacrylamide gel electrophoresis (SDS-PAGE) 來分離不同分子量大小的蛋白。配製 12 %分離膠(Resolving gel)、4 %的焦集膠(Stacking gel)及 1XSDS 電泳緩衝液(Running buffer)，並將 1XSDS 電泳緩衝液倒至整個壓克力槽中，蓋過所需的最低高度，取每管含總濃度 50 μg 的蛋白質樣品，加入適量之 2XSDS / Protein loading buffer，在 100 ℃沸水中煮沸三分鐘，以利蛋白質樣本的展開(Denature)，之後立即放入冰中冷卻，再注入 12 % SDS-PAGE 的 well 中，然後以 120 V 進行電泳分離，待指示染劑，跑至適當位置時(約距膠體底部一公分處)，停止電泳取出膠體，直接進行免疫轉漬分析(Immunoblot transfer analysis)。

4. 轉漬(Transfer)：

蛋白質檢體在跑完 SDS-PAGE 之後，我們接著進行轉漬，也就是將跑完電泳的 gel 的蛋白質透過電轉印緩衝液(Electrotransfer buffer)和電轉印槽

(Electrotransfer tank)轉漬到 PVDF 薄膜(PVDF membrane)上。首先裁剪二張 3MM filter paper 及預先準備適當大小之 PVDF 薄膜，以甲醇(Methanol)浸潤一分鐘，使其活化，之後將活化後的 PVDF 薄膜及 3MM filter paper 浸於電轉印緩衝液中，去掉 Stacking gel，小心拿起 Resolving gel，先以轉漬緩衝液浸濕，依序以 3MM filter paper、gel、PVDF membrane、3MM filter paper 的鋪疊方式，再以二張海綿網夾住置於電轉印槽，在安培數 400 毫安培的電流自負極到正極，約 1 個小時的條件下，將電泳凝膠上的蛋白質由膠體轉漬到 PVDF 薄膜上。

5. 覆蓋膜之非特異性的結合位置(Blocking)：

配製 10 mL 含 1 % BSA 的 Blocking buffer，將完成轉漬作用的 PVDF 薄膜浸泡於其中，置於雙向震盪器(ORBITAL SHAKER)上緩慢震盪，於 4 ℃隔夜反應，目的是將薄膜上的空隙填滿。

6. 抗原、抗體結合反應(Hybridization)：

第二天將 Blocking buffer 倒掉，以 0.1% PBST buffer 清洗三次，每次 5 分鐘，然後配一次抗體(Primary antibody)，以 TBST buffer 稀釋之(稀釋倍數依不同的一次抗體所需要的條件也會不同)。接著將 PVDF 薄膜放到含一次抗體的 TBST buffer 中，置於雙向震盪器(ORBITAL SHAKER)上緩慢震盪，室溫一小時，目的是讓 PVDF 薄膜吸附表面的抗原蛋白。之後將含一次抗體的 TBST buffer 倒掉，以 0.1% PBST buffer 清洗三次，每次 5 分鐘，再放入含二次抗體(Second antibody)的 TBST buffer，於室溫緩慢震盪一個小時，最後以 0.1% PBST buffer 清洗三次，每次 5 分鐘。

7. 呈色、壓片：

實驗於暗房中避光進行，取 1 mL 的呈色劑 A 和呈色劑 B 混合均勻，將 PVDF 薄膜放入，反應 1 分鐘，之後使 PVDF 薄膜正面朝上，固定於感光夾內的透明投影片，再將 X 光感底片(X-film)覆蓋其上，夾住後控制時間進行壓片，時間到將 X 光感底片拿出，洗片於沖片機。

（四）二維凝膠電泳(Two-dimensional electrophoresis)

壹、樣品處理：

當細胞達到八~九成滿時（注意：同一批實驗所用的細胞需培養時間需相同，且至少需 48 小時培養），移除舊的 Medium，以 1XPBS 緩衝液清洗二次，加 Trypsin Incubation 數分鐘並輕拍 Dish，加新的 Medium 中和，離心 1000-1500 rpm，5 min。用 1 × PBS Wash 一次，離心 1000-1500 rpm，5 min，移除上清液，加入 200 μL Lysis Buffer 並 Vortex，15000 rpm，15 min，4 ℃，收上清液(注意不要吸到黏稠物)，置於冰上。(細胞處理的空檔，可先將 Strip 泡在 Rehydration buffer，6 hrs 以上最多不超過 24 hrs (Strip pH = 3-10，Rehydration buffer 必須也是 pH = 3-10)。(Rehydrate Immobiline DryStrip gels using Immobiline DryStrip Reswelling Tray，2-3 ml/well Rehydration Buffer，storage

in -20 ℃) Strip 與 Rehydration buffer 之間不能有氣泡)。

貳、蛋白質定量：

利用 Amersham 的 2-D Quant Kit 來定量蛋白質，測定方法依照廠商所附之 Protocol。

參、First dimensional electrophoresis：

先取 Sample 與 Sample buffer (等體積 1：1)混合均勻之後，超音波震盪(Sonication) (室溫，10 min)，再移置 37 ℃水浴(30 min)，最候離心(15000 rpm，10 min)，收上清液，將 Sample 注入 Cup 裡，跑等電位點聚焦(Iso-electric focusing, IEF)。

IEF 之條件:

(1) 500 V, 3 hrs

(2) 1000 V, 3 hrs

(3) 2000 V, 10 hrs

(4) 2000 V, 6 hrs

肆、Secondary dimensional electrophoresis：

取出 Strip，將膠面朝上(有 Sample 那面)在擦手紙上把 Cover oil 吸淨，將 Strip 置於 Box 上，倒入 Balance buffer(一個 Box 10 mL) (Shaker, 40 rpm, 15 min)，取出 Strip 在擦手紙上把 Balance buffer 吸淨並放入 Strip，放 Sample APPL PIECE 於正極處，並接觸 Separating gel，開始電泳分析。

Separating 之條件:

(1) 200 V

(2) 40 mA (一片 gel 20 mA)

(3) 最高可跑 250 V，一片 gel 25 mA

(4) 藍色的 Dye 跑到跳海為止

伍、銀染(Silver stain)：

(1) 配 Fixation solution：

Ethanol 100 mL

Acetic acid glacial 25 mL

Add ddH_2O to 250 mL

取下 Gel 在右上角切一角作記號，倒入 Fixation solution，Shaker 40 rpm (可 Overnight 或 30 min 繼續下一個步驟)。

(2) 配 Sensitizer solution：

Ethanol 75 mL

Glutardialdehyde (25%) 1.25 mL

Sodium thiosulphate (5%) 10 mL

Sodium acetate 17g

Add ddH_2O to 250 mL

吸淨Fixation solution，倒入Sensitizer solution (Shaking 40 rpm)，30 min。以

ddH_2O Wash 3 次，每次五分鐘(Shaker, 40 rpm)。

(3) 配 Silver reaction：

Silver nitrate solution (2.5%) 25 mL

Formaldehyde (37%) 0.1 mL (要用再加)

Add ddH_2O to 250 mL

倒入Silver reaction (Shaking 40 rpm)，20 min。以ddH_2O Wash 2 次，每次一分鐘(Shaker, 40 rpm)。

(4) 配 Developing solution：

Sodium carbonate 6.25 g

Formaldehyde (37%) 0.05 mL (要用再加)

Add ddH_2O to 250 mL

倒入 Developing solution 並以手搖晃，當 2 片 Gel 所呈現出的 Spots 約相當時，即可停止。

(5) 配 Stopping solution：

EDTA – $Na_2 \cdot 2H_2O$ 3.65 g

Add ddH_2O to 250 mL

吸淨Developing solution，倒入Stopping solution (Shaking 40 rpm)，10 min。以ddH_2O Wash3 次，每次五分鐘(Shaker, 40 rpm)。將gel夾在二片投影片中，進行掃描。

<u>陸、In-gel Digestion：</u>

前置作業：

(1) 將 650 μL Microtubes (Siliconized)與 Tips (Siliconized)，先用甲醇浸泡過，再用去離子水洗掉甲醇並烘乾。

(2) 將 200 μL Tips 尖端剪成直徑約 1 mm ~ 2 mm 的大小。

方法：

在無菌操作台(Laminar flow)裡將 Spots 挖下，放入 650 μL Microtubes (Siliconized)中，把水去除留下 Gel。

(1) **退染：**加入 100 μL Destain solution (30 mM Potassium ferricyanide 與 100 mM Sodium thiosulfate，以 1：1 體積混合均勻)。用手彈至棕色不見(Gel 呈淡黃色)，去離子水 Wash 2~3 次，使 Gel 呈現透明無色。

(2) **Reduction / Akylation：**加入 100 μL (50 mM DTT / 25 mM Ammonium bicarbonate, pH = 8.5)，37 ℃反應一小時。去掉 50 mM DTT / 25 mM Ammonium bicarbonate, pH = 8.5 溶液，加入 100 μL (100 mM IAA / 25 mM Ammonium bicarbonate, pH = 8.5)避光反應一小時。去掉 100 mM IAA / 25 mM Ammonium bicarbonate, pH = 8.5 溶液。加入 100 μL (50 % Acetonitrile / 25 mM Ammonium bicarbonate, pH = 8.5) Wash gel 二次(將 DTT 與 IAA 去除)。加 100% Acetonitrile 使 Gel 脫水(Gel 會變成米白色的)。去掉上清液，低溫真空離心抽氣乾燥(1900 rpm, 10 ℃, 10 min)。

(3) **Digestion**：加入 1.5 ~ 2μL Trypsin。用 Microtube pestles 對 Gel 直接旋轉使 Gel 碎裂。離心(10000 rpm, 4 ℃, 2 ~ 3 min)。若溶液無超過 Gel，則再加 25 mM Ammonium bicarbonate, pH = 8.5 溶液淹過 Gel 即可。37 ℃反應至少十六小時以上。

(4) **Extraction**：加入(50 % Acetonitrile + 5 % Formic acid)萃取蛋白質片段，超音波震盪(Sonication) (4 ℃，10 min)，收集上清液並重複一次。將二次所收集之上清液以低溫真空離心抽氣乾燥之。

柒、質譜儀鑑定：

做完 In-gel digestion 之樣品於本校 LC/MSMS 分析。

（五）細胞週期分析（Cell cycle assay）:

將數盤 10 cm 細胞培養皿各種 3 x 10^5顆細胞，每盤處理藥物於一定時間後，將培養皿的細胞培養液移至離心管，以 1XPBS清洗培養皿二次，再以 1XTrypsine-EDTA處理後，待細胞剝落，立即加入細胞培養液，收取所有細胞至離心管，以 2000 rpm離心 5 分鐘後，移除上層液，再以 1XPBS清洗二次，以 2000 rpm離心 5 分鐘後，去除上清液，加入 250 μL之 1XPBS，將細胞打散後，加 750 μL 99.9%的冰乙醇，置於-20 ℃將細胞固定 30 分鐘。之後以 2000 rpm，4 ℃下離心 5 分鐘，去除上清液，並以 1XPBS清洗一次，加入 20μL RNase A (100 μg/mL)，在 37 ℃下作用 30 分鐘，後加入 1 mL 50μg/ml Propidium Iodide，最後用流式細胞測定儀(Flow cytometer)分析，並利用WinMDI 2.8 軟體分析 Sub-G1 與Cell cycle的Peak與含量(Contents)。

結果

cDNA microarray 結果：

以 cDNA 基因列陣找出具不同化學敏感度腫瘤之特殊基因表現模式(TableI-III)，接著嘗試挑選幾組基因進一步以 real-time PCR, Western blotting 和免疫組織染色法確認 cDNA microarray 結果，在 NTUB1/Arsenic trioxide NTUB1/Cisplatin 和 NTUB1/Gemcitabine 分別選出 HO-1,SUI1 和 TRAP-1，分別進行分析，結果發現 HO-1 與 NTUB1/Arsenic trioxide 對抗性是有關係，不管 real-time PCR 與 Western blotting 結果是和 cDNA microarray 結果一致(Fig.1-2)，不過以免疫組織染色分析 arsenic-related 與 arsenic-unreleated UC HO-1 表現量現並無明顯差異(Fig. 3)。SUI1 和 TRAP-1 real-time PCR 結果與 cDNA microarray 結果有點出入(Fig. 4,5)。因此我們決定直接探討蛋白質層次，以蛋白質學(Proteomics)技術，探討在不同抗藥性之膀胱癌細胞株中，有那些分子受到影響而有表現量的變化，藉以尋找膀胱癌之抗藥機轉。

利用蛋白質體學(Proteomics) 分析方法篩選人類泌尿上皮細胞癌中具抗藥性之蛋白質：

本篇論文主要探討利用蛋白質體學(Proteomics)與西方點墨法(Western blotting)分析方法篩選人類泌尿上皮細胞癌中具抗藥性之蛋白質。我們得到初步研究的結果如下:

利用蛋白質體學分析 NTUB1、NTUB1/Cisplatin (14 μM)及 NTUB1/Arsenic trioxide (0.5 μM)：

由蛋白質體學分析中我們比對 NTUB1、NTUB1/Cisplatin (14 μM)與 NTUB1/Arsenic trioxide (0.5 μM)，發現共有 24 個我們所感興趣之 Spot，並經過 LC/MSMS 及 MASCOT MS/MS Ions Search 分析比對之後，將其蛋白質身分鑑定出來，並依據蛋白質 up-regulation、down-regulation 身分、分子量、pI 值與生化功能製作成表格(Table IV.)。由表格中選出我們所感興趣之 Spot 12：GTP-binding nuclear protein，做進一步確認，因為我們所使用之 Proteomics 技術有它之偵測極限，所以必須利用 Western blotting 或 real-time PCR 的方法來確認。

(b) 鑑定 Spot 12：GTP-binding nuclear protein：

由本篇論文之緒論中可知，GTP-binding nuclear protein 是隸屬於 Rho 蛋白家族成員之一，而 Rho 蛋白家族成員主要有三個蛋白：Rac 1、Rho A 和 Cdc42，所以我們先確認這三個蛋白質或基因之表現量。利用 Western blotting 之方法我們發現 Rho A 蛋白的表現量，在人類泌尿上皮細胞癌細胞株與抗藥株並無明顯差異，但 Rac 1 蛋白之表現量就有明顯差異，其中 BFTCC909、N/T 及 N/P 有被 up-regulation 之現象，其它細胞株則是 down-regulation 之現象(Fig. 6,7)。另外，我們先跑 RT-PCR 確認我們所合成的引子(Primer)，有無 heterodimer 的現

象，因為若有 heterodimer，則會影響 real-time PCR 的定量結果(Fig. 8A)。再運用 Real-time PCR 的技術分析 *cdc42* 之基因表現量，發現 N/P 有較明顯的 down-regulation，而其它細胞株則是落在誤差範圍內，並無明顯差異(Fig. 8B)。

(c) 以 Lovastatin 抑制 Rac1 之表現：

過去文獻曾指出，Lovastatin 能抑制細胞膜上之膜蛋白，又 Fig 4.發現 Rac1 在 N/P 有大量表現，所以我們以 Lovastatin = 10 μM 加入 N/P，經過六小時、十二小時、二十四小時及四十八小時之後，萃取蛋白質進行 Western blotting 分析，結果在十二小時 Rac1 有被抑制下來，但在二十四小時及四十八小時之後，Rac1 似乎有回復的現象(Fig. 9)。

(d) Flow Cytometry 分析 NTUB1/P 經 Lovastatin 處理後之 Sub-G1 及 Cell cycle arrest 的現象：

我們將 NTUB1/P 處理 Lovastatin = 10 μM，經過 6、8、12、24 小時之後，分別再加入 14 μM 的 Cisplatin，經過 48 小時之後，利用 Flow cytometry 分析細胞的 Sub-G1 及 Cell cycle arrest 的現象。發現在 8 小時細胞有 18.8 %產生 Sub-G1 (Fig. 10)，另外在 Cell cycle arrest 的部份，在 6、8、12 小時細胞有停留在 S 期的現象(Fig. 11)。

（三）以 Western blotting 之方法篩選人類泌尿上皮細胞癌細胞株與抗藥株之蛋白質表現差異：

(a) Kinase and Phosphatase 在人類泌尿上皮細胞癌之表現量：

以相同條件下培養人類泌尿上皮細胞癌，24 小時後，以 Western blotting 分析其蛋白表現量，結果發現人類泌尿上皮細胞癌中：Serine/threonine kinase (Akt1/2)、Protein kinase C-ζ (PKC-ζ)與 Extracellular signaling-regulated kinase 1 and 2 (ERK1/2)的蛋白質表現量並無明顯差異；而 Jun N-terminal kinase (JNK)與 Phospho-extracellular signaling-regulated kinase 1 and 2 (p-ERK1/2)有些許差異，(Fig. 12,13)。

(b) Tumor Suppressors / Apoptosis 在人類泌尿上皮細胞癌之表現量：

以相同條件下培養人類泌尿上皮細胞癌，24 小時後，Western blotting 分析其蛋白表現量，結果發現人類泌尿上皮細胞癌中：Bcl-xL、Bcl-2 與 Bad 的蛋白質表現量並無明顯差異；而 p53 在 N/T 與 N/P 有被抑制下來；在 BFTCC909 並無 p21 蛋白質的表現量；另外，N/P 的 Caspase-3 則有被抑制下來的現象(Fig. 14,15)。

(c) Transcrition Regulators 在人類泌尿上皮細胞癌之表現量：

以相同條件下培養人類泌尿上皮細胞癌，24 小時後，以Western blotting分析其蛋白表現量，結果發現人類泌尿上皮細胞癌中：Signal transducer and activator of transcription 3 (STAT3)、IκB、NF-κB p^{65}與Nuclear respiratory factors (Nrf-2)的蛋白質表現量並無顯著差異；而CCAAT-enhancer binding protein (C/EBPβ)在N/P與N/As有顯著差異(Fig. 16,17)。

(d) Signaling Intermediates 在人類泌尿上皮細胞癌之表現量：

以相同條件下培養人類泌尿上皮細胞癌，24 小時後，以 Western blotting 分析其蛋白表現量，結果發現人類泌尿上皮細胞癌中：Cyclooxygenase 2 (COX-2)在 N/T 及 N/P 有較高之表現；Suppressor of cytokine signaling 3 (SOCS-3)在 BFTCC909 及 N/T 有較高之表現；在 N/G 和 N/T 的 Heat shock protein 70 (Hsp70)有被抑制下來；Heme oxygenase 1 (HO-1)在 N/As 有較高之表現；superoxide dismutase (SOD)在 N/P 和 N/As 有較高之表現；另外 transforming growth factor receptor associated binding protein (TRAP-1)並無顯著差異(Fig. 18)。

(e) Growth Factor and Hormones 在人類泌尿上皮細胞癌之表現量：

以相同條件下培養人類泌尿上皮細胞癌，24 小時後，以 Western blotting 分析 Breast and kidney-expressed chemokine (BRAK)與 Interleukin-6 (IL-6) 的表現量，結果發現人類泌尿上皮細胞癌中：BRAK 的表現量並無顯著差異；在 N/As 抗藥株中 IL-6 的蛋白質表現量有 up-regulation 的現象(Fig. 19)。

(f) Cell cycle proteins 在人類泌尿上皮細胞癌之表現量：

以相同條件下培養人類泌尿上皮細胞癌，24 小時後，以 Western blotting 分析其蛋白表現量，結果發現人類泌尿上皮細胞癌中：cyclin D1 在 N/G、N/P 和 N/As 有 up-regulation 的現象；另外，cyclin E 在 N/P 與 N/As 亦有 up-regulation 的現象(Fig. 20)。

(g) Membrane Receptors 在人類泌尿上皮細胞癌之表現量：

以相同條件下培養人類泌尿上皮細胞癌，24 小時後，以 Western blotting 分析 epidermal growth factor receptor (EGFR)的表現量，結果發現人類泌尿上皮細胞癌中：EGFR 的蛋白質表現量在 N/As 抗藥株中有 up-regulation 的現象(Fig. 21)。

(四) Paclitaxe(太平洋紫杉醇)在細胞毒性機制之研究

(I) Paclitaxe 誘發 T24 細胞 reactive oxygen species 形成

Paclitaxel使T24 細胞產生ROS. 將 T24 細胞以paclitaxel 處理後顯著地使Amplex 紅色螢光強度增加. 這個作用會因抗氧劑antioxidents、superoxide dismutase (SOD), catalase、丙酮酸鹽pyruvate, 和硒(Fig. 22A)而減少. 這些結果指出, paclitaxel 處理後會增加細胞內H_2O_2 水平. Paclitaxel 處理後也會增加一測量O2 ˉ探針L-012(Fig. 22B)的chemiluminescent 強度. O2ˉ 的生產會因SOD的存在而減少. 以標準的彗星分析法(standard comet assay)分析發現使用paclitaxel處理T24 細胞並不會導致任何DNA鏈斷裂. 但是, 很多DNA鏈斷裂是因paclitaxel處理過的T24 細胞與endonuclease III 或formamidopyrimidine DNA glycosylase一起培養而產生, 這是因為endonuclease III 移除被氧化的嘧啶且formamidopyrimidine-DNA glycosylase 移除被氧化的嘌呤的緣故. 這些結果暗示著paclitaxel 導致氧化DNA 損傷(Fig. 22C)

(II) Paclitaxe 誘發細胞凋亡

同樣地, 在抗氧劑pyruvate或者硒存在下特殊DNA鏈斷裂造成氧化鹼基的程度顯著地減少 (Fig. 23A) . Paclitaxel 導致G2-M 停滯、核破碎, 及細胞生長被抑制. Paclitaxel 處理細胞明顯地導致細胞停聚在G_2-M階段(Fig. 23B), 產生核碎裂的比例增加(Fig. 23C), 和抑制細胞生長(Fig. 23D). 所有這些由paclitaxel產生的細胞毒素作用可由pyruvate或者硒部份地壓制著.

(III) Paclitaxel 誘發 T24 細胞 nitric oxide 形成

在 T24 細胞方面, Paclitaxel 導致硝酸氧化物產生. 以 Paclitaxel 處理 T24 細胞並藉由培養基亞硝酸鹽水平的增加證明一氧化氮(NO)增加(Fig. 24A). NO 的產生會被(NO synthase inhibitor)一氧化氮合成酶抑制劑 NN-nitro-L-arginine methyl ester (NAME), NO scavenger manganese (III) 及 2-(4-carboxyphenyl)-4,4,5,5- tetramethylimidazoline-1-oxyl- 3-oxide (c-PTIO) 所抑制.依照彗星分析法((Fig. 23B), 這些 NO 調控者也顯示部份地搶救了 paclitaxel 引發的 DNA 氧化損傷.

(IV) 抗氧化劑與 NO 調控劑可以抑制 Paclitaxel 細胞毒性

抗氧化劑與NO調節物可在不同細胞株中抑制paclitaxel的毒性。到目前為止研究結果指出H_2O_2, O_2^-以及NO可能都和T24 細胞中經由paclitaxel所誘導的細胞毒性有關。為了研究此一現象是否具有細胞專一特性，我們在此針對抗氧化劑(pyruvate加上selenium)以及NO調節物(NAME or c-PTIO)的影響作進一步的研究，在這個實驗之中，我們利用DNA flow cytometry來檢測除了T24 cell以外的一些細胞株之中由paclitaxel所誘導的sub-G1 fraction累積情形。我們檢測了兩株人類的urothelial carcinoma cell lines (BFTC905 and NTUB1), 以及SV40-transformed 的人類urothelial cell line (SV-HUC-1), 還有人類lung epidermoid carcinoma cell line (H1355)和breast cancer cell line (MCF-7; Fig. 25)。研究結果指出pyruvate plus selenium、NAME,以及c-PTIO可以減少上述那些細胞株中paclitaxel-induced sub-G1 fraction的累積(Fig.25A and B)。此外，利用 buthionine sulfoximine(BSO) 阻止 glutathione 的合成作用或是以 2-methoxyestradiol (2-ME)抑制SOD的活性，都增強了paclitaxel的細胞毒性，此一現象可由sub-G1 fractions累積的增加情形得到證實(Fig. 25C and D)。這些實驗結果指出在大部分的細胞株中，ROS以及NO兩者都與paclitaxel所誘導的細胞毒性有關。

(V) 總體抗氧化能力與 paclitaxel 的抗性有關聯。

因為H_2O_2, O_2^-以及NO被發現與被paclitaxel所誘導的細胞毒性有關，我們因而假設那些具有較高抗氧化能力的腫瘤細胞會比其他那些抗氧化能力較低的腫瘤細胞更能夠抵抗paclitaxel。為了證實這個假設，我們分別量測 16 株不同細胞株的整體抗氧化能力(Fig. 26A)以及對paclitaxel的IC50(Fig. 26B)。經由MTT實驗分析所得到的結果，可以得知整體抗氧化能力與paclitaxel的IC50 呈現正相關(Pearson's correlation coefficient $r = 0.90$, $P < 0.0001$; Fig. 26D)。我們更進一

步的進行colony formation assay來確認這些結果(Fig. 26D)。我們挑選了MCF-7 (對paclitaxel高度敏感的細胞株), T24 (對paclitaxel敏感的細胞株), T24/A (具doxorubicin抗性的T24 subline), and NTUB1/P and NTUB1/T (具有cisplatin and paclitaxel抗性的NTUB1 sublines)。由colony formation assay所得到的實驗數據確認了我們先前實驗的結果，證實總體抗氧化能力的確與paclitaxel的 IC50有關(Pearson's correlation coefficient r = 0.93, P = 0.024; Fig. 26D)。

(VI) 不同細胞株對 paclitaxel 的抗性與細胞總抗氧化能力的正相關性

以上結果暗示腫瘤細胞的paclitaxel IC_{50} 越高，其抗氧化能力越高。我們以實驗來檢視是否可以降低paclitaxel 抗性的試劑也可以降低細胞總抗氧化能力。結果顯示在MCF-7(最敏感的細胞株)、NTUB1/T(最具抗性細胞株)、PD98059(一種有絲分裂活化蛋白及MEK/ERK抑制劑)、U0126(一種MEK/ERK抑制劑)、LY294002(一種PI3K/Akt抑制劑)、BSO、2-ME以及As_2O_3(一種ROS生成劑)這些實驗組別中其細胞存活率都有顯著降低(Fig. 27A,B)，而其細胞總抗氧化能力也有降低(Fig. 27C,D)。類似的結果也在其他細胞株被觀察到，包含T24、T24/A，還有NTUB1/P細胞株(資料沒有列出)

討論

膀胱癌在臨床上多採用外科手術切除，之後再併用化學藥物或放射性治療；但是許多研究發現，其中大約有三分之一的病人會對化學藥物治療產生抗藥性 (drug resistance)，造成治療與預後上相當程度的瓶頸。於是，我們決定針對膀胱癌細胞株，對其抗藥性做分析。

首先，我們先利用 Proteomics 的技術對人類泌尿上皮細胞癌細胞株與抗藥株做分析，將 NTUB1 當控制組；NTUB1/P 及 NTUB1/As 當實驗組，將所得之實驗組的圖譜與控制組作比對，找出差異性的 Spots。目前我們得到具差異的 24 個 Spots，整理出 Table 4.的結果。從中我們先對 Spot 12：GTP-binding nuclear protein 這個點做進一步確認，我們利用 Western blotting 與 real-time PCR 做鑑定，發現 Rac1 在人類泌尿上皮細胞癌細胞株與抗藥株有極大之差異性(Fig. 6)；而 Rho A 和 Cdc42 則無差異性(Fig. 7,8)。在 Fig. 6 中我們發現 NTUB1/P 與 NTUB1 比較之後，NTUB1/P 的 Rac1 有很高的表現，故我們先把焦點放在 cisplatin 所產生之抗藥性作用機制做一探討。

從前人文獻指出，Rac 1、Rho A 和 Cdc42 它們是膜蛋白，且已有證據證實它們會分別啟動各種不同的訊息傳遞路徑(16)，所以我們持續探討下游訊息傳遞路徑。先前研究已發現 Platelet-derived growth factor receptor (PDGFR)會促進 Phosphatidylinositol 3'-Kinase (PI3K)的活化，而 PI3K 會調控 Rac 1 之活化，進一步開啟各種不同之訊息傳遞路徑。在 1999 年有人發現，Rac 1 會啟動 cyclin D1 的表現(17)，而 cyclin D1 又是調控 cell cycle 的調控子(regulator)，促進細胞不斷分裂，在 Fig. 20 也是相同情況，所以我們進一步推測 cyclin D1 會調控 Retinoblastoma (Rb) 蛋白(47, 48)，而 Rb 是一種腫瘤抑制蛋白，它的功能應是抑制腫瘤細胞。又從 Fig. 17 中我們發現 NTUB1/P 的 p53 是 down regulation 的現象，根據文獻指出，p53 會與 Mdm2 形成 complex，使 p53 經由 Ubiquitin pathway，將 p53 失去活性(49, 50)，而 Mdm2 是一個致癌蛋白，它會抑制 Rb 的活性，使得 Rb 無法發揮它抑制腫瘤的功能(51, 52)，所以說這可能是具 Cisplatin 抗藥性之癌細胞的一種生存能力。另外，Lovastatin 可經由抑制 Isoprenylation 而降低細胞膜上 Rho 蛋白之活性及含量，所以我們加入 10 μM 的 Lovastatin，經過 Time-course 之後，發現 Lovastatin 有抑制 Rac1 的能力(Fig. 9)，但是 Lovastatin 似乎沒有專一性的抑制效果，從結果中在十二小時 Rac1 有被抑制下來，不過四十八小時之後，Rac1 好似有被回復過來。另外在 Flow cytometry 分析方面，我們證明 Lovastatin 有使細胞停留在 S 期的能力，促使細胞產生 Sub-G1 的現象，這也與我們 Western 的結果相符合，不過在十二小時之後都有被回復的情況。所以我們推斷 Lovastatin 可能有它一定的時效及濃度；又有一可能是 Lovastatin 雖然能抑制膜蛋白，但癌細胞可能有多重機制來合成所需之膜蛋白，當主要之合成路徑被抑制住，它可能會衍生出其他合成路徑，故我

們可能要再尋找新的具專一性小分子化學抑制劑，完全針對 Rac1 做專一性的抑制，看能否增加 cisplatin 的毒殺效果。

在C/EBPβ這個Transcription factor上，我們發現NTUB1/P有較高之表現(Fig. 17)，C/EBPβ會調控p21的表現(18)，而我們知道p53的下游是p21，在Fig. 14中NTUB1/P有p21的表現，但是NTUB1/P並無p53的表現，所以我們推斷C/EBPβ會調控p21的表現。另一方面，從前人研究指出，在細胞進行分化(Differentiation)時，會大量產生C/EBPβ，有證據顯示C/EBPβ會受到MAPK pathway所調控(53)，又在血管平滑肌細胞(Vascular Smooth Muscle Cells)研究指出(54)，當細胞受到一些inflammatory cytokines刺激時而啟動PI3K pathway，會活化C/EBPβ進而增加*c-fos*的Promoter之活性(55)，而*c-fos*它含有 serum-response element (SRE)會開啟很多成長因子(growth factors)的活化。在Fig. 14中，我們發現一些腫瘤抑制之相關蛋白質：Bad、Bcl-2與Bcl-xL並無明顯差異，但是caspase-3這個細胞凋亡蛋白質，在NTUB1/P有被抑制下來(Fig. 15)，而caspase-3它在整個細胞凋亡(apoptosis)的訊息傳遞路徑中，為一個重要的關鍵點，故我們推論cisplatin抗藥性之癌細胞不會使癌細胞走向細胞凋亡(apoptosis)，caspase-3被抑制可能是扮演一個重要之角色。

根據前人研究指出，Rac 會刺激 JNK/p38 MAP kinase 路徑(19-21)，在 Fig. 12,13 中，我們發現 JNK 與 p-ERK 在 NTUB1/P 有較高之表現，在這個 JNK/p38 MAP kinase 路徑中，mitogen-activated protein kinase (MAPK)會被 MEK 的雙重特異性 (dual specificity ; tyrosine threonine)的磷酸化作用而活化。MAPK 有兩種異構型 (isoform)：extra cellular regulated kinase (ERKs) 1 和 2。它們能位移至核內並且能被磷酸化及調控 DNA 合成和細胞分裂的重要轉錄因子。使得細胞走向生存(survival)、分化(differentiation)、增生(proliferation)及轉移(metastasis)，所以說我們推斷，cisplatin 抗藥性之癌細胞會經由 JNK/p38 MAP kinase 路徑，使細胞不會產生毒殺效果。

綜合以上結論，在 cisplatin 抗藥性之癌細胞它會經由多重之訊息傳遞路徑，以達到不被毒殺之效果，但是它是如何產生抗藥性的呢？有可能是，透過 PI3K 活化 multidrug resistance 1(*mdr1*)基因或 multidrug resistance protein-1 (MRP-1)，以啟動細胞排毒之能力(22, 23)。

許多研究早已發現，在巨噬細胞中，「內毒素」所誘導「前發炎物質」，如：腫瘤壞死因子—alfa (tumor necrosis factor alfa)、介白素-1 (interleukin-1)、介白素-6 (interleukin-6)、一氧化氮(NO)等的表現，可以透過介白素-10 (interleukin-10)將其抑制，因此，在「介白素」大家族中，「介白素-10」被科學家認為具有很強的抗發炎效果，「介白素-10」可以透過磷酸化細胞內 Mitogen-Activated Protein Kinase (MAPK)中的 p38 這路徑，而非 JNK 或 ERK，活化「血紅素氧化酵素-1」 (heme oxygenase-1, HO-1) mRNA 與蛋白質表現，來抑制「內毒素」所誘導「前發炎物質」如：腫瘤壞死因子、一氧化氮、MMP-9 等，但是分別使用 antisense 方式與血紅素氧化酵素抑制劑—ZnPP，阻斷「血

紅素氧化酵素-1」表現後，「介白素-10」抑制「內毒素」的現象也隨即消失，這暗示著介白素-10」抑制「內毒素」誘導發炎反應的訊息傳遞路徑中，「血紅素氧化酵素-1」扮演著舉足輕重的角色。 在尋找「血紅素氧化酵素-1」的調控機制時，其進一步發現，「血紅素氧化酵素-1」代謝血紅素之後，所產生一氧化碳(CO)，才是「介白素-10」作用的關鍵；從動物實驗中，也看到「介白素-10」可以大幅提高了已注射內毒素老鼠的存活率；相同於細胞階段的發現，「血紅素氧化酵素-1」、一氧化碳(CO) 確實是「介白質-10」避免內毒素在老鼠體內引起劇烈發炎反應的重要原因(44)。在 Growth Factor and Hormones 在人類泌尿上皮細胞癌之表現量中發現，interleukin-6 (IL-6) 的表現量在抗藥株都有被抑制下來的現象，所以我們推測可能是被 IL-10 抑制下來，不過這二者的先後順序可能還需要實驗證明。

在Fig. 18 中，Signaling Intermediates在人類泌尿上皮細胞癌之表現量中，Superoxide dismutase (SOD)於N/P和N/As有被up-regulation的現象，而heme oxygenase-1 (HO-1) 於N/As有被up-regulation的現象，故我們從自由基之觀點切入。何謂自由基：是指帶有不成對電子的分子、原子、或離子，因存在未成對電子，因此特性。自由基 ─ 非常不穩定、具高度活性、它會去搶奪其他物質的電子，而併發一連串連鎖反應，對身體有一定毒性；可能影響一些生物分子如蛋白質、脂質、醣類、DNA等正常結構，及代謝反應造成不可回復的傷害，氧自由基(O_2)、氫氧自由基(OH)，其含有不穩定的氧分子，具有強烈的氧化作用，會給組織細胞帶來氧化壓力，破壞細胞膜、血管壁、蛋白質及基因，使人體產生老化及疾病，尤其是慢性病，包括癌症等。自由基是如何形成的：自由基隨時隨地會產生，人體中自由基產生的原因可能來自身體能量產生的過程所釋放出來；人體遭受感染、受傷等發炎狀態時，會啟動身體殺菌機制來清除外來物，例噬中性球及巨噬細胞會立即進行respiratory burst，以增加氧氣攝入，活化HMS並產生H_2O_2及O_2；正常健康情況下，產生之殺菌自由基可為身體抗氧化營養素（如維生素A、C、E、Se和Zn等）或酵素機轉(superoxide dismutase、glutathione peroxidase、catalase與thioredoxin reductase）所清除；但若在感染結束後，宿主沒有足夠的保護機制，清除此過多的自由基，將造成細胞傷害（如細胞膜脂質過氧化、DNA傷害等）。自由基造成傷害原因：造成胞膜脂質過氧化作用、蛋白質間雙硫鍵形成、 DNA傷害。自由基與DNA反應可能造成癌症，自由基可攻擊細胞核，導致細胞死亡或受損，突變等；自由基造成胞膜脂質過氧化作用、並使低密度脂蛋白氧化，為造成心血管疾病、冠狀動脈硬化的主因(45)。從Fig. 18 中，一些與自由基有關的marker：COX-2、HO-1 和SOD，在抗藥株中都有表現的差異，有可能是因為當細胞在癌化的過程中，細胞會產生reactive oxygen species (ROS)，而這個內生性的ROS會與抗癌藥物或放射線使得DNA產生突變，經由粒腺體(mitochondrial)的呼吸傳遞鏈(respiratory chain)增加ROS的產生，最後使DNA不穩定、產生突變與抗藥性的發生(56)。

我們將 Western blotting 之方法所篩選人類泌尿上皮細胞癌細胞株與抗藥株之蛋白質表現差異整理，發現在四株抗藥株：N/G、N/T、N/P 和 N/As 的 RhoA、JNK、ERK1/2、p-ERK1/2、 C/EBPβ 與 Cyclin D1 都有被 up-regulation 之現象，其中 RhoA 和 Cyclin D1 是調控 cell cycle 之調控子；JNK、ERK1/2、p-ERK1/2 和 C/EBPβ 會開啟一些 survival 的基因，使細胞走向 survival 的狀況。在四株抗藥株：N/G、N/T、N/P 和 N/As 的 Bcl-xL、Nrf-2 和 Hsp70 都有被 down-regulation 之現象，其中 Bcl-xL 為一腫瘤抑制蛋白，它在四株抗藥株中都被抑制下來，所以可能無法達到抑制腫瘤的能力。熱休克蛋白(heat shock protein, Hsp 70)是生物用來對抗外在高溫環境的蛋白質，細胞中如果缺少這種蛋白質，就會比較容易發生癌症反應。文獻指出(46)，研究細胞染色體分裂所需的端粒酶(telomerase)時發現，一般細胞只有在染色體要分離時，才會產生端粒酶，幫助染色體分離。然而，癌症細胞的端粒酶卻一直存在，此外，Hsp70 蛋白質也同時存在。

Paclitaxe(太平洋紫杉醇)在細胞毒性機制研究，在這項研究中, 收集證據來證實paclitaxel 能藉由提高細胞內O_2^-, H_2O_2及 NO 水平來產生毒性的概念. 這種理論由下列的結果說明 : (a) paclitaxel 導致O_2^- , H_2O_2及 NO的產生; (b) paclitaxel 導致的DNA氧化損傷; (c) 減少製造H_2O_2及 NO 的試劑會抑制paclitaxel 引起的DNA 損傷、G2-M 停滯、細胞凋亡, 和抑制細胞生長; (d) 抑制SOD or glutamylcysteine synthase 會增加paclitaxel 引起細胞凋亡; (e) 高總抗氧化容量的細胞株對於paclitaxel 細胞毒性更有抗性; 以及(f) 減少群落生存的試劑對於paclitaxel處理的細胞也會減少細胞總抗氧化容量. 因而, paclitaxel chemoresistance 化療藥物抗藥性與細胞內抗氧化容量有很好的關聯。許多化學療法試劑對癌細胞藉由產生自由基來引發毒性反應, 導致細胞不可逆的傷害, 並且在癌細胞中過度產生ROS可能會耗盡SOD容量及其他適當抗氧化防禦容量. 這個概念與我們的結果是一致的表示, 耗盡細胞的抗氧化容量會增加paclitaxel 毒性。最近, 據報導, paclitaxel 處理可活化MEK/ERK 和phosphatidylinositol 3-kinase/Akt 訊息傳遞(57)，據報導, paclitaxel 可能導致單股DNA鏈斷裂(58-60). 我們的資料顯示, paclitaxel 能夠藉由增加H_2O_2及 NO 水平引起DNA氧化傷害. 在DNA 損傷方面, 細胞能夠停止細胞週期的進行來修復損傷. 他們也能夠初步控制細胞死亡或允許細胞週期繼續進行而不修復損傷甚至有過多突變或分子改變. 對於paclitaxel 處理的細胞而言, DNA 損傷和G2-M 停滯之間或DNA損傷及續發突變的仍是未知的. 這裡, 我們的結果顯示, 在T24 細胞以0.02 mol/L低濃度paclitaxel處理後會導致的氧化DNA 併攏. 這個paclitaxel 的水平比產生核碎裂, sub-G1 聚積及G_2M停滯所需濃度還低. 的確, 這發現能夠解釋為什麼基因突變從minor DNA insults能夠促進抗藥性細胞生長而不是死亡。這些結果我們已經寫成論文並發表在Cancer Res期刊中(61)。

這些現象只能說明具抗藥性細胞株生存之能力，不能證明與抗藥性之關係，

就從參考文獻中推斷，有可能藉由 PI3K 的訊息傳遞路徑，活化 MRP-1 以產生抗藥性，後面的實驗證明待留後人進一步研究。

參考文獻

1. Human Physiology 10/e 2006
2. 民國九十四年行政院衛生署之統計資料
3. Sternberg CN, de Mulder PH, Schornagel JH, Theodore C, Fossa SD, van Oosterom AT, Witjes F, Spina M, van Groeningen CJ, de Balincourt C, Collette L; European Organization for Research and Treatment of Cancer Genitourinary Tract Cancer Cooperative Group. Randomized phase III trial of high-dose-intensity methotrexate, vinblastine, doxorubicin, and cisplatin (MVAC) chemotherapy and recombinant human granulocyte colony-stimulating factor versus classic MVAC in advanced urothelial tract tumors: European Organization for Research and Treatment of Cancer Protocol no. 30924. *J Clin Oncol*. (2001) **19**: 2638-46.
4. Bergman AM, Pinedo HM, Peters GJ. Determinants of resistance to 2',2'-difluorodeoxycytidine (gemcitabine). *Drug Resist Updat*. (2002) **5**: 19-33.
5. Kondratov RV, Komarov PG, Becker Y, Ewenson A, Gudkov AV. Small molecules that dramatically alter multidrug resistance phenotype by modulating the substrate specificity of P-glycoprotein. *Proc Natl Acad Sci U S A*. (2001) **98**:14078-83.
6. Bergman AM, Pinedo HM, Peters GJ. Determinants of resistance to 2',2'-difluorodeoxycytidine (gemcitabine). *Drug Resist Updat.* (2002) **5**: 19-33.
7. Miller WH Jr, Schipper HM, Lee JS, Singer J, Waxman S. Mechanisms of Action of Arsenic Trioxide. *Cancer Research* (2002) **62**: 3893-3903.
8. Olson RD, Boerth RC, Gerber JG, Nies AS. Mechanism of adriamycin cardiotoxicity: evidence for oxidative stress. *Life Sci*. (1981) **29**: 1393-401.
9. Wernyj RP, Morin PJ. Molecular mechanisms of platinum resistance: still searching for the Achilles' heel. *Drug Resist Updat.* (2004) **7**: 227-32.
10. Cozzarelli NR. The mechanism of action of inhibitors of DNA synthesis. *Annu Rev Biochem*. (1977) **46**: 641-68.
11. Tobert JA. LOVASTATIN AND BEYOND: THE HISTORY OF THE HMG-COA REDUCTASE INHIBITORS. *Nature Reviews Drug Discovery* (2003) **2**: 517-526.
12. McFarlane SI, Muniyappa R, Francisco R, Sowers JR. Pleiotropic effects of statins: Lipid reduction and beyond. *J Clin Endocrinol Metab* (2002) **87:** 1451-8.
13. O'Donnell MP, Kasiske BL, Kim Y, Schmitz PG, Keane WF. Lovastatin

retards the progression of established glomerular disease in obese Zucker rats. *Am J Kidney Dis* (1993) **22:** 83-9.

14. Fukata M and Kaibuchi K. Rho-family GTPases in cadherin-mediated cell-cell adhesion. *Nat Rev Mol Cell Biol*. (2001) **2**: 887-97.
15. Wennerberg K and Der CJ. Rho-family GTPases: it's not only Rac and Rho (and I like it). *J Cell Sci.* (2004)**117**: 1301-12.
16. Aznar S. and Lacal C. Rho signals to cell growth and apoptosis. *Cancer Letters* (2001) **165**: 1-10.
17. Page K, Li J, Hodge JA, Liu PT, Vanden Hoek TL, Becker LB, Pestell RG, Rosner MR, Hershenson MB. Characterization of a Rac1 signaling pathway to cyclin D(1) expression in airway smooth muscle cells. *J Biol Chem*. (1999)**274**: 22065-71.
18. Hour TC, Chen J, Huang CY, Guan JY, Lu SH, Pu YS. Curcumin enhances cytotoxicity of chemotherapeutic agents in prostate cancer cells by inducing p21(WAF1/CIP1) and C/EBPbeta expressions and suppressing NF-kappaB activation. *Prostate*. (2002) **51**: 211-8.
19. Brown JL, Stowers L, Baer M, Trejo J, Coughlin S, Chant J. Human Ste20 homologue hPAK1 links GTPases to the JNK MAP kinase pathway. *Curr Biol*. (1996) **6**: 598-605.
20. Bagrodia S, Derijard B, Davis RJ, Cerione RA. Cdc42 and PAK-mediated signaling leads to Jun kinase and p38 mitogen-activated protein kinase activation. *J Biol Chem*. (1995) **270**: 27995-8.
21. Zhang S, Han J, Sells MA, Chernoff J, Knaus UG, Ulevitch RJ, Bokoch GM. Rho family GTPases regulate p38 mitogen-activated protein kinase through the downstream mediator Pak1. *J Biol Chem.* (1995) **270**: 23934-6.
22. Kuo MT, Liu Z, Wei Y, Lin-Lee YC, Tatebe S, Mills GB, Unate H. Induction of human MDR1 gene expression by 2-acetylaminofluorene is mediated by effectors of the phosphoinositide 3-kinase pathway that activate NF-kappaB signaling. *Oncogene*. (2002) **21**: 1945-54.
23. Lee JT Jr, Steelman LS, McCubrey JA. Phosphatidylinositol 3'-kinase activation leads to multidrug resistance protein-1 expression and subsequent chemoresistance in advanced prostate cancer cells. *Cancer Res*. (2004) **64**: 8397-404.
24. Otto JJ. Vinculin. *Cell Motil Cytoskeleton*. (1990)**16**: 1-6.
25. Ryazanov AG. Elongation factor-2 kinase and its newly discovered relatives. *FEBS Lett*. (2002) **514**: 26-9.
26. Kubota H, Hynes G, Willison K. The chaperonin containing t-complex polypeptide 1 (TCP-1). Multisubunit machinery assisting in protein folding

and assembly in the eukaryotic cytosol. *Eur J Biochem*. (1995) **230**: 3-16.
27. Pancholi V. Multifunctional alpha-enolase: its role in diseases. *Cell Mol Life Sci.* (2001) **58**: 902-20.
28. Bedard KM, Walter BL, Semler BL. Multimerization of poly(rC) binding protein 2 is required for translation initiation mediated by a viral IRES. *RNA*. (2004) **10**:1266-76.
29. Rescher U, Gerke V. Annexins--unique membrane binding proteins with diverse functions. *J Cell Sci*. (2004) **117**: 2631-9.
30. Janssens V, Goris J, Van Hoof C. PP2A: the expected tumor suppressor. *Curr Opin Genet Dev.* (2005) **15**: 34-41.
31. Minarik P, Tomaskova N, Kollarova M, Antalik M. Malate dehydrogenases--structure and function. *Gen Physiol Biophys.* (2002) **21**: 257-65.
32. Tanaka K, Tsurumi C. The 26S proteasome: subunits and functions. *Mol Biol Rep*. (1997) **24**: 3-11.
33. Fothergill-Gilmore LA, Watson HC. The phosphoglycerate mutases. *Adv Enzymol Relat Areas Mol Biol.* (1989) **62**: 227-313.
34. Olah J, Orosz F, Keseru GM, Kovari Z, Kovacs J, Hollan S, Ovadi J. Triosephosphate isomerase deficiency: a neurodegenerative misfolding disease. *Biochem Soc Trans*. (2002) **30**: 30-8.
35. Moore JD. The Ran-GTPase and cell-cycle control. *Bioessays*. (2001) 23: 77-85.
36. Mauro VP, Edelman GM. The ribosome filter hypothesis. *Proc Natl Acad Sci U S A.* (2002) **99**: 12031-6.
37. Das KC. Thioredoxin system in premature and newborn biology. *Antioxid Redox Signal.* (2004) **6**: 177-84.
38. Paavilainen VO, Bertling E, Falck S, Lappalainen P. Regulation of cytoskeletal dynamics by actin-monomer-binding proteins. *Trends Cell Biol*. (2004)**14**: 386-94.
39. Chauhan D, Hideshima T, Anderson KC. Proteasome inhibition in multiple myeloma: therapeutic implication. *Annu Rev Pharmacol Toxicol.* (2005) **45**: 465-76.
40. Hayes JD, Flanagan JU, Jowsey IR. Glutathione transferases. *Annu Rev Pharmacol Toxicol*. (2005) 45: 51-88.
41. Le Roy C, Wrana JL. Clathrin- and non-clathrin-mediated endocytic regulation of cell signalling. *Nat Rev Mol Cell Biol*. (2005) **6**: 112-26.
42. Stanier P, Abu-Hayyeh S, Murdoch JN, Eddleston J, Copp AJ. Paralogous sm22alpha (Tagln) genes map to mouse chromosomes 1 and 9: further

evidence for a paralogous relationship. *Genomics*. (1998) **51**: 144-7.
43. Witke W. The role of profilin complexes in cell motility and other cellular processes. *Trends Cell Biol.* (2004) **14**: 461-9.
44. Lee TS, Chau LY. Heme oxygenase-1 mediates the anti-inflammatory effect of interleukin -10 in mice. *Nat Med.* (2002) **8**: 240-6.
45. Fattman CL, Schaefer LM, Oury TD. Extracellular superoxide dismutase in biology and medicine. *Free Radic Biol Med*. (2003) **35**: 236-56.
46. Pandita TK, Higashikubo R, Hunt CR. HSP70 and genomic stability. *Cell Cycle*. (2004) **3**: 591-2.
47. Azechi H, Nishida N, Fukuda Y, Nishimura T, Minata M, Katsuma H, Kuno M, Ito T, Komeda T, Kita R, Takahashi R, Nakao K. Disruption of the p16/cyclin D1/retinoblastoma protein pathway in the majority of human hepatocellular carcinomas. *Oncology*. (2001) **60**: 346-54.
48. Sumrejkanchanakij P, Tamamori-Adachi M, Matsunaga Y, Eto K, Ikeda MA. Role of cyclin D1 cytoplasmic sequestration in the survival of postmitotic neurons. *Oncogene*. (2003) **22**: 8723-30.
49. Meek DW. The p53 response to DNA damage. *DNA Repair*. (2004) **3**: 1049-56.
50. Yang Y, Li CC, Weissman AM. Regulating the p53 system through ubiquitination. *Oncogene*. (2004) **23**: 2096-106.
51. Yap DB, Hsieh JK, Chan FS, Lu X. mdm2: a bridge over the two tumour suppressors, p53 and Rb. *Oncogene*. (1999) **18**: 7681-9.
52. Haines DS. The mdm2 proto-oncogene. *Leuk Lymphoma*. (1997) **26**: 227-38.
53. Piwien Pilipuk G, Galigniana MD, Schwartz J. Subnuclear localization of C/EBP beta is regulated by growth hormone and dependent on MAPK. *J Biol Chem*. (2003) **278**: 35668-77.
54. Sekine O, Nishio Y, Egawa K, Nakamura T, Maegawa H, Kashiwagi A. Insulin activates CCAAT/enhancer binding proteins and proinflammatory gene expression through the phosphatidylinositol 3-kinase pathway in vascular smooth muscle cells. *J Biol Chem*. (2002) **277**: 36631-9.
55. Hanlon M, Sturgill TW, Sealy L. ERK2- and p90(Rsk2)-dependent pathways regulate the CCAAT/enhancer-binding protein-beta interaction with serum response factor. *J Biol Chem*. (2001) **276**: 38449-56.
56. Pelicano H, Carney D, Huang P. ROS stress in cancer cells and therapeutic implications. *Drug Resist Updat*. (2004) **7**: 97-110.
57. Ling X, Bernacki RJ, Brattain MG, Li F. Induction of survivin expression by taxol (paclitaxel) is an early event, which is independent of taxol-mediated

G2/M arrest. *J Biol Chem* (2004) **279**:15196–203.

58. Ollikainen T, Knuuttila A, Suhonen S, et al. In vitro sensitivity of normal human mesothelial and malignant mesothelioma cell lines to four new chemotherapeutic agents. *Anticancer Drugs* (2000);**11**:93–9.
59. Digue L, Orsiere T, De Meo M, et al. Evaluation of the genotoxic activity of paclitaxel by the in vitro micronucleus test in combination with fluorescent in situ hybridization of a DNA centromeric probe and the alkaline single cell gel electrophoresis technique (comet assay) in human T-lymphocytes. Environ Mol Mutagen (1999) **34**:269–78.
60. Branham MT, Nadin SB, Vargas-Roig LM, Ciocca DR. DNA damage induced by paclitaxel and DNA repair capability of peripheral blood lymphocytes as evaluated by the alkaline comet assay. *Mutat Res* (2004) **560**:11–7.
61. Ramanathan, B., Chen, C. H., Jan, K .Y., Hour, T. C., Yu, H. J., and Pu, Y. S. (2005) Resistance to paclitaxel is proportional to total cellular antioxidation capacity. *Cancer Res* **65**(18):8455-8460.

圖表

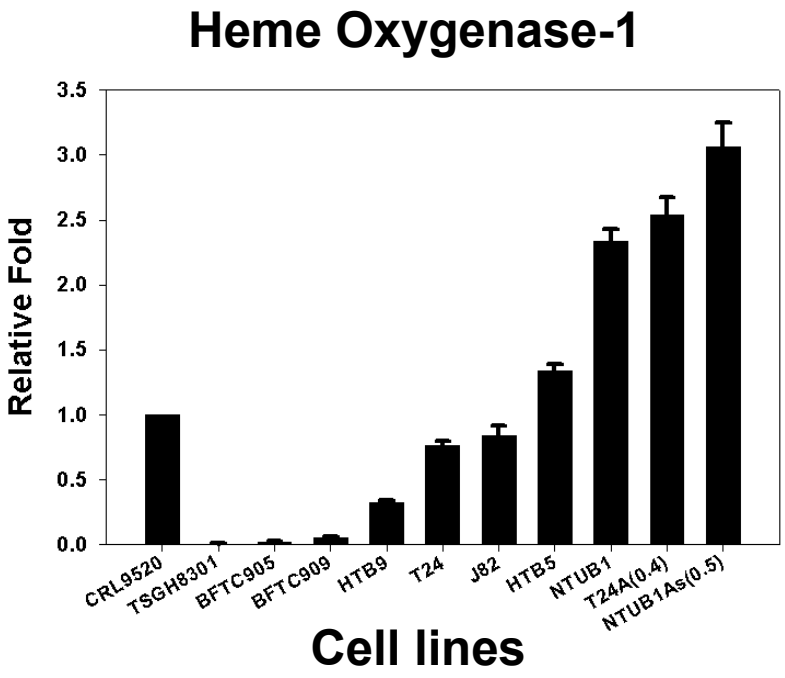

Fig.1 Real-time PCR 分析人類泌尿上皮細胞癌 **HO-1** 基因表現量

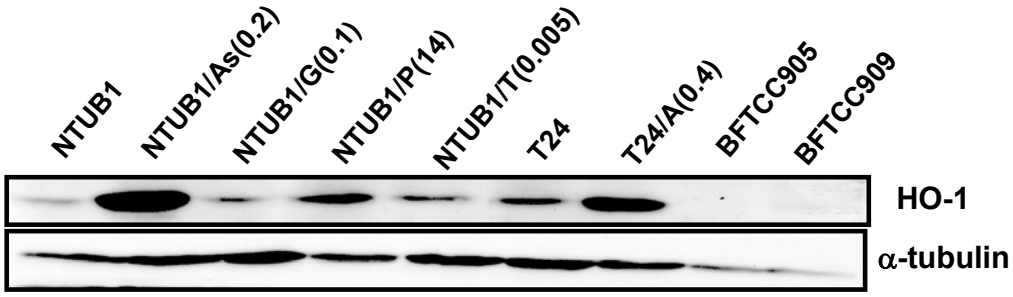

Fig. 2 Western blotting 分析人類泌尿上皮細胞癌 **HO-1** 蛋白質表現量

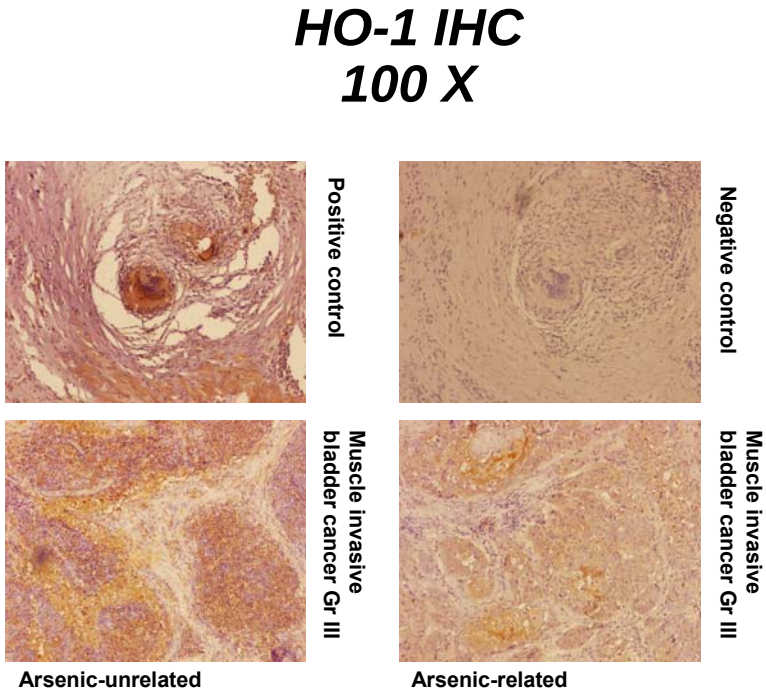

Fig. 3 免疫組織染色分析人類泌尿上皮細胞癌組織內 **HO-1** 表現量

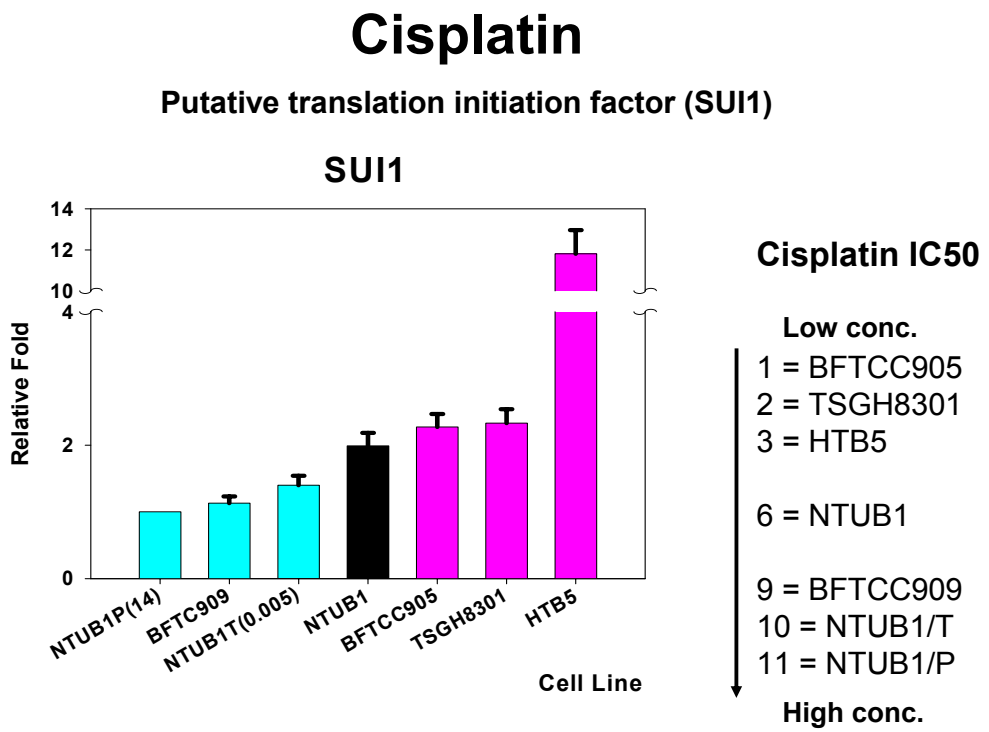

Fig. 4 Real-time PCR 分析具 cisplatin 抗性/敏感人類泌尿上皮癌細胞株之 SUI1 基因表現量

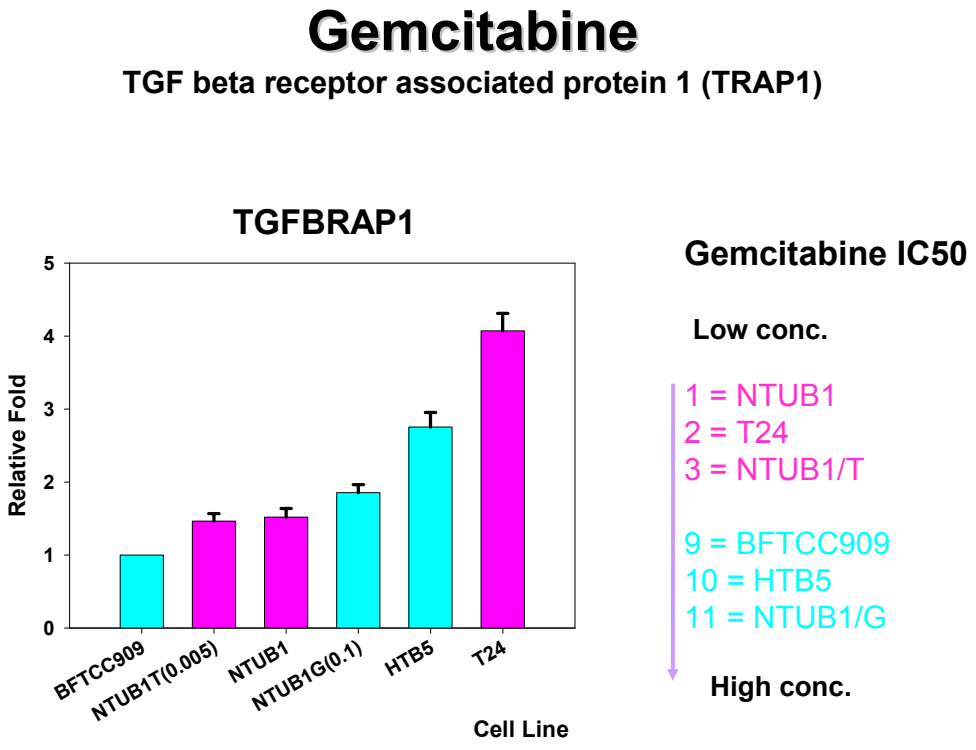

Fig. 5 Real-time PCR 分析具 cisplatin 抗性/敏感人類泌尿上皮癌 TRAP1 基因表現量

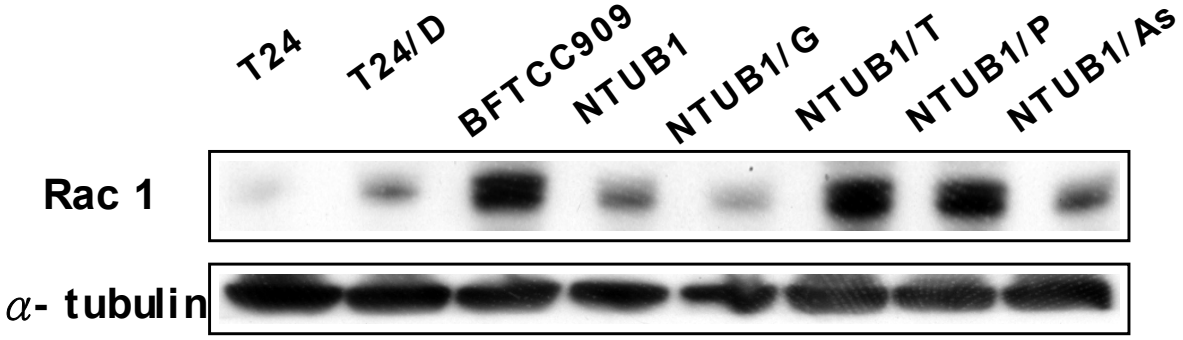

Fig. 6.為使用 **Western blotting** 分析 **Rac1** 在人類泌尿上皮細胞癌細胞株與抗藥株之含量。

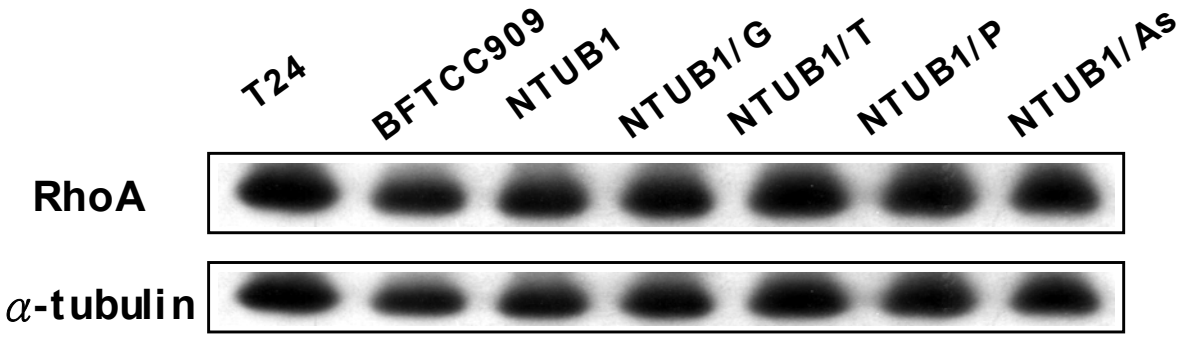

Fig. 7 為使用 **Western blotting** 分析 **RhoA** 在人類泌尿上皮細胞癌細胞株與抗藥株之含量。

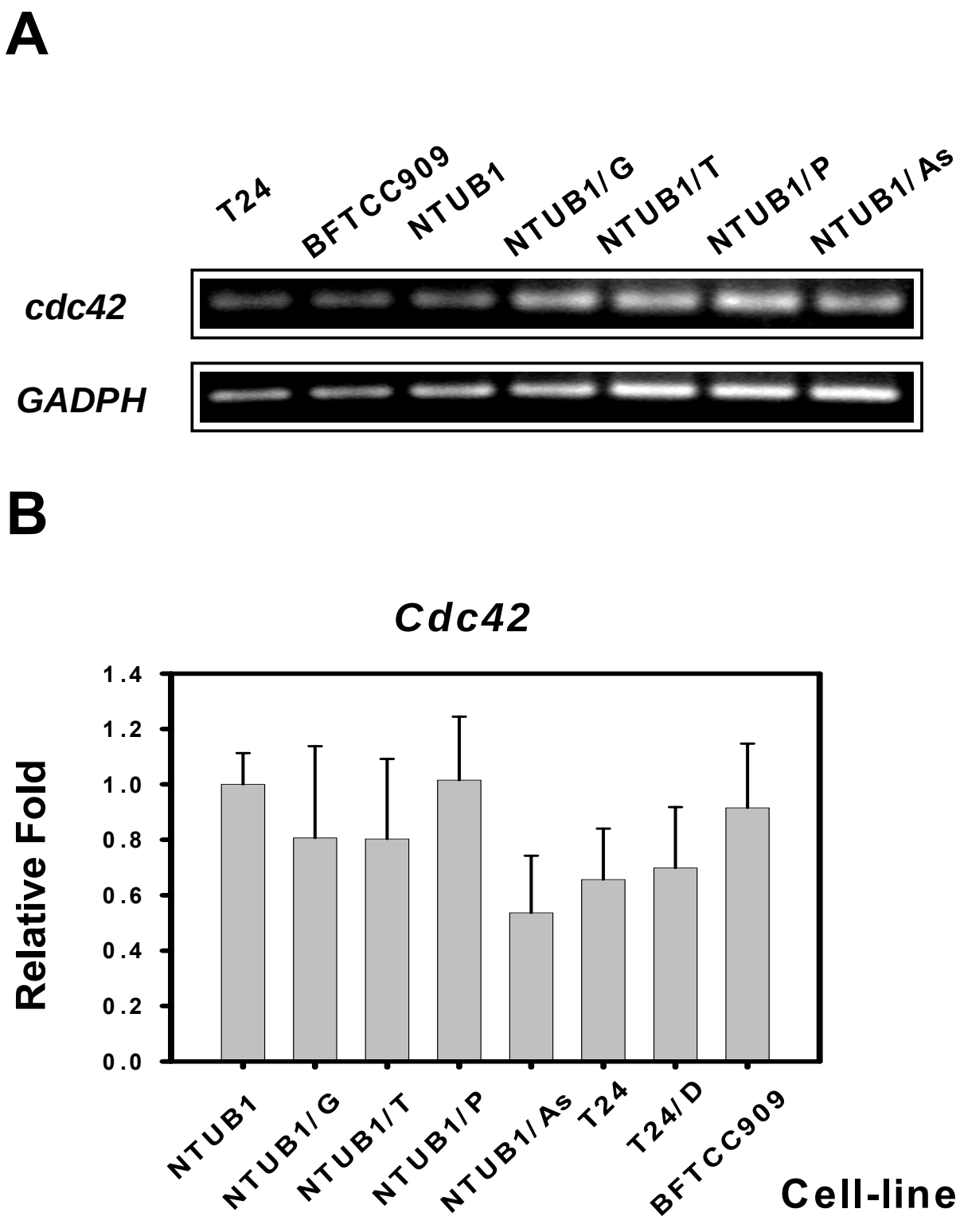

Fig. 8 A 為使用 **RT-PCR** 分析 ***cdc42*** 在人類泌尿上皮細胞癌細胞株與抗藥株之含量；**B** 為利用 **Real-time PCR** 定量之結果。

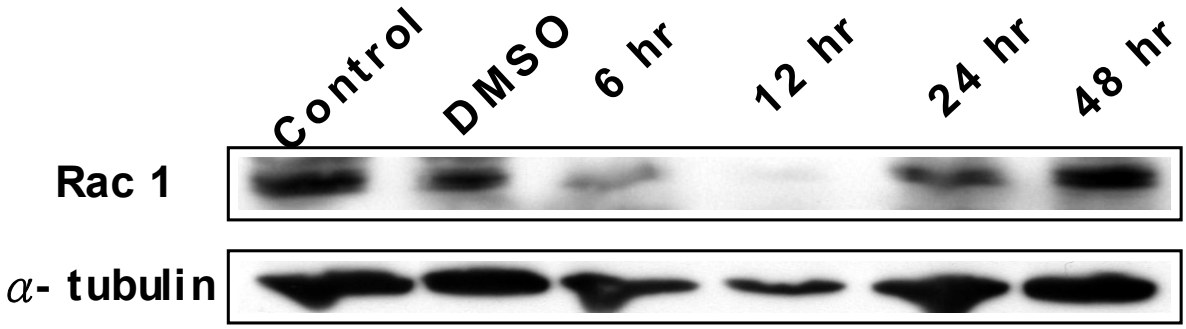

Fig. 9 NTUB1/Cisplatin (14 μM)-resistant 細胞株先處理 Lovastatin = 10 μM，經由 Time-course 之後，以 Western blotting 分析 Rac 1 蛋白質之表現量。

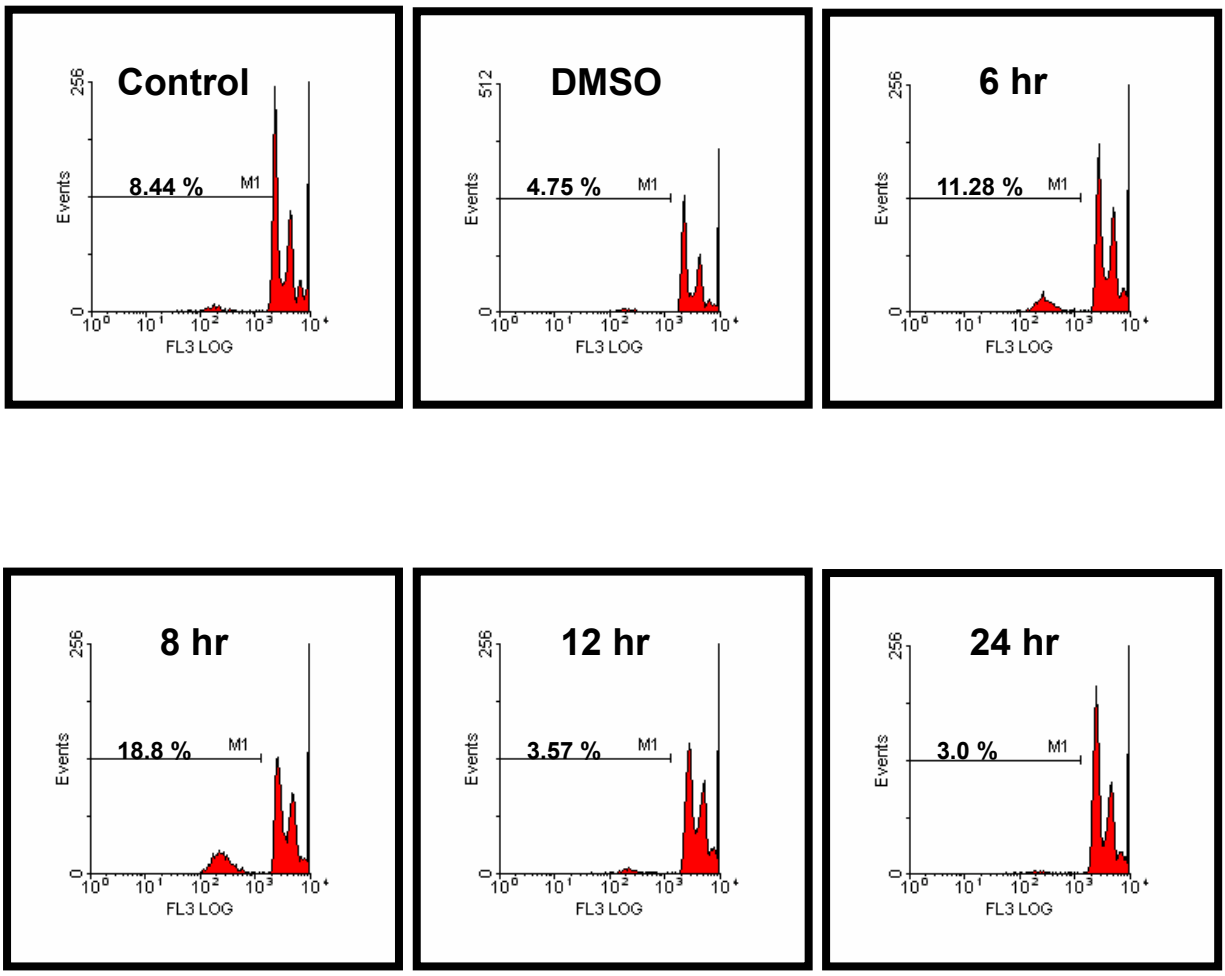

Fig. 10 NTUB1/P細胞處理Lovastatin = 10 μM後，產生Sub-G_1 fractions的現象。時間經由 6、8、12、24 小時後，發現Lovastatin對NTUB1/P細胞產生sub-G1 fractions的程度在 8 小時有增加的現象，但是在 12 小時之後有回復的現象。

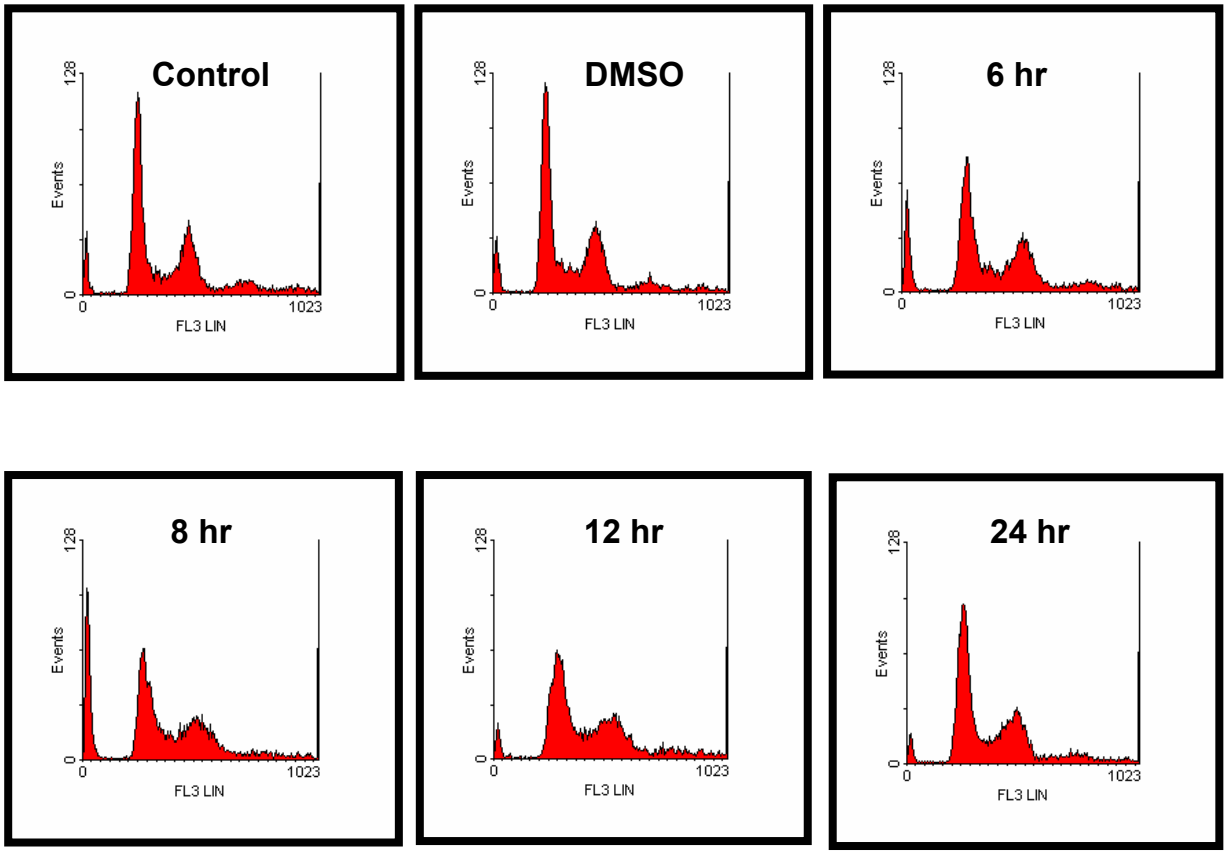

	G_0/G_1 phase	S phase	G_2/M phase
Control %	42.49	11.87	20.90
DMSO %	46.66	14.22	20.78
6 hr %	19.91	26.05	20.03
8 hr %	22.71	21.99	19.09
12 hr %	20.63	29.16	20.08
24 hr %	43.94	16.43	22.77

Fig. 11 NTUB1/P 細胞處理 Lovastatin = 10 μM 後，產生 Cell cycle arrest 的現象。時間經由 6、8、12、24 小時後，發現 Lovastatin 對 NTUB1/P 細胞產生 Cell cycle arrest 的程度在 6、8、12 小時，細胞在 S 期有停滯的現象。

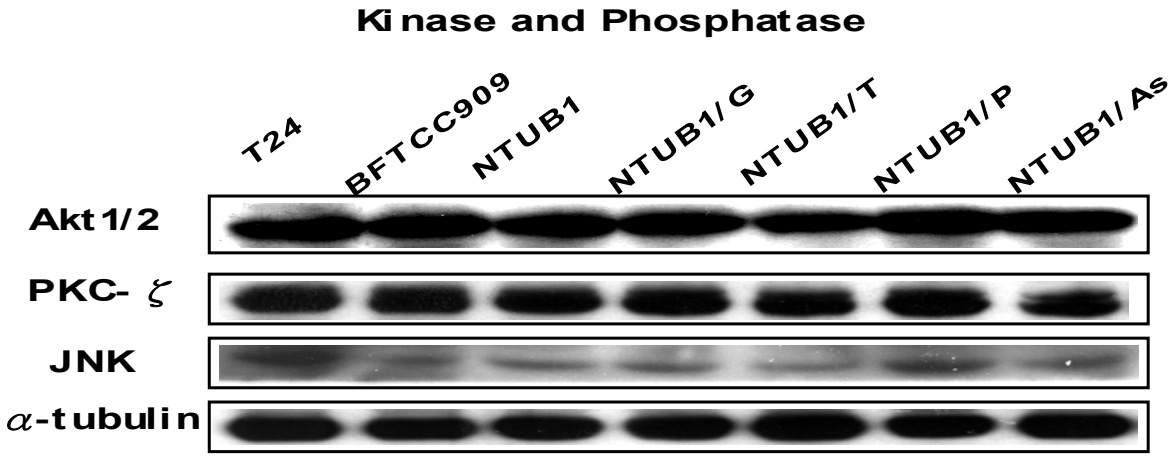

Fig. 12 以 **Western blotting** 分析 **Kinase and Phosphatase** 在人類泌尿上皮細胞癌之表現量。

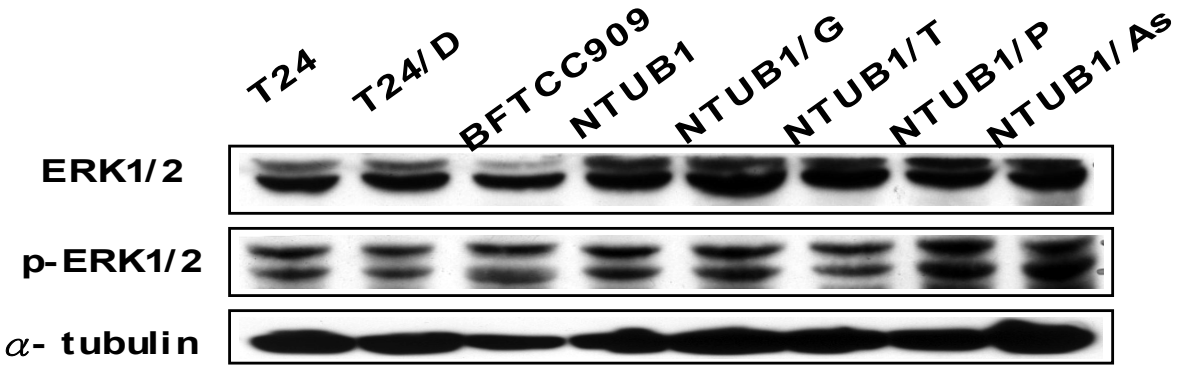

Fig. 13 以 **Western blotting** 分析 **Kinase and Phosphatase** 在人類泌尿上皮細胞癌之表現量。結果發現具抗藥性之人類泌尿上皮細胞癌中 **ERK1/2** 和 **p-ERK1/2** 則有些許差異。

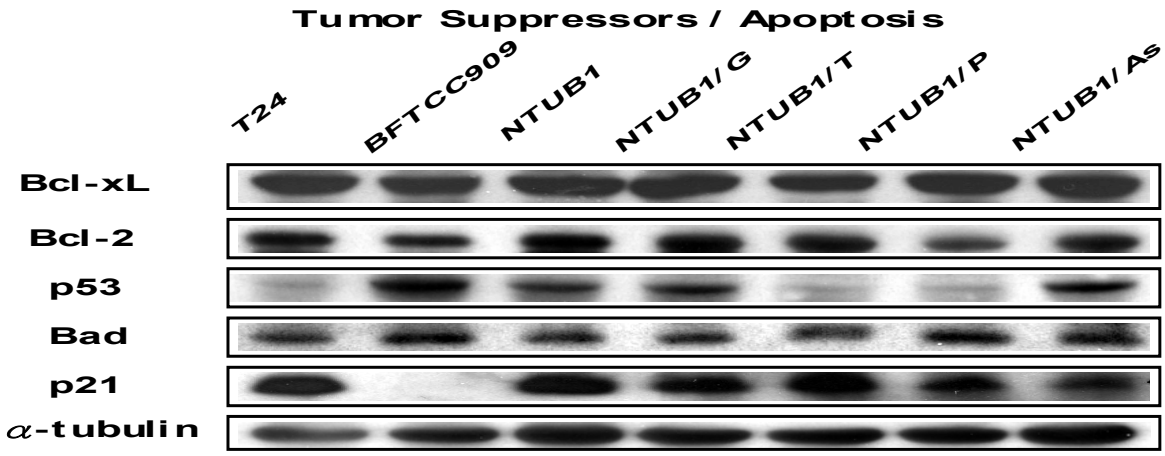

Fig. 14 以 **Western blotting** 分析 **Tumor suppressor/Apoptosis** 在人類泌尿上皮細胞癌之表現量。結果發現人類泌尿上皮細胞癌 **Bcl-xL**、**Bcl-2** 與 **Bad** 並無明顯差異，而 **p53** 及 **p21** 的蛋白質表現量則有些許差異。

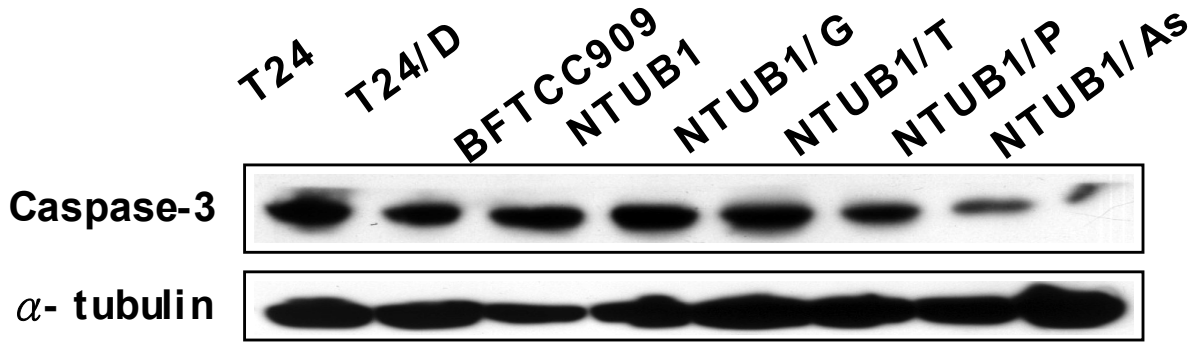

Fig. 15 以 **Western blotting** 分析 **Tumor suppressor/Apoptosis** 在人類泌尿上皮細胞癌之表現量。結果發現人類泌尿上皮細胞癌 **Caspase-3** 的蛋白質表現量則有些許差異。

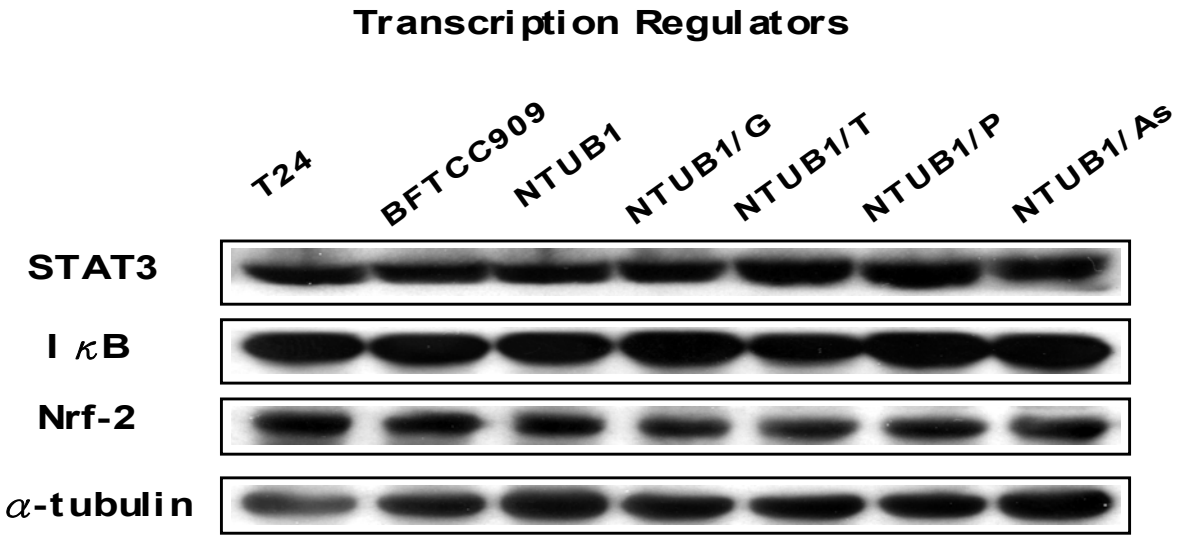

Fig. 16 以 **Western blotting** 分析 **transcrition regulators** 在人類泌尿上皮細胞癌之表現量。結果發現人類泌尿上皮細胞癌 **STAT3**、**IκB** 與 **Nrf-2** 的蛋白質表現量並無顯著差異。

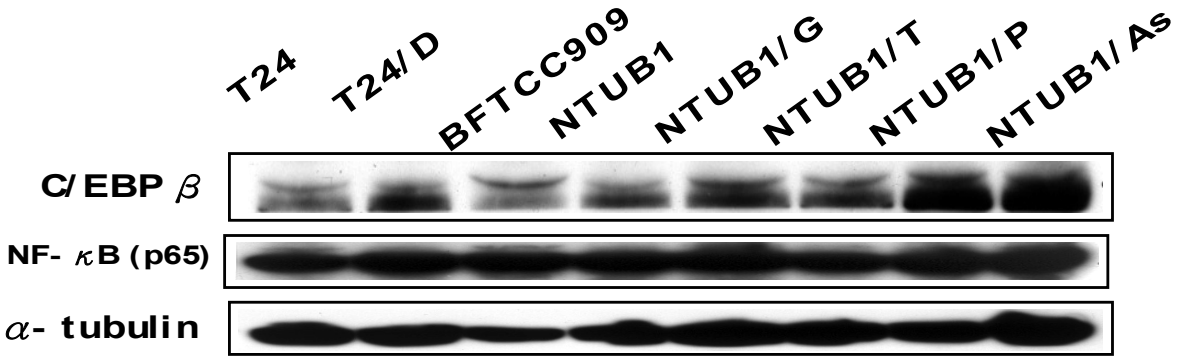

Fig. 17 以 **Western blotting** 分析 **transcrition regulators** 在人類泌尿上皮細胞癌之表現量。結果發現人類泌尿上皮細胞癌 **NF-κB** 的蛋白質表現量並無顯著差異，而 **C/EBP**β則有些許差異。

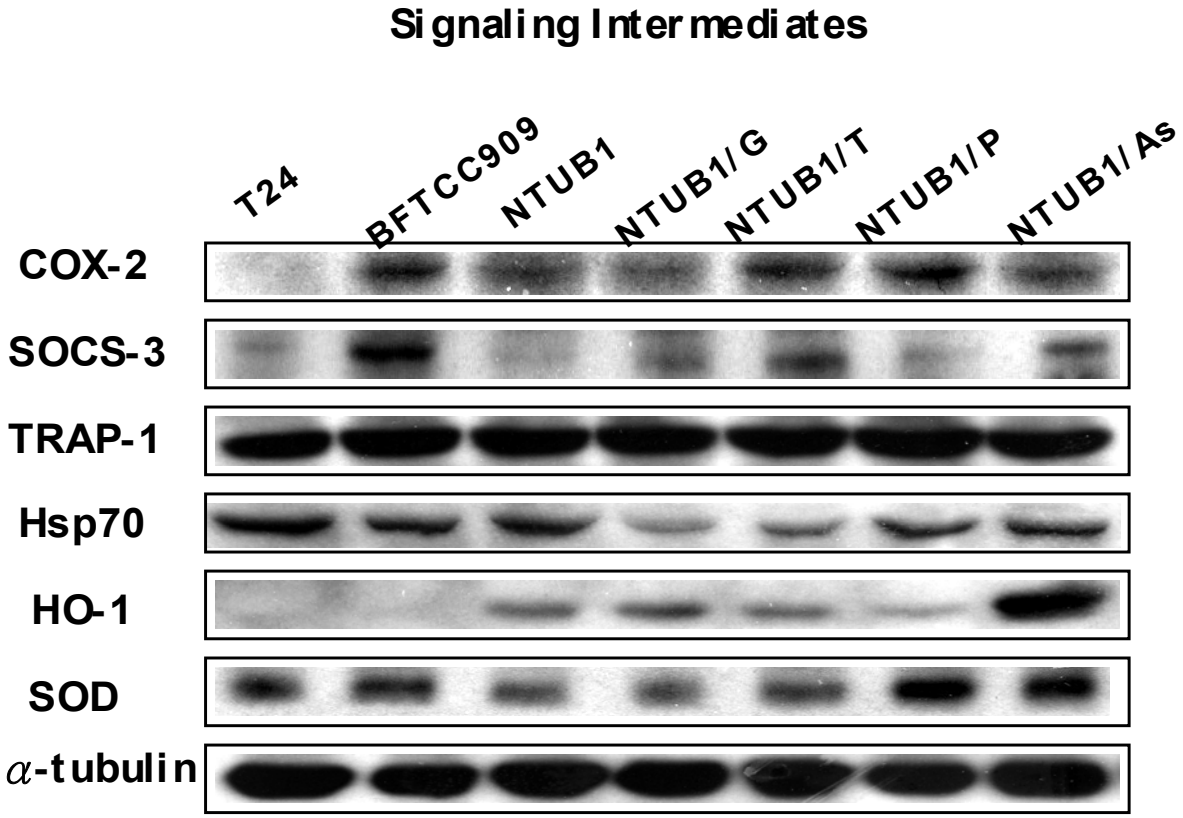

Fig. 18 以 **Western blotting** 分析 **Signaling Intermediates** 在人類泌尿上皮細胞癌之表現量。結果發現人類泌尿上皮細胞癌中 **COX-2**、**SOCS-3**、**Hsp70**、**HO-1** 和 **SOD** 的蛋白質表現量有些許差異，而 **TRAP-1** 並無差異。

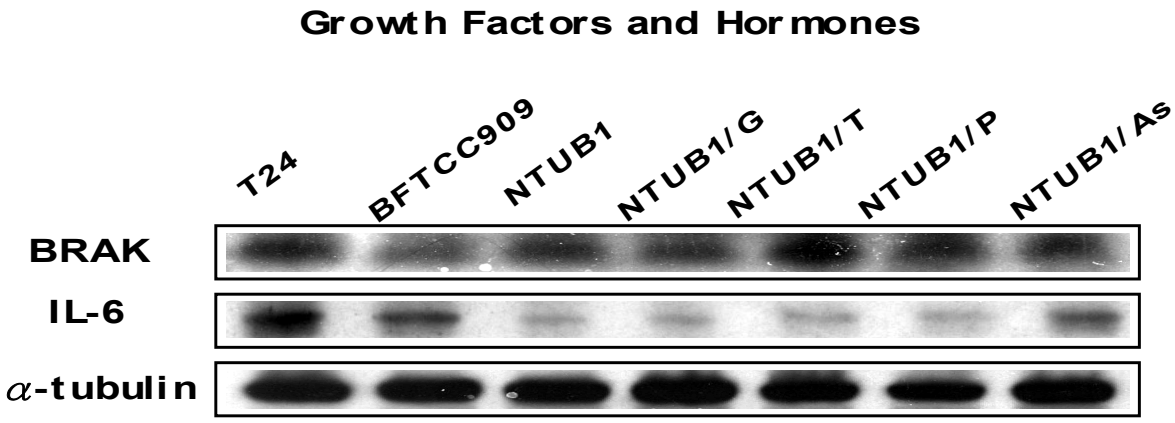

Fig. 19 以 **Western blotting** 分析 **Growth Factor and Hormones** 在人類泌尿上皮細胞癌之表現量。結果發現具抗藥性之人類泌尿上皮細胞癌中 **IL-6** 的蛋白質表現量有些許差異，而並 **BRAK** 無明顯差異。

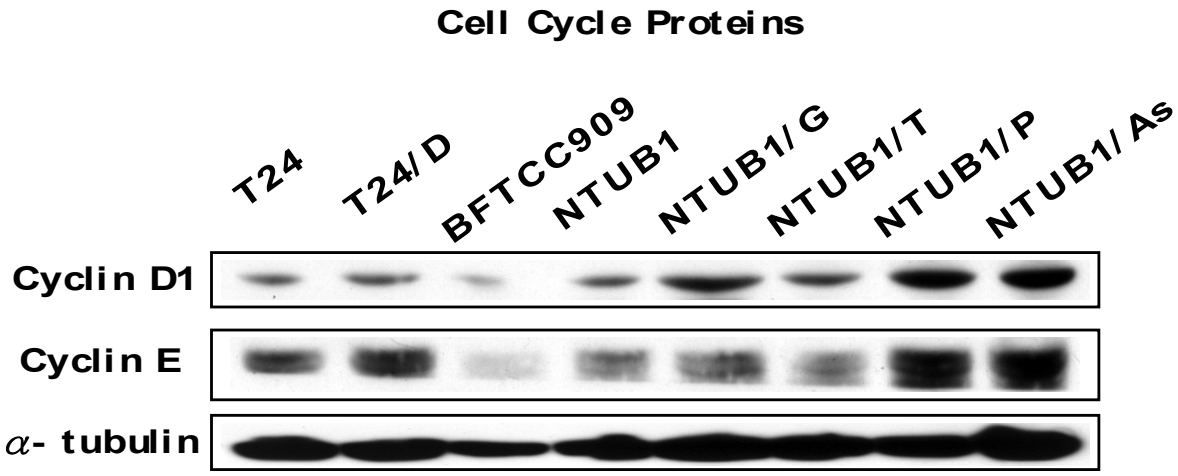

Fig. 20 以 **Western blotting** 分析 **cell cycle proteins** 在人類泌尿上皮細胞癌之表現量。結果發現具抗藥性之人類泌尿上皮細胞癌 **cyclin D1** 與 **cyclin E** 的蛋白質表現量有些許差異。

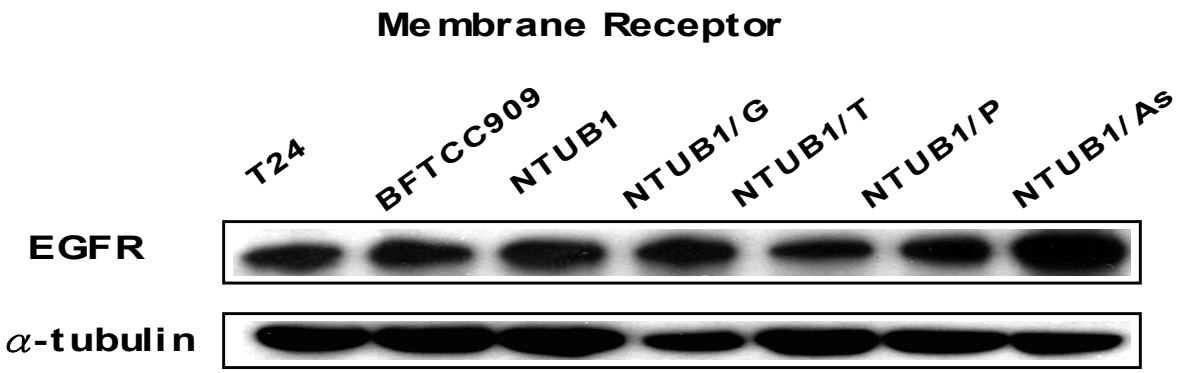

Fig. 21 以 **Western blotting** 分析 **membrane receptor** 在人類泌尿上皮細胞癌之表現量。結果發現具抗藥性之人類泌尿上皮細胞癌 **EGFR** 的蛋白質表現量有些許差異。

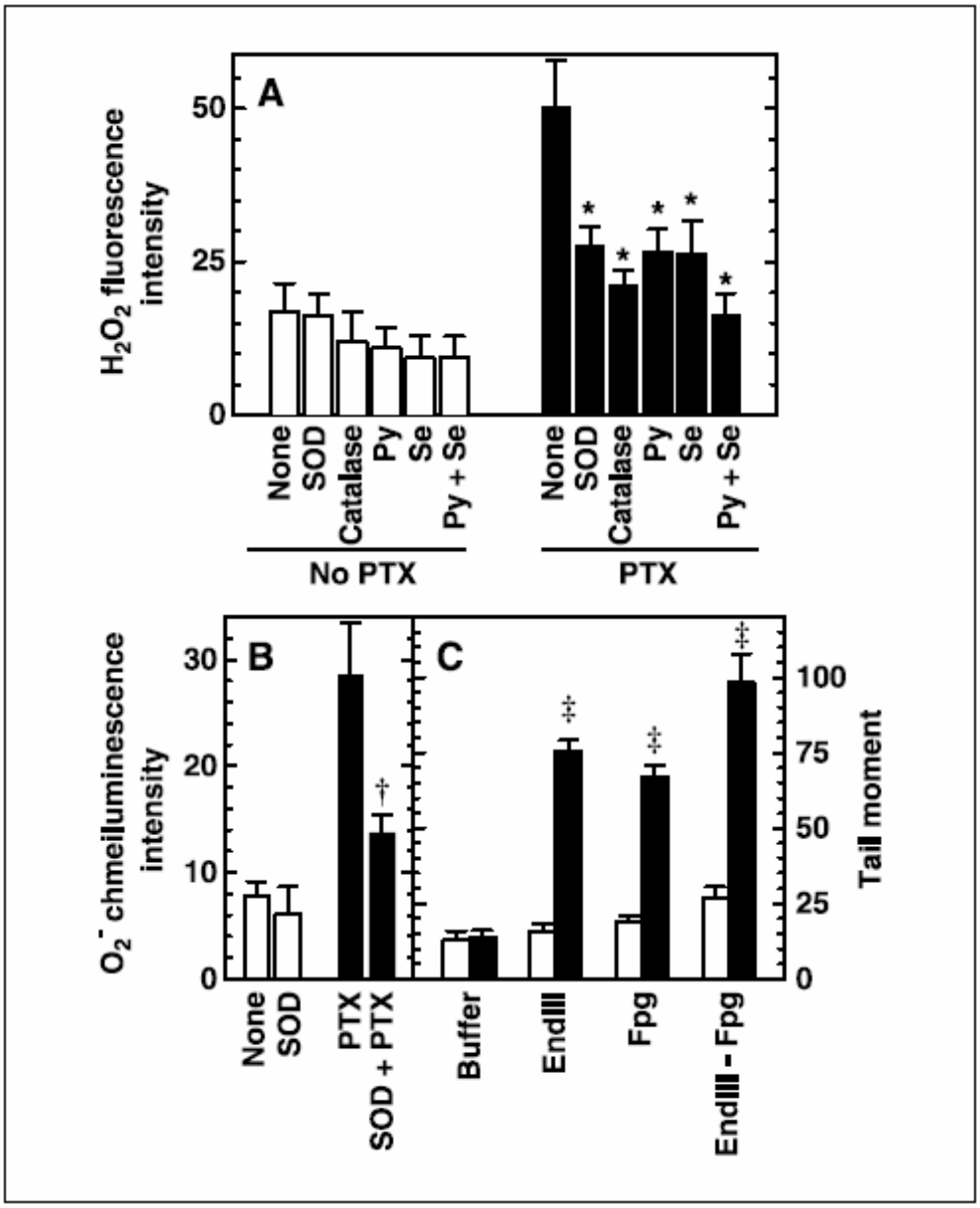

Fig. 22 使用 paclitaxel 處理 T24 細胞造成 ROS 水平的增加及 DNA 氧化傷害

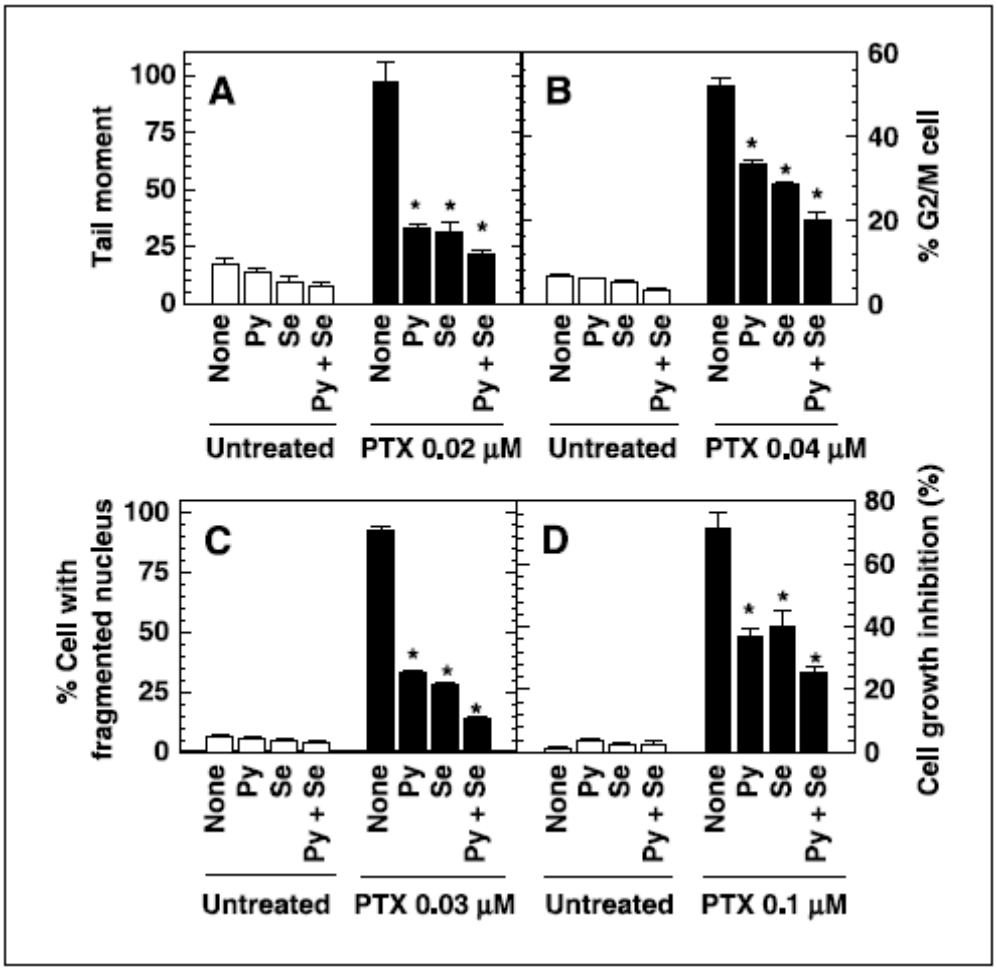

Fig. 23 抗氧化劑, pyruvate 及硒會抑制 paclitaxel 導致特有 DNA 鏈斷裂產生氧化鹼基

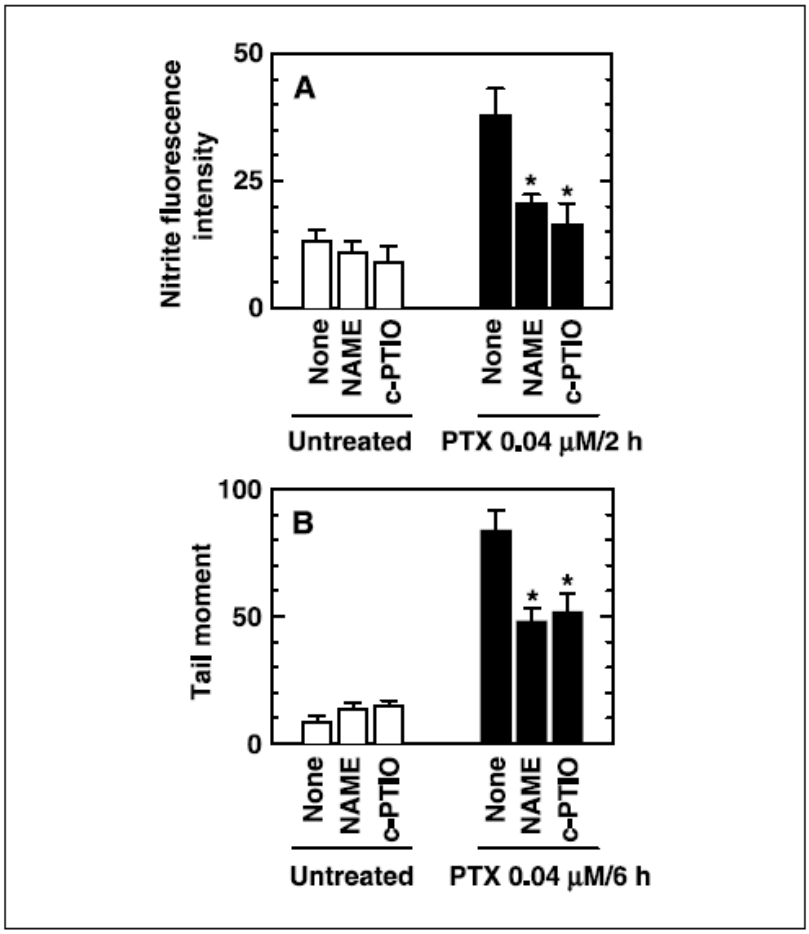

Fig. 24 (A)以 paclitaxel 處理 T24 細胞增加了 NO levels。(B) BNO modulators、NAME 以及 c-PTIO 減少 paclitaxe 誘導 DNA 受損。

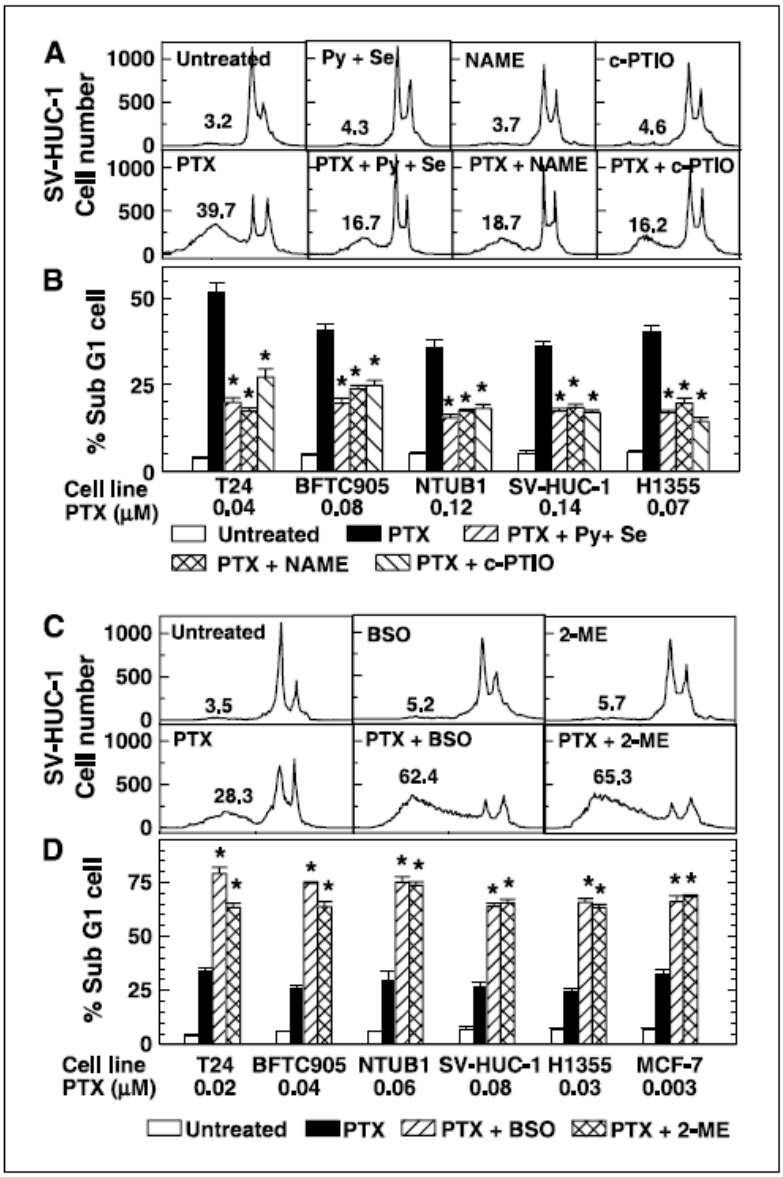

Fig. 25 (A)和(B)，抗氧化劑與 NO 調控物減少 paclitaxel 所誘導的凋亡作用。(C)和(D)，BSO 與 2-ME 增加細胞凋亡，以藥物處理細胞 48 小時。

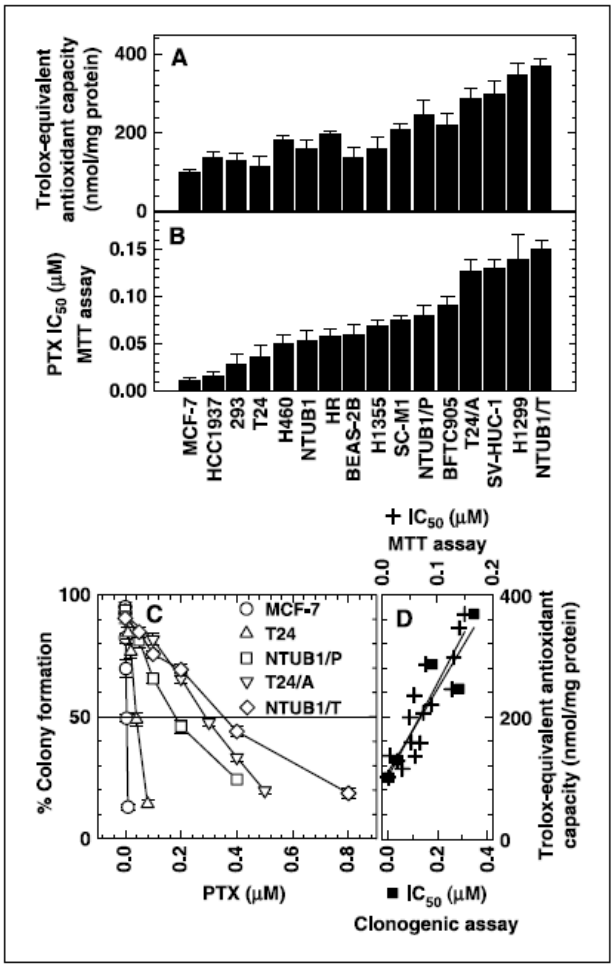

Fig. 26 不同細胞株對 paclitaxel 的抗性與細胞總抗氧化能力的正相關性

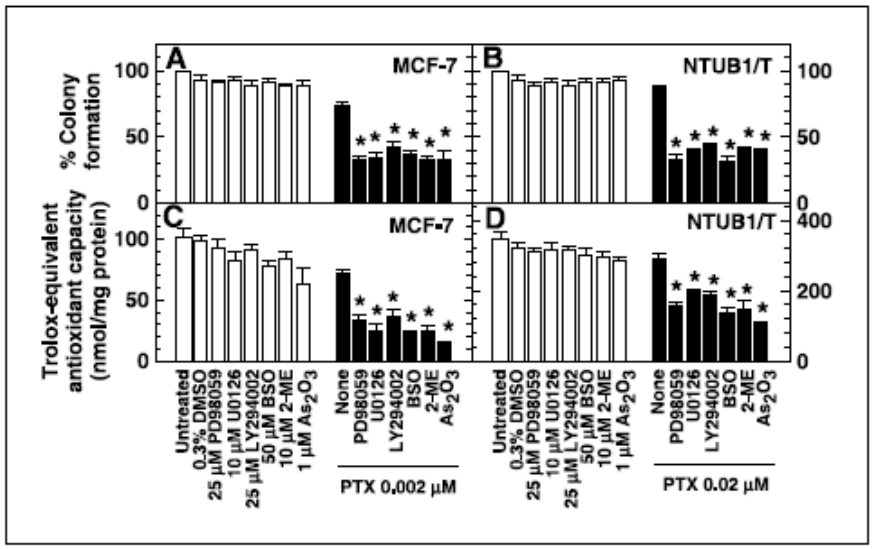

Fig. 27 PD98059、U0126、LY294002、BSO、2-ME以及As_2O_3會降低細胞總抗氧化能力，以及降低經paclitaxel處理過的MCF7(對paclitaxel敏感)和NTUB1/T(對paclitaxel具抗性)細胞的存活率。

Table I: Drug-Selecting Algorithm of Arsenic by microarray analysis

• NTUB1/As compared to NTUB1:

Up-regulated					
	Fold	Gene category	HsID	gene name (revised on Jan.31, 2001)	acc. NO
				HO-1	
Down-regulated					
1614	0.12	Transcriptional factor	Hs.77900	general transcription factor IIB	H23978
1750	0.14		Hs.250811	stathmin 1/oncoprotein 18	
572	0.16	Growth factor or cytokine	Hs.44	pleiotrophin (heparin binding growth factor 8, neurite growth-promoting factor 1)	H84345
1204	0.19		Hs.292378	ESTs, Moderately similar to 810024E cytochrome oxidase III [H.sapiens]	
1555	0.2		Hs.62349	RAB5 interacting protein 2	
1582	0.2		Hs.194478	Homo sapiens, clone IMAGE:3677155, mRNA	
1286	0.21		Hs.182825	ribosomal protein L35	
1273	0.24	Phosphatase	Hs.76780	protein phosphatase 1, regulatory (inhibitor) subunit 1A	AA086411

Table II: Drug-Selecting Algorithm of Cisplatin by microarray analysis

• NTUB1/As compared to NTUB1:

	Fold	Gene category	HsID	gene name (revised on Jan.31, 2001)	acc. NO
Up-regulated					
1987	9.3	Translation	Hs.155558	putative translation initiation factor	N91944
878	4.3	Adhesion & ECM	Hs.87268	annexin A8	H58091
1299	4.1	Kinase & signaling	Hs.256697	histidine triad nucleotide-binding protein	T57556
Down-regulated					
731	0.036	Proteolytic activity	Hs.93002	ubiquitin carrier protein E2-C	T86744
1775	0.08	Growth factor or cytokine	Hs.80976	antigen identified by monoclonal antibody Ki-67	N52414
2011	0.14		Hs.347052	ESTs	
403	0.16	Receptor	Hs.150402	activin A receptor, type I	R45384
101	0.22	Miscellaneous	Hs.118778	ESTs	N93946
1297	0.22		Hs.250895	ribosomal protein L34	
1376	0.24	Kinase & signaling	Hs.78305	RAB2, member RAS oncogene family	N20071
194	0.25		Hs.83135	similar to RIKEN cDNA 2310040G17 gene	
1827	0.25		Hs.241392	small inducible cytokine A5 (RANTES)	

Table III. Drug-Selecting Algorithm of Gemcitabine by microarray analysis

	Fold	Gene category	HsID	gene name (revised on Jan.31, 2001)	acc. NO
Up-regulated					
1256	18.03	Differentiation	Hs.101766	TGF beta receptor associated protein -1	H22171
2011	11.16		Hs.347052	ESTs	
1282	7.13	Kinase & signaling	Hs.78793	protein kinase C, zeta	R27361
1206	6.94	DNA replication and repair	Hs.80409	growth arrest and DNA-damage-inducible, alpha	H24346
1263	6.15	Cell-cycle control	Hs.73986	CDC-like kinase 2	H15069
1693	5.68	unknown	Hs.208286	ESTs	H56611
1473	5.3		Hs.288856	prefoldin 5	
1908	5.24		Hs.180877	H3 histone, family 3B (H3.3B)	
344	4.77		Hs.171723	TAF9-like RNA polymerase II, TATA box binding protein (TBP)-associated factor, 31 kD	
1388	4.17		Hs.278503	regulated in glioma	
786	4.08	Transcriptional factor	Hs.155172	adaptor-related protein complex 3, beta 1 subunit	N23968
Down-regulated					
111	0.21		Hs.348397	phosphatidylinositol glycan, class F	
170	0.23	Transcriptional factor	Hs.306	human immunodeficiency virus type I enhancer-binding protein 1	T80276
1013	0.16	Proteolytic activity	Hs.152978	proteasome (prosome, macropain) activator subunit 3 (PA28 gamma; Ki)	T53317
1190	0.22		Hs.2186	eukaryotic translation elongation factor 1 gamma	

Table IV: Drug-Selecting Algorithm of Doxorubicin by microarray analysis

Up-regulated	Fold	Genbank TCL	Plasmid	Gene category	HsID	gene name (revised on Jan.31, 2001)	acc. NO
Down-regulated							
1969	0.09	05-H11	05-H11				
1809	0.11	07-B11	07-B11		Hs.227059	chloride channel, calcium activated, family member 4	
1762	0.14						
988	0.19	10-G07	10-G07				
1773	0.19	08-H10	08-H10				
28	0.2	07-A09	07-A09		Hs.155560	calnexin	
1643	0.2	M02F06	M02F06	Kinase & signaling	Hs.155609	protein kinase, cAMP-dependent, regulatory, type I, alpha	R43147
1982	0.22	06-F03	06-F03		Hs.18895	tousled-like kinase 1	
1542	0.24	M05H01	M05H01	Stress protein	Hs.111779	secreted protein, acidic, cysteine-rich (osteonectin)	AA021304

Table V: Drug-Selecting Algorithm of Paclitaxel by microarray analysis

Up-regulated	Fold	Genbank TCL	Plasmid	Gene category	HsID	gene name (revised on Jan.31, 2001)	acc. NO
885	4.27	07-G11	07-G11		**Hs.135265**	**Homo sapiens, clone MGC:10965**	
461	4.25	M03A11	M03A11	Kinase & signaling	Hs.79391	huntingtin (Huntington disease)	R38170
502	4.1	11-C03	11-C03				
Down-regulated							
1604	0.12	07-D07	07-D07		**Hs.8858**	**bromodomain adjacent to zinc finger domain, 1A**	
1720	0.15	M05D08	M05D08	DNA replication and repai	Hs.35120	eukaryotic translation initiation factor 4A, isoform 2	H54752
1524	0.17	M03F08	M03F08	Transcriptional factor	Hs.235887	HMT1 (hnRNP methyltransferase, S. cerevisiae)-like 1	R17824
1689	0.17	08-B10	08-B10				
692	0.21	M03A09	M03A09	Kinase & signaling	Hs.198891	serine/threonine-protein kinase PRP4 homolog	R55052
1531	0.21	M01F06	M01F06	House keeping	Hs.8102	ribosomal protein S20	AA147674
1437	0.24	05-H10	05-H10				

Table VI: Drug-Selecting Algorithm of Metotrexate by microarray analysis

Up-regulated	Fold	Genbank TCL	Plasmid	Gene category	HsID	gene name (revised on Jan.31, 2001)	acc. NO
154	7.55	01-C02	01-C02		Hs.3436	CDK2-associated protein 1	
243	4.93	11-A05	11-A05				
337	4.1	09-G12	09-G12				
464	5.07	04-A08	04-A08		Hs.183842	ubiquitin B	
672	4.68						
860	4.48	M04E09	M04E09	Oncogene & suppressor gene	Hs.151134	oxidase (cytochrome c) assembly 1-like	T78436
1008	4.45						
1117	5.31	M06H12	M06H12	Vascular disorder	Hs.82085	serine (or cysteine) proteinase inhibitor, clade E	N28858
1153	4.4	M02D10	M02D10	Oncogene & suppressor gene	Hs.110713	DEK oncogene (DNA binding)	H09636
1301	5.77	M01F11	M01F11	Miscellaneous	Hs.83753	small nuclear ribonucleoprotein polypeptides B and B1	AA126968
1406	4.67	05-F01	05-F01				
1526	4.26	04-F02	04-F02		Hs.1880	hypothetical protein MGC5363	
1562	5.07	02-H03	02-H03		Hs.248549	ESTs	
1587	4.05	M02B06	M02B06	Oncogene & suppressor gene	Hs.50984	sarcoma amplified sequence	T64826
1704	4.76	04-B09	04-B09		Hs.100194	arachidonate 5-lipoxygenase-activating protein	
1789	4.09	04-H12	04-H12			House keeping GAPDH(200X)	
1897	4.51	M04H12	M04H12	Translation	Hs.155558	putative translation initiation factor	N91944

Table VII: Drug-Selecting Algorithm of 5-Fluorouracil by microarray analysis

Up-regulated	Fold	Genbank TCL	Plasmid	Gene category	HsID	gene name (revised on Jan.31, 2001)	acc. NO
13	5.23	11-A10	11-A10		Hs.204038	indolethylamine N-methyltransferase	
Down-regulated							
30	0.14	M01C01	M01C01	Adhesion & ECM	Hs.85266	integrin, beta 4	AA158877
1761	0.24	04-F12	04-F12		Hs.301198	roundabout, axon guidance receptor, homolog 1	

Table VIII: Drug-Selecting Algorithm of Vinblastine by microarray analysis

Up-regulated	Fold	Genbank TCL	Plasmid	Gene category	HsID	gene name (revised on Jan.31, 2001)	acc. NO
885	10.1	07-G11	07-G11		Hs.135265	Homo sapiens, clone MGC:10965 IMAGE:3633884, mRNA, complete cds	
1986	4.58						
Down-regulated							
1474	0.15	M01B03	M01B03	Kinase & signaling	Hs.178695	mitogen-activated protein kinase 13	AA158169
1773	0.16	08-H10	08-H10				
1672	0.19	M02H09	M02H09	Adhesion & ECM	Hs.83968	integrin, beta 2 (antigen CD18 (p95), lymphocyte function-associated antigen 1	H17426
1524	0.19	M03F11				Egr1	X52541

Table IX. Polypeptides deregulated in drug-resistant urothelial cell line

NTUB1/As (0.5 μM) **Up-regulation**

Number	Identity	Molecular mass (KDa)	pI	Function
1	Vinculin splice isoform2	123	5.6	a key element in the transmembrane assemblages that link cells to each other or to the substrate[24]
2	Elongation factor 2	95	6.4	regulate protein synthesis[25]
3	T-complex protein 1, beta subunit	57	6.0	regulated protein folding and functional conformation [26]
4	Alpha enolase	47	7.0	a key glycolytic enzyme[27]
5	Poly (rC)-binding protein 2 (Alpha-CP2)	45	6.3	mediate mRNA stability and down-regulation of translation[28]
6	Annexin A1	38	8.5	regulated phospholipid-binding and membrane-binding proteins[29]
7	Serine/threonine protein Phosphatase PP1-alpha Catalytic subunit	37	5.9	regulation of different signal transduction pathways, cell cycle progression, DNA replication, gene transcription and protein Translation[30]
8	Malate dehydrogenase	36	5.9	catalyze the NAD/NADH-dependent interconversion of the substrates malate and oxaloacetate[31]
9	26S proteasome non-ATPase Regulatory subunit	34	6.1	regulation of activity to the protease[32]
10	Phosphoglycerate mutase 1	28	6.7	a glycolytic enzymes[33]
11	Triosephosphate isomerase	26	6.5	a glycolytic enzyme, which catalyses the interconversion of d-glyceraldehyde 3-phosphate to dihydroxyacetone phosphate (DHAP)[34]
12	Ran GTP-binding protein	24	7.0	regulated cell-cycle[35]
13	40S ribosomal protein S12	14	6.8	regulated posttranscriptional mechanisms[36]

(To be continued)

NTUB1/P (14μM) Up-regulation

Number	Identity	Molecular mass (KDa)	pI	Function
14	Annexin A1	38	8.5	regulated phospholipid-binding and membrane-binding proteins[29]
15	Peroxiredoxin 6	25	6.2	to play a role in the removal of H_2O_2[37]
16	Peroxiredoxin 1	22	8.2	to play a role in the removal of H_2O_2[37]
17	Cofilin	18	8.2	to increase actin dynamics by depolymerizing filaments from their pointed ends[38]
18	Rac GTP binding protein	20	7.0	cell cycle differentiation and regulation of the cytoskeleton

(To be continued)

NTUB1 **Down-regulation**

Number	Identity	Molecular mass (KDa)	pI	Function
18	39S ribosomal protein L46	31	6.5	regulated posttranscriptional mechanisms[36]
19	Proteasome activator	28	5.7	to degrade proteins and regulate the cell cycle, cell growth, and differentiation [39]
20	Glutathione transferase Omega-1	27	6.2	to detoxify drugs[40]
21	Clathrin light chain A	23	4.4	that assembles into a polyhedral cage on the cytosolic side of a membrane so as to form a clathrin-coated pit[41]
22	Peroxiredoxin	22	8.3	to play a role in the removal of H_2O_2[36]
23	Transgelin-2	22	8.4	one of the earliest markers of differentiated smooth muscle [42]
24	Profilin-1	14	8.5	regulated the dynamics of actin polymerization [43]

Related Published Articles:

1. **Urology** (2002) 60(2):346-350**:** Cytotoxicity of arsenic trioxide to transitional carcinoma cells

2. **Anticancer Drug** (2002)13(3):293-300: Arsenic trioxide as a novel anticancer agent against human transitional carcinoma⊥characterizing its apoptotic pathway

3. **Anticancer Drug** (2004) 15, 779-785**:** Characterization of molecular events in a series of bladder urothelial carcinoma cell lines with progressive resistance to arsenic trioxide

4. **Cancer Res** (2005) 65(18):8455-8460**:** Resistance to paclitaxel is proportional to total cellular antioxidation capacity.

5. **Anticancer Res** (2005 Oct. accepted): Expression of molecular markers in arsenic-related bladder urothelial carcinoma: distinction from non-arsenic related BUC in Taiwan

ELSEVIER

CYTOTOXICITY OF ARSENIC TRIOXIDE TO TRANSITIONAL CARCINOMA CELLS

YEONG-SHIAU PU, TZYH-CHYUAN HOUR, JUN CHEN, CHAO-YUAN HUANG, JING-YI GUAN, AND SHIU-HUI LU

ABSTRACT

Objectives. To explore the therapeutic efficacy of arsenic trioxide (As_2O_3) in human transitional cell carcinomas, we investigated the potential use of the compound as a chemotherapeutic agent and the possible cross-resistance with cisplatin in this malignancy.

Methods. Three bladder transitional carcinoma cell lines, NTUB1, NTUB1/P (cisplatin-resistant), and NTUB1/As (As_2O_3-resistant), were used. The chemosensitivity of the three cell lines to cisplatin and As_2O_3 was determined by the microculture tetrazolium assay. The modulatory effect of buthionine sulfoximine (BSO) on As_2O_3 cytotoxicity was studied by combining the two agents simultaneously or sequentially and evaluated using the median-effect analysis. Cellular glutathione contents were determined using a biochemical method.

Results. There was evident cross-resistance between cisplatin and As_2O_3 in the cell model used. BSO significantly enhanced As_2O_3 cytotoxicity in the three cell lines, indicating synergism in combination. In the presence of 3 μM BSO, the sensitivity of NTUB1, NTUB1/P, and NTUB1/As to As_2O_3 was increased 3, 7.4, and 8.4-fold, respectively. Among the three different combination schedules, greater cytotoxic effects were obtained by concurrent exposure to both agents. A significant dose-response relationship was found between the BSO concentrations and glutathione contents in NTUB1 ($P = 0.007$) and NTUB1/As ($P = 0.05$) but not NTUB1/P ($P = 0.1$) cells.

Conclusions. As_2O_3 in the presence of BSO may be an active agent against transitional cell carcinoma. Our results have clinical implications and warrant further investigation. UROLOGY **60:** 346–350, 2002. © 2002, Elsevier Science Inc.

Arsenic is a natural substance that has been used medicinally for centuries. In the 1970s, Thomas Fowler developed "Fowler's solution" (potassium arsenite) for the treatment of a variety of diseases, including asthma, pernicious anemia, and Hodgkin's disease.[1] In 1910, Paul Ehrlich, the founder of chemotherapy, introduced salvarsan, an organic arsenical that could cure syphilis.[1] Recently, arsenic compounds, such as arsenic trioxide (As_2O_3) were used to treat acute promyelocytic leukemia.[2] The mechanism appeared to be associated with the induction of apoptosis and differentiation.[3] Clinically achievable concentrations of As_2O_3 could trigger apoptosis of leukemia[4] and lymphoma[5] cells, as well as some solid tumor cells in vitro, including esophageal cancer,[6] prostate cancer,[7] ovarian cancer,[7] etc. This suggests that As_2O_3-induced apoptosis may be seen in a variety of tumors. However, little is known about the cytotoxic effects of As_2O_3 in human transitional carcinoma cells.

About 30% to 50% of advanced transitional cell carcinomas do not respond to cisplatin-based chemotherapy. Effective salvage regimens for cisplatin-refractory tumors are urgently needed. The interaction or cross-resistance between As_2O_3 and cisplatin has never been reported in transitional cell carcinoma. If As_2O_3 is to be used as a second-line agent, its cross-resistance to cisplatin should be investigated. Data on the cross-resistance be-

This study was supported by National Science Council, Executive Yuan, Republic of China with Grants NSC 89-2314-B-002-153, NSC 89-2314-B-002-572, and NSC 91-2314-B-002-215.

From the Department of Urology, National Taiwan University Hospital and National Taiwan University College of Medicine, Taipei; and Institute of Biochemistry, Kaohsiung Medical University, Kaohsiung, Taiwan, Republic of China

Reprint requests: Yeong-Shiau Pu, M.D., Ph.D., Department of Urology, National Taiwan University Hospital, 7 Chung-Shan South Road, Taipei, Taiwan 100, Taiwan

Submitted: November 20, 2001, accepted (with revisions): March 7, 2002

0090-4295/02/$22.00
PII S0090-4295(02)01699-0

tween the two agents are lacking, except in ovarian and head-and-neck cancers.[8]

It has previously been shown that intracellular glutathione (GSH) content has a decisive effect on As_2O_3-induced apoptosis.[9] Cells of low GSH content are sensitive to As_2O_3 and up-modulation of GSH contents may decrease the sensitivity.[5] It was also demonstrated that buthionine sulfoximine (BSO) may sensitize cells to As_2O_3 by depleting GSH contents.[5] It would be clinically significant if modulators such as BSO are capable of potentiating As_2O_3 cytotoxicity in human transitional cell carcinomas.

On the basis of these facts, we hypothesized that arsenic compounds, typically As_2O_3, can be an effective antitumor agent against human transitional cell carcinoma. This study was designed to explore its potential therapeutic use in this malignancy.

MATERIAL AND METHODS

Cell Lines and Chemicals

Three human bladder transitional carcinoma cell lines were used: NTUB1,[10] NTUB1/P (cisplatin-resistant subline),[11] and NTUB1/As (As_2O_3-resistant subline). NTUB1/P and NTUB1/As were generated by culturing NTUB1 in progressively increased concentrations of cisplatin and As_2O_3, respectively, and could thrive at 14 μM cisplatin and 0.4 μM As_2O_3, respectively. The cisplatin concentration that inhibits 50% (IC_{50}) of NTUB1/P and the As_2O_3 IC_{50} of NTUB1/As was 36.6 μM and 5.0 μM, respectively, 15.3-fold and 4.2-fold higher than those of NTUB1. All cells were maintained in an RPMI-1640 medium (Gibco BRL, Gaithersburg, Md) containing 10% heat-inactivated fetal calf serum (Gibco BRL) at 37°C in humidified air with 5% carbon dioxide.

Cisplatin was obtained as a clinical preparation (Pharmacia & Upjohn, Milan, Italy) and was used after appropriate reconstitution with distilled water. As_2O_3 was purchased from Sigma Chemical (St. Louis, Mo) and dissolved in hot distilled water as a high-concentration stock (20 mM). It was further dissolved in a culture medium immediately before use.

In Vitro Chemosensitivity

In vitro chemosensitivity was assayed with a modified microculture 3-(4,5-dimethylthiazol-2-yl)-2,5-diphenyl tetrazolium (MTT) method to determine cell viability.[12] In brief, 3000 (NTUB1), 9000 (NTUB1/P), or 5000 (NTUB1/As) cells per well in 100 μL culture medium were seeded into 96-well microplates and incubated at 37°C for 24 hours before drug exposure. Plated cell numbers were titrated to keep the control cells growing in the exponential phase throughout the 72-hour incubation period. For one-drug exposures, cells were treated with either graded concentrations of cisplatin or As_2O_3 for 24 hours, washed with the regular medium, and incubated for another 48 hours before using the MTT assay.

The combined effects of As_2O_3 and BSO (Sigma) on the three cell lines were studied using three different schedules to determine whether the combinations were schedule dependent: (a) concurrent incubation with As_2O_3 and BSO for 24 hours; (b) BSO pretreatment for 24 hours followed by 24 hours of As_2O_3; and (c) 24 hours of As_2O_3 followed by 24 hours of BSO. The MTT assay was carried out 72 hours after the first drug exposure. Three separate experiments with triplicate data were done. The IC_{50} of these cells was calculated by the median-effect equation, as previously described.[13]

The combined effects of As_2O_3 and BSO at two combination ratios (1:1 and 1:10) were subjected to the median-effect analysis with the mutually nonexclusive model, as previously described.[14] To generate the combined effects, we first determined the effects of BSO and As_2O_3 alone and then in different combinations. In brief, by combining two agents at graded concentrations, numerous combined effects of growth inhibition were obtained and analyzed using the computer software, Calcusyn (version 1.1.1, 1996, Biosoft, Cambridge, United Kingdom). For each combined dose effect (or fraction affected), a combination index was generated. The effects of the combinations were then transformed into and displayed in fraction affected–combination index plots. A combination index less than 1, equal to 1, and greater than 1 indicated synergism, additivity, and antagonism, respectively. Synergism of two agents indicates a greater positive effect, and antagonism refers to having a less than desired treatment outcome. Different fraction affected levels may have different degrees of synergism or antagonism.

GSH Contents

To determine whether BSO could alter GSH contents, we treated the three cell lines with BSO at 0.1, 3, and 10 μM. Cells were treated with BSO for 24 hours, because we noticed in the combined treatments that 24 hours of BSO treatment had a great impact on As_2O_3 sensitivity. Treated cells (3×10^6) were resuspended in 0.5 mL of 5% metaphosphoric acid and put on ice for 20 minutes. Cells were lysed by three freeze-and-thaw cycles. After centrifugation at 4°C for 20 minutes, the supernatant was collected. GSH contents were determined using the GSH-400 kit (Oxis International, Portland, Ore) according to the instructions of the manufacturer. Fifty microliters of supernatant was incubated with 0.4 mL of the reaction buffer. Then, 25 μL of chromogenic reagent in 0.2 N HCl and 25 μL of 30% NaOH were sequentially added and mixed thoroughly. The mixture was allowed to react in the dark at room temperature for at least 10 minutes. The colorimetric density of the chromogen was determined at 400 nm by a spectrophotometer (DU640i; Beckman, Fullerton, Calif). Three separate experiments were performed.

Statistical Analysis

All symmetric numeric data are presented as the mean ± standard error of the means. The drug IC_{50} between cells and GSH levels of two groups of cells were compared using the Student *t* test. To determine whether BSO could modify the GSH contents in a dose-dependent manner, linear regression analysis was used, with the GSH contents and BSO concentrations (transformed into ordinal variables) the dependent and independent variables, respectively. The regression analysis was carried out using Statistical Analysis System software for an IBM-compatible PC (version 8.0, 2000).

RESULTS

Chemosensitivity Assay

Cross-resistance was evident between cisplatin and As_2O_3 in the cell model used (Table I). The cisplatin IC_{50} of NTUB1/As was significantly higher than that of NTUB1 (1.4-fold, $P = 0.011$), indicating that As_2O_3-resistant cells were cross-resistant to cisplatin. Similarly, the As_2O_3 IC_{50} of NTUB1/P was higher than that of NTUB1 (6.2-fold, $P = 0.0006$), indicating that cisplatin-resistant cells also showed a cross-resistance to As_2O_3.

TABLE I. ***IC_{50} of cisplatin and As_2O_3 in three transitional carcinoma cell lines***

Cell Line	Cisplatin IC_{50} (μM)	As_2O_3 IC_{50} (μM)
NTUB1	2.4 ± 0.27*	1.2 ± 0.19†
NTUB1/P	36.6 ± 2.91	7.4 ± 0.69†
NTUB1/As	3.3 ± 0.65*	5.0 ± 0.53

KEY: IC_{50} = concentration that inhibits 50%; As_2O_3 = Arsenic trioxide.
* P = *0.011.*
† P = *0.0006.*
Data presented as the mean ± standard error of the means.

Of note, the As_2O_3 IC_{50} of NTUB1/P was even higher than that of NTUB1/As.

BSO was nontoxic to the three cell lines at concentrations up to 1000 μM (only 4% of growth inhibition, detailed data not shown). As shown by the median-effect analysis, combinations of As_2O_3 and BSO were grossly synergistic (combination index less than 1) in cell killing ability (Fig. 1). Of the two combination ratios tested, higher synergism was obtained when As_2O_3 and BSO were combined at a ratio of 1:10. In the presence of 3 μM BSO, the sensitivity of NTUB1, NTUB1/P, and NTUB1/As to As_2O_3 increased 3, 7.4, and 8.4-fold, respectively, by the concurrent treatment schedule. It indicates that BSO significantly potentiates As_2O_3 cytotoxicity to the three cell lines. Among the three cell lines, the synergism appeared more profound in the two resistant cell lines than in the sensitive parental cell line (Fig. 1).

Schedule Dependence

Although combinations of BSO and As_2O_3 were grossly synergistic in cytotoxicity, minor differences in the combined effects among different schedules were noticed (Fig. 1). For the two resistant cell lines, explicit synergism was shown in a wide range of fractions affected in all three schedules, except for NTUB1/P cells pretreated with BSO followed by As_2O_3, for which antagonism (combination index greater than 1) was shown in the low fraction affected range (fraction affected less than 0.3). For the parental NTUB1 cells, synergism was seen in all three schedules, except for a small range of fractions affected (less than 0.3 and greater than 0.8) in the two sequential schedules. In general, the concurrent treatment schedule was more effective in cell killing than the two sequential schedules.

Cellular GSH Contents

BSO at 10 μM significantly reduced the GSH contents in NTUB1, NTUB1/P, and NTUB1/As cells by 60%, 36%, and 33% (P = 0.01, 0.005, and 0.05, respectively, Student's t test, Fig. 2). A dose-dependent reduction of GSH contents by BSO was found in NTUB1 and NTUB1/As by regression analysis (P = 0.007 and 0.05, respectively). The trend of GSH reduction in NTUB1/P did not reach statistical significance (P = 0.1).

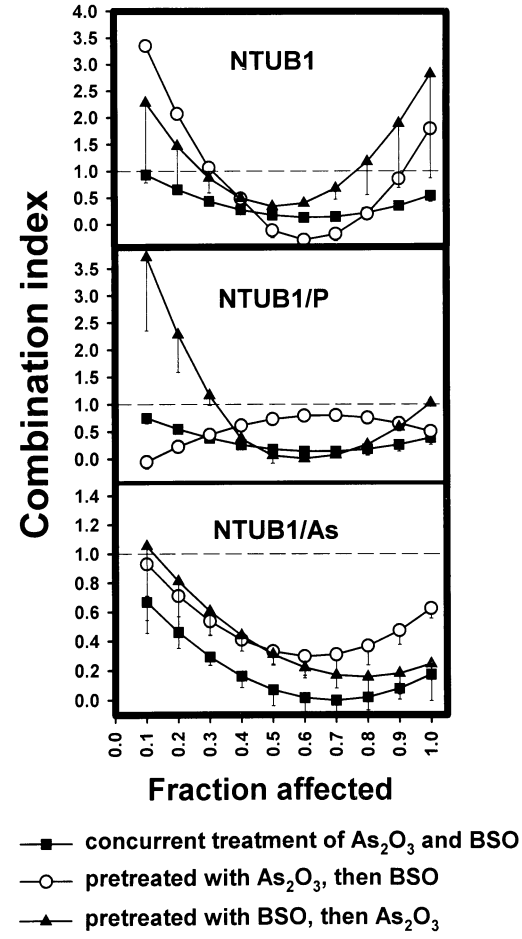

FIGURE 1. *Median-effect analyses of the combination of As_2O_3 and BSO in NTUB1, NTUB1/P, and NTUB1/As cell lines. Data presented as the mean ± SEM of three separate experiments.*

COMMENT

Two facts suggest that transitional cell carcinomas may be sensitive to As_2O_3. First, cells exposed to arsenic compounds in vitro, typically As_2O_3, go through the classic apoptotic pathways that can be found in many tissue systems. We also demonstrated that classic apoptotic events occurred in As_2O_3-treated transitional cell carcinoma cells.[15] Second, among 17 different cancer cell lines, NTUB1 appeared to be one of the most sensitive ones to As_2O_3 in a previous report.[9] It is therefore hypothesized that arsenic compounds may be used as antitumor agents against human transitional cell carcinomas.

In this study, an evident cross-resistance existed between cisplatin and As_2O_3. Although the mech-

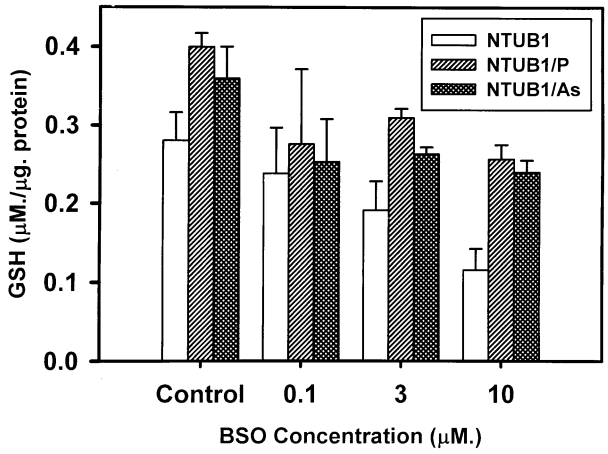

FIGURE 2. *Cellular GSH contents modified by BSO in three transitional carcinoma cell lines. Data presented as the mean ± SEM of three separate experiments. BSO at 10 μM significantly lowered GSH levels of all three cell lines compared with those without any BSO treatment. A significant dose-response relationship was found between BSO concentrations and GSH contents in NTUB1 (P = 0.007) and NTUB1/As (P = 0.05) but not NTUB1/P (P = 0.1) cell lines.*

anisms of cisplatin resistance have been extensively studied,[11] reports on arsenic resistance in transitional cell carcinomas were lacking. Because most first-line chemotherapies for advanced or metastatic transitional cell carcinomas are cisplatin based, the cross-resistance between cisplatin and any second-line agents should be taken into consideration before the initiation of salvage treatments. Cross-resistance between cisplatin and As_2O_3 has been described in ovarian and head-and-neck cancers in vitro.[8] Although the molecular events responsible for the cross-resistance are not clear, several factors may be responsible. The elevation of GSH levels and glutathione S transferase-π (GST-π) activity have been demonstrated in arsenic-resistant Chinese hamster ovary cells.[16] GST-π may catalyze the conjugation of GSH to organic or inorganic arsenic.[17] GSH-arsenic complexes may then be excluded by way of the GSH-conjugate export pump. By using a series of As_2O_3-resistant NTUB1 cells, we have also shown that the chemoresistance of transitional carcinoma cells to As_2O_3 may involve upregulation of the GSH-related detoxification system but not GST-π, upregulation of an reactive oxygen species (ROS)-scavenger (superoxide dismutase [Zn/Cu]), induction of a DNA mismatch repair enzyme (hMSH2), downregulation of nuclear transcription factors (NF-κB, AP-1, and c-Myc), and upregulation of cell cycle regulators (p53 and $p21^{waf1}$) (unpublished data). Among these, the GSH-related detoxification system,[11] ROS-scavengers,[18] DNA mismatch repair machinery,[19] nuclear transcription factors,[20] and cell cycle regulator activity[21] have all been reported to be involved in cisplatin resistance and may be responsible for the cross-resistance.

Among all thiol compounds, GSH is present at a high concentration in cells of nearly all organs. GSH has many physiologic functions, including the defense mechanism against ROS. It was shown that GSH is involved in the disposition of peroxides by cancer cells and in the protection against ROS-generating anticancer drugs.[22] In addition, As_2O_3 selectively induces leukemic cell apoptosis by way of a hydrogen peroxide-dependent pathway.[23] We have also demonstrated that As_2O_3-mediated apoptosis in transitional cell carcinoma is associated with ROS production.[15] However, it was also suggested that disposition of arsenic may be associated with the direct conjugation of GSH to arsenic and exclusion by way of the GSH-conjugate export pump.[17] Therefore, GSH may prevent As_2O_3-induced apoptosis through two pathways: an ROS-dependent scavenging pathway and a direct conjugation of GSH to arsenic.

Although arsenic may very likely act by depleting sulfhydryl groups, other pathways may be involved in the arsenic activity.[24] It has been shown that As_2O_3 is a potent stimulator of AP-1 transcriptional activity and an efficient inducer of c-fos and c-jun gene expressions. In addition, low levels of As_2O_3 can stimulate proliferative signals in primary vascular cells through an arsenic-induced ROS accumulation, subsequent activation of tyrosine phosphorylation, and NF-κB-dependent transcription.[25] The two transcription factors, NF-κB and AP-1, were both found to respond to ROS.[26] In summary, As_2O_3 may act by way of two distinct pathways: (a) induction of phase 2 enzymes, such as GST-π and (b) ROS-dependent activation of NF-κB or AP-1 to regulate cell proliferation.

BSO reduced intracellular GSH levels and potentiated arsenic cytotoxicity in both sensitive and resistant cells. After BSO modulation, the GSH contents of the two resistant cell lines returned to levels similar to that of NTUB1. It seemed that BSO may only be able to deplete the "inducible" portion of GSH that was generated by the resistant cells. It is also possible that higher BSO concentrations (greater than 10 μM) are needed to deplete the GSH contents further. In fact, plasma concentrations of BSO as high as 670 to 7250 μM can be reached after intravenous infusion at 13 g/M^2 that caused patients only mild nausea and vomiting in a clinical study.[27]

CONCLUSIONS

As_2O_3 may serve as an active agent against human transitional cell carcinomas. A cross-resistance between cisplatin and As_2O_3 is present and

should be considered in clinical applications. BSO reduces GSH contents and the As_2O_3 resistance in both sensitive and resistant cells. Our results have clinical implications and warrant further investigation.

REFERENCES

1. Klaassen CD: Heavy metals and heavy-metal antagonists, in Hardman JG, Gilman AG, and Limbird LE (Eds): *Goodman & Gilman's The Pharmacological Basis of Therapeutics.* New York, McGraw-Hill, 1996, pp 1649–1672.
2. Shen ZX, Chen GQ, Ni JH, *et al:* Use of arsenic trioxide (As_2O_3) in the treatment of acute promyelocytic leukemia (APL): II. Clinical efficacy and pharmacokinetics in relapsed patients. Blood **89:** 3354–3360, 1997.
3. Chen GQ, Zhu J, Shi XG, *et al:* In vitro studies on cellular and molecular mechanisms of arsenic trioxide (As_2O_3) in the treatment of acute promyelocytic leukemia: As_2O_3 induces NB4 cell apoptosis with downregulation of Bcl-2 expression and modulation of PML-RAR alpha/PML proteins. Blood **88:** 1052–1061, 1996.
4. Zhu XH, Shen YL, Jing YK, *et al:* Apoptosis and growth inhibition in malignant lymphocytes after treatment with arsenic trioxide at clinically achievable concentrations. J Natl Cancer Inst **91:** 772–778, 1999.
5. Dai J, Weinberg RS, Waxman S, *et al:* Malignant cells can be sensitized to undergo growth inhibition and apoptosis by arsenic trioxide through modulation of the glutathione redox system. Blood **93:** 268–277, 1999.
6. Shen ZY, Tan LJ, Cai WJ, *et al:* Arsenic trioxide induces apoptosis of oesophageal carcinoma in vitro. Int J Mol Med **4:** 33–37, 1999.
7. Uslu R, Sanli UA, Sezgin C, *et al:* Arsenic trioxide-mediated cytotoxicity and apoptosis in prostate and ovarian carcinoma cell lines. Clin Cancer Res **6:** 4957–4964, 2000.
8. Naredi P, Heath DD, Enns RE, *et al:* Cross-resistance between cisplatin, antimony potassium tartrate, and arsenite in human tumor cells. J Clin Invest **95:** 1193–1198, 1995.
9. Yang CH, Kuo ML, Chen JC, *et al:* Arsenic trioxide sensitivity is associated with low level of glutathione in cancer cells. Br J Cancer **81:** 796–799, 1999.
10. Yu HJ, Tsai TC, Hsieh TS, *et al:* Characterization of a newly established human bladder carcinoma cell line, NTUB1. J Formosan Med Assoc **91:** 608–613, 1992.
11. Hour TC, Chen J, Huang CY, *et al:* Characterization of chemoresistance mechanisms in a series of cisplatin-resistant transitional carcinoma cell lines. Anticancer Res **20:** 3221–3225, 2000.
12. Carmichael J, DeGraff WG, Gazdar AF, *et al:* Evaluation of a tetrazolium-based semiautomated colorimetric assay: assessment of chemosensitivity testing. Cancer Res **47:** 936–942, 1987.
13. Chou TC: Derivation and properties of Michaelis-Menten type and Hill type equations for reference ligands. J Theor Biol **59:** 253–276, 1976.
14. Chou TC, and Talalay P: Quantitative analysis of dose-effect relationships: the combined effects of multiple drugs or enzyme inhibitors. Adv Enzyme Regul **22:** 27–55, 1984.
15. Pu, YS, Hour TC, Chen J, *et al:* Arsenic trioxide as a novel anti-cancer agent against human transitional carcinoma-characterizing its apoptotic pathway. Anticancer Drugs **13:** 293–300, 2002.
16. Lee TC, Wei ML, Chang WJ, *et al:* Elevation of glutathione levels and glutathione S-transferase activity in arsenic-resistant Chinese hamster ovary cells. In Vitro Cell Dev Biol **25:** 442–448, 1989.
17. Scott N, Hatlelid KM, MacKenzie NE, *et al:* Reactions of arsenic(III) and arsenic(V) species with glutathione. Chem Res Toxicol **6:** 102–106, 1993.
18. Sasada T, Iwata S, Sato N, *et al:* Redox control of resistance to cis-diamminedichloroplatinum (II) (CDDP): protective effect of human thioredoxin against CDDP-induced cytotoxicity. J Clin Invest **97:** 2268–2276, 1996.
19. Lin X, Ramamurthi K, Mishima M, *et al:* p53 modulates the effect of loss of DNA mismatch repair on the sensitivity of human colon cancer cells to the cytotoxic and mutagenic effects of cisplatin. Cancer Res **61:** 1508–1516, 2001.
20. Maldonado V, Melendez-Zajgla J, and Ortega A: Modulation of NF-kappa B, and Bcl-2 in apoptosis induced by cisplatin in HeLa cells. Mutat Res **381:** 67–75, 1997.
21. Davol PA, Goulette FA, Frackelton ARJ, *et al:* Modulation of p53 expression by human recombinant interferon-alpha2a correlates with abrogation of cisplatin resistance in a human melanoma cell line. Cancer Res **56:** 2522–2526, 1996.
22. Hall AG: Review: the role of glutathione in the regulation of apoptosis. Eur J Clin Invest **29:** 238–245, 1999.
23. Jing Y, Dai J, Chalmers-Redman RM, *et al:* Arsenic trioxide selectively induces acute promyelocytic leukemia cell apoptosis via a hydrogen peroxide-dependent pathway. Blood **94:** 2102–2111, 1999.
24. Muller JM, Rupec RA, and Baeuerle PA: Study of gene regulation by NF-kappa B and AP-1 in response to reactive oxygen intermediates. Methods **11:** 301–312, 1997.
25. Barchowsky A, Roussel RR, Klei LR, *et al:* Low levels of arsenic trioxide stimulate proliferative signals in primary vascular cells without activating stress effector pathways. Toxicol Appl Pharmacol **159:** 65–75, 1999.
26. Cavigelli M, Li WW, Lin A, *et al:* The tumor promoter arsenite stimulates AP-1 activity by inhibiting a JNK phosphatase. EMBO J **15:** 6269–6279, 1996.
27. Bailey HH, Mulcahy RT, Tutsch KD, *et al:* Phase I clinical trial of intravenous L-buthionine sulfoximine and melphalan: an attempt at modulation of glutathione. J Clin Oncol **12:** 194–205, 1994.

Characterization of molecular events in a series of bladder urothelial carcinoma cell lines with progressive resistance to arsenic trioxide

Tzyh-Chyuan Hour[a], Chao-Yuan Huang[b], Chia-Chi Lin[c], Jun Chen[b], Jing-Yi Guan[b], Jen-Mei Lee[a] and Yeong-Shiau Pu[b]

Our previous studies have shown that arsenic trioxide (As_2O_3), a novel anti-cancer agent, may be active against urothelial carcinomas. A series of bladder urothelial carcinoma cells with progressive As_2O_3 resistance were established and studied to reveal molecular events in relation to the mechanisms of resistance to As_2O_3. A sensitive parental line (NTUB1) and three As_2O_3-resistant sublines (NTUB1/As) were used with their IC_{50}s being 0.9, 1.2, 2.5 and 4.9 μM, respectively. Cellular resistance to As_2O_3 was associated with a lowered proliferation profile (increased p53 and p21$^{Waf1/Cip1}$ and decreased c-Myc levels) and a greater resistance to apoptosis (elevated Bcl-2 levels). Cells with a stronger resistance had higher expressions of superoxide dismutase (Cu/Zn) and hMSH2 (but not hMLH1). GSH contents were up-regulated in resistant cells in a dose-dependent manner. The DNA-binding activities of NF-κB and AP-1 were down-regulated in resistant cells in a dose-dependent manner. Profound molecular alterations occur during the acquisition of secondary As_2O_3 resistance. Our *in vitro* cellular model may help to reveal resistance mechanisms to As_2O_3 in bladder urothelial carcinoma cells. *Anti-Cancer Drugs* 15:779–785 © 2004 Lippincott Williams & Wilkins.

Anti-Cancer Drugs 2004, **15**:779–785

Keywords: arsenicals, DNA repair, drug resistance, p53, reactive oxygen species

[a]Institute of Biochemistry, Kaohsiung Medical University, Kaohsiung, Taiwan, ROC, [b]Department of Urology, National Taiwan University College of Medicine, Taipei, Taiwan, ROC and [c]Department of Oncology, National Taiwan University Hospital, Taipei, Taiwan, ROC.

Sponsorship: This work was supported by grants NSC 90-2314-B-002-215, 91-3112-B-002-010 and 92-3112-B-002-024 from the National Science Council, Executive Yuan, Taiwan, ROC.

Correspondence to Y.-S. Pu, Department of Urology, National Taiwan University Hospital, 7 Chung-Shan South Road, Taipei 100, Taiwan, ROC.
Tel: +886 2 23123456 extn 5249; Fax: +886 2 23219145;
e-mail: yspu@ha.mc.ntu.edu.tw

Received 30 March 2004 **Revised form accepted** 9 June 2004

Introduction

Although arsenic compounds are known as poisons, they have also been used medicinally for centuries. In 1970s, Thomas Fowler developed a solution (known as Fowler's solution) of potassium arsenite for the treatment of a variety of diseases including asthma, pernicious anemia, Hodgkin's disease, eczema, pemphigus and psoriasis. In 1910, Paul Ehrlich, a Nobel laureate and a pioneer of chemotherapy, introduced salvarsan, an organic arsenical that could cure syphilis and is still used today to treat trypanosomiasis.

Recently, arsenic compounds, such as arsenic trioxide (As_2O_3) and arsenic disulfide, have been used to treat acute promyelocytic leukemia (APL) [1]. The mechanisms of action were shown to be associated with the induction of apoptosis and differentiation [2]. *In vitro* studies revealed that clinically achievable concentrations of As_2O_3 could trigger apoptosis of leukemia [3] and lymphoma [4] cells as well as some solid tumor cells, including those from esophageal cancer [5], prostate cancer [6] and ovarian cancer, etc [6]. This suggests that As_2O_3 may be active against a wide variety of human tumors.

Cell line models that are selected to be secondarily resistant to anti-tumor agents can provide valuable information as to how cells survive toxic environments. Although As_2O_3 has been used in preclinical or clinical settings to treat human cancers, the mechanisms of chemoresistance are not completely understood. Most of the knowledge about arsenic resistance was obtained from a non-cancer models, including those of trypanosoma [7], Chinese hamster ovary cells [8] and human fibroblast cells [9]. The mechanisms of arsenic resistance in human cancer cells have been much less explored. Although it has been suggested that human cells relatively lack the inducible tolerance to arsenite seen in hamster cells [8], we have succeeded in establishing a series of bladder urothelial carcinoma cells that harbor progressive resistance to As_2O_3. These cells are, to our knowledge, the first series of urothelial carcinoma cells that have been selected for resistance to As_2O_3. This is also the first report characterizing the molecular alterations in a series of urothelial carcinoma cells that harbored progressive resistance to As_2O_3. Molecular alterations occurring in these cells may exhibit a dose–response relationship depending on the intensity of arsenic resistance. These cells therefore may represent an

0959-4973 © 2004 Lippincott Williams & Wilkins

excellent cellular model for revealing the arsenic-mediated molecular events and its chemoresistance mechanisms in human cancer cells.

Materials and methods

Cell lines and chemicals

NTUB1 is an immortalized human urothelial carcinoma cell line raised from a high-grade bladder cancer [10]. A series of As_2O_3-resistant sublines were developed by chronically exposing NTUB1 to progressively increased concentrations of As_2O_3 (Sigma, St Louis, MO). Three sublines that can survive at 0.1, 0.2 and 0.4 μM As_2O_3 were used in the study, and were designated as NTUB1/As(0.1), NTUB1/As(0.2) and NTUB1/As(0.4), respectively. All cells were cultured in an RPMI 1640 medium (Gibco/BRL, Gaithersburg, MD) supplemented with 10% heat-inactivated fetal calf serum (Gibco/BRL) at 37°C in humidified air with 5% CO_2.

Chemosensitivity assay

Cellular chemosensitivity to As_2O_3 was studied using a modified MTT (Sigma) assay to determine cell viability *in vitro* [11]. Cells (NTUB1: 4000, NTBU1/As(0.1): 5000, NTUB1/As(0.2): 7000 and NTUB1/P(0.4): 9000 cells/well, respectively) were cultured in 96-well microplates and incubated with graded concentrations of As_2O_3 at 37°C for 72 h. Plated cell numbers were titrated to keep control cells growing in the exponential phase throughout the 72-h incubation period. After exposure for 72 h, 50 μl of MTT (2 mg/ml in RPMI medium) was added to each well and allowed to react for 2.5 h. The blue formazan crystals that formed were pelleted to well bottoms by centrifugation, separated from the supernatant and dissolved in 150 μl of dimethylsulfoxide. The proportion of surviving cells was determined by the absorbance spectrometry at 492 nm using an MRX-2 microplate reader (Dynex, Chantilly, VA). Three independent experiments with triplicate data were performed. The As_2O_3 IC_{50}s of these cells were calculated by the median-effect equation [12] and presented as mean ± SEM.

Cellular growth rate curve

The cellular growth rate curve was also studied using the MTT assay, similar to the chemosensitivity assay using a modified MTT (Sigma) assay to determine cellular growth *in vitro*. The four kinds of cells (5000 cells/well) were cultured in 96-well microplates and incubated with various concentrations of As_2O_3 (0, 0.1, 0.2 and 0.4 μM, respectively) at 37°C for 0, 24, 48, 72 and 96 h, respectively. After exposure for various time course, the following steps were previously described as MTT assay. Three independent experiments with triplicate data were performed and data presented as mean ± SEM.

Western blotting

To dissect the molecular alterations occurring in the series of cells, we studied the protein levels of the three cell cycle regulators (p53, $p21^{Waf1/Cip1}$ and c-Myc), the anti-apoptosis factor (Bcl-2), the reactive oxygen species (ROS) scavenger [superoxide dismutase (Cu/Zn)], and the two DNA mismatch repair enzymes (hMSH2 and hMLH1) by using Western blotting analysis. Cellular protein collected and concentration determinations were carried out as described in a previous study [13]. Cells scraped from a 100-mm Petri dish were resuspended in 100 μl of gold lysis buffer (10% glycerol, 1% Triton X-100, 137 mM NaCl, 10 mM NaF, 1 mM EGTA, 5 mM EDTA, 1 mM sodium pyrophosphate, 20 mM Tris–HCl, pH 7.9, 100 μM β-glycerophosphate, 1 mM sodium orthovanadate, 0.1% SDS, 10 μg/ml aprotinin, 1 mM phenylmethylsulfonyl fluoride and 10 μg/ml leupeptin) and put on ice for 30 min. The lysate was then centrifuged at 18 000 *g* for 30 min at 4°C to collect the supernatant for protein concentration determination with the BCA Protein Assay Reagent (Pierce Life Science, Rockford, IL) and for Western blotting analysis. Briefly, protein extracts (50 μg) were separated on 10% SDS–polyacrylamide gels and transferred to microporous PVDF membranes (Boehringer Mannheim, Mannheim, Germany). After blocking with the TBST buffer (10 mM Tris–HCl, pH 7.5, 100 mM NaCl and 0.1% Tween-20) plus 1% bovine serum albumin, the membranes were incubated with human-specific antibodies at 4°C for 12–18 h against the target proteins. These antibodies were purchased from Santa Cruz Biotechnology, (Santa Cruz, CA; Bcl-2 and p53) and PharMingen [San Diego, CA; $p21^{Waf1/Cip1}$, superoxide dismutase (Cu/Zn) and c-Myc] as monoclonal antibodies, and from Santa Cruz Biotechnology (hMSH2 and hMLH1) as polyclonal antibodies. The membranes were washed 3 times with the TBST buffer (20 min each) and incubated with a horseradish peroxidase-conjugated secondary antibody at room temperature for 1 h. After 3 washes with the TBST buffer, these proteins were detected by Western blotting Luminol reagent (Santa Cruz Biotechnology).

Electrophoretic mobility shift assay (EMSA)

The nuclear DNA-binding activities of the two transcription factors, NF-κB and AP-1, were studied by using EMSA. Nuclear proteins were extracted based on our previously described methods [14] by adding 500 μl of cold hypotonic buffer [20 mM HEPES, pH 7.8, 10 mM KCl, 0.1 mM EDTA, 1 mM dithiothreitol (DTT) and 0.5 mM PMSF] to the cell pellets that were put on ice for 15 min. The mixture was then added to 30 μl of 10% NP-40 and vortexed for 10 s. The mixture was centrifuged at 3000 *g* for 5 min at 4°C to collect the pellets that were then resuspended in 50 μl of cold hypertonic buffer (20 mM HEPES, pH 7.8, 10 mM KCl, 0.1 mM EDTA, 1 mM DTT, 0.5 mM PMSF and 400 mM NaCl) and agitated vigorously at 4°C for 15 min. Cell debris was removed by centrifugation at 3000 *g* at 4°C for 5 min. Binding reactions were performed while on ice for 20 min with 5 μg nuclear protein in 15 μl of 10 mM Tris–HCl

(pH 7.5), 50 mM NaCl, 1 mM EDTA, 10% glycerol, 2 μg poly(dI–dC), 1 mM DTT, 1 mM PMSF and 30 000 c.p.m. ^{32}P-labeled oligonucleotides. DNA–protein complexes were separated from unbound DNA probes on native 6% polyacrylamide gels. Gels were vacuum dried and exposed to Kodak films at –20°C for 16–48 h. The sequences of the NF-κB and AP-1 oligonucleotides were as follows: NF-κB: 5′-AGTTGAGGGGACTTTCC-CAGG-3′; AP-1: 5′-TGACTA-3′.

Cellular glutathione (GSH) content

Cells (3×10^6) were resuspended in 0.5 ml of 5% metaphosphoric acid (Sigma) and put on ice for 20 min. Cells were then lysed by 3 cycles of freeze–thaw. After centrifugation at 4°C for 20 min, the supernatant was collected. Cellular GSH content was determined using the GSH-400 kit (Oxis International, Portland, OR) according to the instructions of the manufacturer [13]. Briefly, 50 μl of supernatant was incubated with 0.4 ml of the reaction buffer (200 mM potassium phosphate, 0.2 mM diethylene-triamine pentaacetic acid and 0.025% lubrol, pH 7.8). Then, 25 μl of chromogenic reagent in 0.2 N HCl and 25 μl of 30% NaOH were sequentially added and mixed thoroughly. The mixture was reacted in the dark at room temperature for at least 10 min. The colorimetric density of the target chromogen was determined by a spectrophotometer (DU640i; Beckman, Fullerton, CA) at 400 nm. Three separate experiments with triplicate data were performed.

Statistical methods

All symmetrical numeric data were presented as mean ± SEM. To determine if higher cellular GSH contents were associated with the stronger As_2O_3 resistance, linear regression analysis was used with the IC_{50}s of the four cell lines, with GSH contents being the independent and dependent variables, respectively. The regression analysis was carried out using SAS software for an IBM-compatible PC (version 8.0, 2000).

Results

IC_{50}s of the series of cell lines

The As_2O_3 IC_{50}s of NTUB1, NTUB1/As(0.1), NTUB1/As(0.2) and NTUB1/As(0.4) were 0.9, 1.2, 2.5 and 4.9 μM, respectively. The IC_{50} of the most resistant subline, NTUB1/As(0.4), is 5.4-fold higher than that of NTUB1 (Fig. 1).

Regulators of cell proliferation and cellular growth rate

As shown in Fig. 2, the p53 and p21$^{Waf1/Cip1}$ protein levels were positively correlated with the As_2O_3 resistance intensity, with an evident dose–response relationship. In sharp contrast, c-Myc levels, the transcription factor that enhances cell proliferation, were down-regulated in the three resistant cells. In accordance with this, the *in vitro* growth rates of the As_2O_3-resistant cells were consistently found to be slower than the parental NTUB1 cells (Fig. 3). It appeared that the proliferation activities of A_2O_3-resistant cells were significantly slowed down compared to the parental NTUB1 cell.

Fig. 1

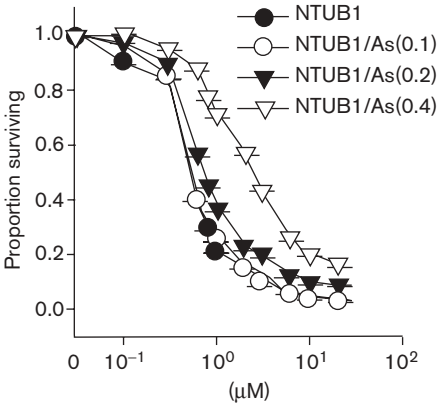

Chemosensitivity assay. Chemosensitivity curves of the four cells to As_2O_3 determined by the MTT assay. The As_2O_3 IC_{50}s of NTUB1, NTUB1/As(0.1), NTUB1/As(0.2) and NTUB1/As(0.4) were 0.9, 1.2, 2.5 and 4.9 μM, respectively, with NTUB1/As(0.4) being 5.4-fold higher than NTUB1. All symmetrical numeric data are presented as mean ± SEM.

Fig. 2

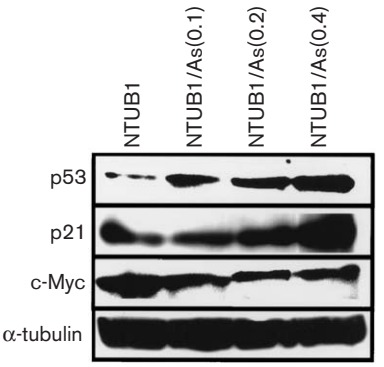

Cell proliferation profiles of the series of As_2O_3-resistant urothelial carcinoma cell lines determined by the Western blotting analysis. The greater the resistance to As_2O_3, the lower the proliferation profile as shown by higher p53 and p21 expressions and lower c-Myc levels. α-Tubulin served as the internal control.

Induction of apoptosis-resistant protein

The protein levels of Bcl-2 were evidently up-regulated in A_2O_3-resistant cells (Fig. 4). However, there was no dose–response relationship between the expression levels and the resistance capacity. This suggests that the resistant cells were more capable of surviving in an unfavorable environment that would normally kill sensitive cells.

Fig. 3

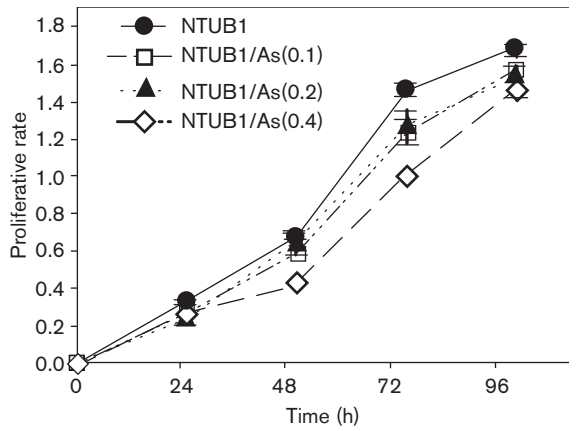

Cellular growth rates. The parental and three As_2O_3-resistant urothelial carcinoma cells were maintained at 0, 0.1, 0.2 and 0.4 μM As_2O_3, respectively. Cellular growth curves of the four cells were determined by the MTT assay. All symmetrical numeric data are presented as mean ± SEM.

Fig. 4

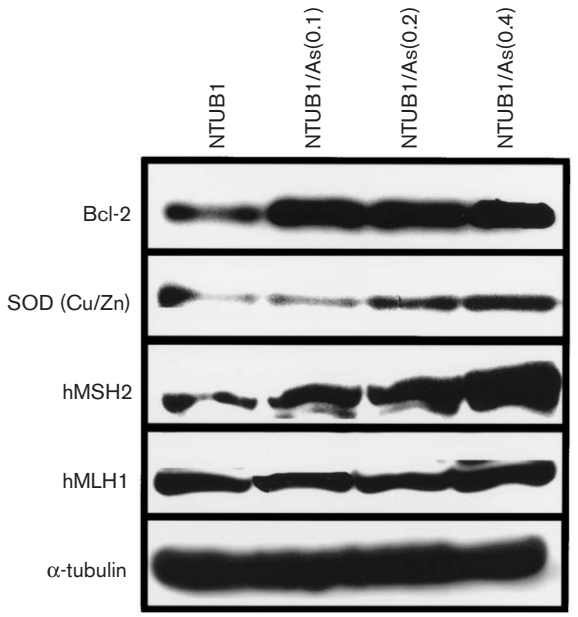

Western blotting of Bcl-2, superoxide dismutase (Cu/Zn) and DNA repair enzymes (hMSH2 and hMLH1) in the series of As_2O_3-resistant urothelial carcinoma cells. Cells with greater resistance had higher levels of Bcl-2, superoxide dismutase (Cu/Zn) and hMSH2, but not hMLH1. α-Tubulin served as the internal control.

Induction of ROS scavenger and DNA repair enzymes

The protein levels of superoxide dismutase (Cu/Zn) were progressively increased in the three resistant cell lines (Fig. 4). Similarly, the DNA mismatch repair enzyme, hMSH2 (but not hMLH1), was up-regulated in the resistant cells in a dose-dependent manner (Fig. 4). These data imply that cellular resistance to A_2O_3 may involve the up-regulation of cells capability to survive oxidative stress and to fix mismatched DNA structures.

GSH contents

The GSH contents of NTUB1, NTUB1/As(0.1), NTUB1/As(0.2) and NTUB1/As(0.4) were 189.3 ± 7.4, 225.4 ± 9.7, 233.2 ± 9.2, and 260.4 ± 10 μM/μg protein, respectively. The stronger cellular As_2O_3 resistance, the higher GSH contents ($p = 0.0002$, $R^2 = 0.48$). This suggests that cellular resistance to As_2O_3 is associated with increased cellular GSH levels.

Nuclear NF-κB and AP-1 DNA-binding activity

The constitutional nuclear DNA binding activity of both NF-κB and AP-1 were significantly reduced in resistant cells in a dose-dependent manner (Fig. 5). Although the binding activity of NF-κB in NTUB1/As(0.1) remained unchanged as compared to the control NTUB1 cells, it was barely detectable in NTUB1/As(0.2) and nearly absent in NTUB1/As(0.4). Control competition experiments using a 50-fold excess of unlabeled (cold) oligonucleotides can significantly block the binding of the two transcription factors to the respective hot oligonucleotides, which indicates that the binding reactions were specific.

Discussion

This is the first report characterizing the molecular alterations in a series of urothelial carcinoma cells that harbored progressive resistance to a novel cytotoxic agent, As_2O_3. Molecular events occurring in a series of cells may provide valuable information since the dose–response relationship between drug resistance and existing molecular events further substantiates the association between them. In this study, we have shown that cellular resistance to As_2O_3 in urothelial carcinoma cells is associated with the down-regulation of cell proliferation activities, and up-regulation of a wide variety of cellular detoxification machineries that include the cellular GSH, DNA repair and ROS scavenging systems. Dose-dependent suppression of NF-κB and AP-1 activation was also demonstrated in resistant cells.

p53 and $p21^{Waf1/Cip1}$ are known to function as a checkpoint in cell cycle progression. They usually halt progression and drive cells toward apoptosis in cases of unrecoverable DNA damages [15]. In contrast, the c-Myc oncoprotein is associated with uncontrolled cell division [16]. In our results, the p53 and $p21^{Waf1/Cip1}$ proteins were up-regulated, and c-Myc was down-regulated in a dose-dependent manner, which together obviously function to put a brake on cell cycle progression and slow down cell proliferation. In accordance with this, the growth rates of the As_2O_3-resistant cells were consistently found to be

Fig. 5

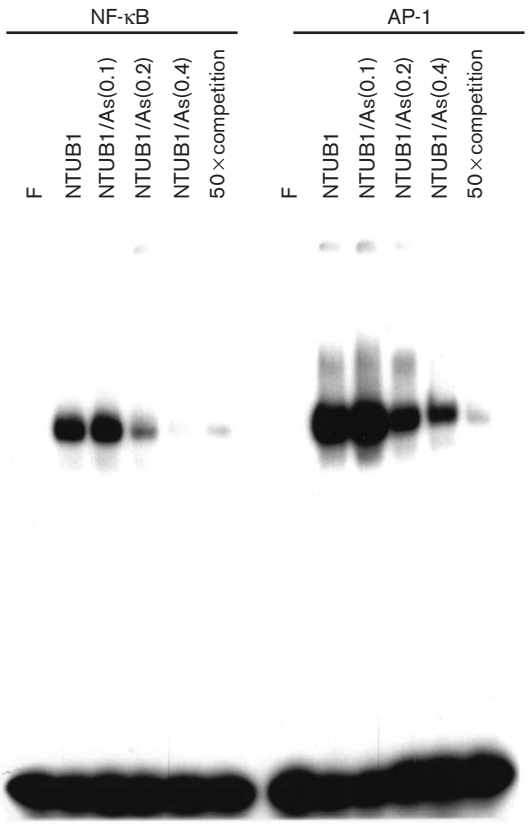

Reduction of NF-κB and AP-1 DNA-binding activity in As_2O_3-resistant urothelial carcinoma cells as determined by EMSAs. The higher the resistance to A_2O_3, the lower the constitutional activity of both NF-κB and AP-1. Control competition experiments using a 50-fold excess of unlabeled (cold) oligonucleotides (× 50 competition) significantly blocked the binding of the two nuclear factors to the respective hot oligonucleotides, indicating specific binding.

slower than the parental NTUB1 cells. The reason why resistant cells had a slower proliferation rate than sensitive cells is not clearly understood. It seems that cells that have to spend the majority of energy to survive in an undesirable toxic environment would have less spare energy for growth and proliferation. In a previous report, we have shown that the expression of *mdr-1*, a membrane-bound energy-dependent efflux pump that is responsible for the phenotype of multiple drug resistance, was seen in 100% of normal urothelial mucosal samples, 70% of clinical urothelial cell tumors, but only 20% of the 10 urothelial carcinoma cell lines [17]. Cultured cancer cells that usually have a higher proliferation rate than tumors and normal tissues may somehow evolve to inactivate various energy-consuming mechanisms, permitting rapid cell growth and proliferation. Conversely, resistant cells that have developed various energy-consuming resistance machineries have to slow down cell growth and proliferation. This may at least in part explain why the As_2O_3 cells had a lowered proliferation profile.

It was shown that As_2O_3 at low doses selectively inhibits growth and induces apoptosis of APL cell line NB4 [2]. The mechanisms of As_2O_3-mediated apoptosis were shown to involve the down-regulation of the Bcl-2 protein [2] and the activation of the ROS-related caspase-3 pathway [18]. The protein levels of Bcl-2 were up-regulated in the three resistant cells, which suggests that cancer cells tend to resist apoptotic stresses by developing a mechanism to survive toxic and lethal environments. In addition, the activated Bcl-2 pathway and its related survival mechanism may help escape from lethal attacks of other cytotoxic agents and thus produce a cross-resistance to agents other than As_2O_3. In a previous report, we first demonstrated that cross-resistance between As_2O_3 and cisplatin may occur in urothelial carcinoma cells [19]. The cross-resistance may arise from the sharing of common resistance mechanisms, such as elevated GSH contents, ROS scavenging capacity and DNA repair capacity [13,20]. This phenomenon should be considered in advance when designing second-line protocols for urothelial carcinomas.

In human cells, five DNA mismatch repair proteins, i.e. hMSH2, hMSH3, hMSH6, hMLH1 and hPMS, have been identified as responsible for the identification and correction of DNA replication errors [21]. Loss of their functions may result in the accumulation of DNA replication errors and mutant phenotypes. In contrast, enhancement of these repair functions may help cells to survive otherwise lethal DNA damage caused by a variety of cytotoxic agents. Previous studies have shown that arsenic compounds may inhibit DNA repair activity and result in DNA damage. Mismatch errors have been identified as a major form of arsenic-mediated DNA insults [22]. In addition to mismatched nucleotides, these repair proteins have been found to recognize specific types of DNA lesions. For example, the complex of hMSH2–hMSH6 may directly recognize cisplatin-induced DNA adducts and facilitate the transcription-coupled DNA repair processes [23]. In fact, it has been shown that As_2O_3-generated ROS could attack DNA and result in the formation of DNA adducts during the carcinogenesis of human skin [24]. In our results, the hMSH2 protein was progressively up-regulated in the three resistant cells, which suggests that As_2O_3-resistant cells manage to up-regulate the DNA mismatch repair machinery which then protects cells from As_2O_3-mediated DNA damage and cell death. These findings imply that hMSH2 is involved in the recognition of As_2O_3-generated DNA adducts and activation of the transcription-coupled repair mechanism in urothelial carcinoma, which is similar to the involvement of hMSH2 in the recognition of cisplatin-mediated DNA adducts.

A previous study showed that the mechanism of self-tolerance to low-dose arsenite in liver epithelial cells was based primarily on reduced cellular disposition of the

metalloid and was not accounted for by changes in levels of GSH or the metalloid [25]. However, we demonstrated that the GSH contents were significantly elevated in As_2O_3-resistant cells in a dose-dependent manner. GSH is the major cellular antioxidant that functions to scavenge free radicals and detoxify cytotoxic substances. In cells of low GSH content, arsenic binds to sulfhydryl group-containing compounds such as GSH. The capacity to eliminate ROS is then decreased, which results in increased oxidative stress and cell death [18]. Except for GSH content, we also showed that the ROS scavenger, superoxide dismutase (Cu/Zn) plays an important role in As_2O_3 resistance. Cells with a higher As_2O_3 resistance were found to have higher levels of superoxide dismutase (Cu/Zn). The above data suggest that the cytotoxic effects and the resistance mechanisms of As_2O_3 are closely related to their cellular abilities to resist oxidative stress. Our recent data have also shown that buthionine sulfoximine may effectively reduce the cellular capacity of anti-oxidation, and restore the sensitivity to both cisplatin and As_2O_3 [19,26].

The constitutional nuclear DNA-binding activities of NF-κB and AP-1 were significantly reduced in resistant cells. Although NF-κB has been implicated in the control of apoptosis and oncogenesis [27], conflicting data exist in relation to the role of NF-κB in programmed cell death. A number of recent studies have shown that NF-κB is an important pro-apoptotic factor for some specific agent-mediated apoptosis [28]. In the progenitor B lymphocytes, inhibition of NF-κB activation delays cytokine withdrawal-induced cell death [29]. However, it was also demonstrated that NF-κB has an anti-apoptotic function in response to tumor necrosis factor-α-induced apoptosis [30]. Therefore, the actual role of NF-κB, as being an anti- or pro-apoptotic protein, may depend on the different responding tissue systems and distinct triggering agents. In our cellular model, it appears that NF-κB is pro-apoptotic so that resistant cells managed to suppress their nuclear DNA-binding activity so as to survive in an unfavorable situation. Interestingly, expression of Fas ligand was found to be regulated by NF-κB and AP-1 [28], which may also suggest that down-regulation of both NF-κB and AP-1 is related to the anti-apoptotic capacity of A_2O_3-resistant cells.

The mechanisms of As_2O_3 resistance in urothelial carcinoma cells involve multiple pathways. Profound molecular events occur during the acquisition of As_2O_3 resistance, including lowered proliferation activity, increased resistance to apoptosis, up-regulated detoxification mechanisms against oxidative stress and elevated DNA mismatch repair functions. Our cellular model may help to reveal molecular events in relation to secondary As_2O_3 resistance in human urothelial carcinomas.

References

1 Shen ZX, Chen GQ, Ni JH, Li XS, Xiong SM, Qiu QY, *et al.* Use of arsenic trioxide (As_2O_3) in the treatment of acute promyelocytic leukemia (APL): II. Clinical efficacy and pharmacokinetics in relapsed patients. *Blood* 1997; **89**:3354–3360.

2 Chen GQ, Zhu J, Shi XG, Ni JH, Zhong HJ, Si GY, *et al. In vitro* studies on cellular and molecular mechanisms of arsenic trioxide (As_2O_3) in the treatment of acute promyelocytic leukemia: As_2O_3 induces NB4 cell apoptosis with downregulation of Bcl-2 expression and modulation of PML-RAR alpha/PML proteins. *Blood* 1996; **88**:1052–1061.

3 Zhu XH, Shen YL, Jing YK, Cai X, Jia PM, Huang Y, *et al.* Apoptosis and growth inhibition in malignant lymphocytes after treatment with arsenic trioxide at clinically achievable concentrations. *J Natl Cancer Inst* 1999; **91**:772–778.

4 Dai J, Weinberg RS, Waxman S, Jing Y. Malignant cells can be sensitized to undergo growth inhibition and apoptosis by arsenic trioxide through modulation of the glutathione redox system. *Blood* 1999; **93**: 268–277.

5 Shen ZY, Tan LJ, Cai WJ, Shen J, Chen C, Tang XM, *et al.* Arsenic trioxide induces apoptosis of oesophageal carcinoma *in vitro*. *Int J Mol Med* 1999; **4**:33–37.

6 Uslu R, Sanli UA, Sezgin C, Karabulut B, Terzioglu E, Omay SB, *et al.* Arsenic trioxide-mediated cytotoxicity and apoptosis in prostate and ovarian carcinoma cell lines. *Clin Cancer Res* 2000; **6**: 4957–4964.

7 Barrett MP, Fairlamb AH. The biochemical basis of arsenical-diamidine crossresistance in African trypanosomes. *Parasitol Today* 1999; **15**: 136–140.

8 Rossman TG, Goncharova EI, Rajah T, Wang Z. Human cells lack the inducible tolerance to arsenite seen in hamster cells. *Mutat Res* 1997; **386**:307–314.

9 Lee TC, Ho IC. Differential cytotoxic effects of arsenic on human and animal cells. *Environ Health Perspect* 1994; **102**(**suppl 3**):101–105.

10 Yu HJ, Tsai TC, Hsieh TS, Chiu TY. Characterization of a newly established human bladder carcinoma cell line, NTUB1. *J Formosan Med Ass* 1992; **91**:608–613.

11 Carmichael J, DeGraff WG, Gazdar AF, Minna JD, Mitchell JB. Evaluation of a tetrazolium-based semiautomated colorimetric assay: assessment of chemosensitivity testing. *Cancer Res* 1987; **47**:936–942.

12 Chou TC. Derivation and properties of Michaelis–Menten type and Hill type equations for reference ligands. *J Theor Biol* 1976; **59**:253–276.

13 Hour TC, Chen J, Huang CY, Guan JY, Lu SH, Hsieh CY, *et al.* Characterization of chemoresistance mechanisms in a series of cisplatin-resistant transitional carcinoma cell lines. *Anticancer Res* 2000; **20**:3221–3225.

14 Hour TC, Chen J, Huang CY, Guan JY, Lu SH, Pu YS. Curcumin enhances cytotoxicity of chemotherapeutic agents in prostate cancer cells by inducing p21(WAF1/CIP1) and C/EBPbeta expressions and suppressing NF-kappaB activation. *Prostate* 2002; **51**:211–218.

15 Divan A, Lawry J, Dunsmore IR, Parsons MA, Royds JA. p53 and p21$^{waf\text{-}1}$ expression correlates with apoptosis or cell survival in poorly differentiated, but not well-differentiated, retinoblastomas. *Cancer Res* 2001; **61**: 3157–3163.

16 Arango D, Corner GA, Wadler S, Catalano PJ, Augenlicht LH. c-*myc*/p53 interaction determines sensitivity of human colon carcinoma cells to 5-fluorouracil *in vitro* and *in vivo*. *Cancer Res* 2001; **61**:4910–4915.

17 Pu YS, Tsai TC, Cheng AL, Tsai CY, Tseng NF, Su IJ, *et al.* Expression of MDR-1 gene in transitional cell carcinoma and its correlation with chemotherapy response. *J Urol* 1996; **156**:271–275.

18 Akao Y, Nakagawa Y, Akiyama K. Arsenic trioxide induces apoptosis in neuroblastoma cell lines through the activation of caspase 3 *in vitro*. *FEBS Lett* 1999; **455**:59–62.

19 Pu YS, Hour TC, Chen J, Huang CY, Guan JY, Lu SH. Cytotoxicity of arsenic trioxide to transitional carcinoma cells. *Urology* 2002; **60**:346–350.

20 Miyajima A, Nakashima J, Yoshioka K, Tachibana M, Tazaki H, Murai M. Role of reactive oxygen species in *cis*-dichlorodiammineplatinum-induced cytotoxicity on bladder cancer cells. *Br J Cancer* 1997; **76**:206–210.

21 Fishel R, Wilson T. MutS homologs in mammalian cells. *Curr Opin Genet Dev* 1997; **7**:105–113.

22 Okui T, Fujiwara Y. Inhibition of human excision DNA repair by inorganic arsenic and the co-mutagenic effect in V79 Chinese hamster cells. *Mutat Res* 1986; **172**:69–76.

23 Mello JA, Acharya S, Fishel R, Essigmann JM. The mismatch-repair protein hMSH2 binds selectively to DNA adducts of the anticancer drug cisplatin. *Chem Biol* 1996; **3**:579–589.

24 Matsui M, Nishigori C, Toyokuni S, Takada J, Akaboshi M, Ishikawa M, et al. The role of oxidative DNA damage in human arsenic carcinogenesis: detection of 8-hydroxy-2′-deoxyguanosine in arsenic-related Bowen's disease. *J Invest Dermatol* 1999; **113**:26–31.
25 Romach EH, Zhao CQ, Del Razo LM, Cebrian ME, Waalkes MP. Studies on the mechanisms of arsenic-induced self tolerance developed in liver epithelial cells through continuous low-level arsenite exposure. *Toxicol Sci* 2000; **54**:500–508.
26 Pu YS, Hour TC, Chen J, Huang CY, Guan JY, Lu SH. Arsenic trioxide as a novel anticancer agent against human transitional carcinoma—characterizing its apoptotic pathway. *Anticancer Drugs* 2002; **13**:293–300.
27 de Martin R, Schmid JA, Hofer-Warbinek R. The NF-kappaB/Rel family of transcription factors in oncogenic transformation and apoptosis. *Mutat Res* 1999; **437**:231–243.
28 Hsu SC, Gavrilin MA, Lee HH, Wu CC, Han SH, Lai MZ. NF-kappa B-dependent Fas ligand expression. *Eur J Immunol* 1999; **29**:2948–2956.
29 Sohur US, Chen CL, Hicks DJ, Yull FE, Kerr LD. Nuclear factor-kappaB/Rel is apoptogenic in cytokine withdrawal-induced programmed cell death. *Cancer Res* 2000; **60**:1202–1205.
30 Zong WX, Edelstein LC, Chen C, Bash J, Gelinas C. The prosurvival Bcl-2 homolog Bfl-1/A1 is a direct transcriptional target of NF-kappaB that blocks TNFalpha-induced apoptosis. *Genes Dev* 1999; **13**:382–387.

Anti-Cancer Drugs 2002, **13,** pp. 293–300

Report

Arsenic trioxide as a novel anticancer agent against human transitional carcinoma—characterizing its apoptotic pathway

Yeong-Shiau Pu,[1] Tzyh-Chyuan Hour,[2] Jun Chen,[1] Chao-Yuan Huang,[1] Jing-Yi Guan[1] and Shiu-Hui Lu[1]

[1]Department of Urology, National Taiwan University Hospital and National Taiwan University College of Medicine, 7 Chung-Shan South Road, Taipei, Taiwan 100, ROC. [2]Institute of Biochemistry, Kaohsiung Medical University, 100 Shih-Chuan 1st Road, Kaohsiung, Taiwan 807, ROC.

Arsenic trioxide (As_2O_3) has been shown to be an active agent against acute promyelocytic leukemia. Little is known about its therapeutic efficacy in human transitional carcinomas. In this study, the arsenic-mediated apoptotic pathway in transitional carcinoma cells was investigated. Three bladder transitional carcinoma cell lines were used, including a parental sensitive line and two resistant daughter lines (cisplatin and As_2O_3 resistant). The As_2O_3-mediated cytotoxicity to the three cell lines was studied *in vitro* in the presence or absence of buthionine sulfoximine (BSO), a chemotherapy modulator. In results, although a lesser extent of apoptosis was seen in cells treated with As_2O_3 alone, more significant apoptotic events were observed in the combined treatment of As_2O_3 and non-toxic concentrations of BSO (up to 10 μM). These included the accumulation of sub-G_1 fractions and internucleosomal DNA breakdown, which were preceded by production of reactive oxygen species, loss of mitochondrial membrane potential and activation of caspase-3. In conclusion, As_2O_3 in the presence of BSO may be an active agent against both chemonaive and cisplatin-resistant transitional carcinomas. The As_2O_3-mediated cytotoxicity appeared to go through the conventional apoptotic pathway. Our results have clinical implications and warrant further investigation. [© 2002 Lippincott Williams & Wilkins.]

Key words: Bladder neoplasms, buthionine sulfoximine, caspases, glutathione, NTUB1 cells, reactive oxygen species.

This study was supported by grant nos NSC 89-2314-B-002-153, NSC 90-2314-B-002-572 and NSC 91-2314-B-002-019 from the National Science Council, Executive Yuan, ROC.

Correspondence to Y-S Pu, Department of Urology, National Taiwan University Hospital, 7 Chung-Shan South Road, Taipei, Taiwan 100, ROC.
Tel: (+886) 2-2312-3456 extn 5249; Fax: (+886) 2-2321-9145; E-mail: yspu@ha.mc.ntu.edu.tw

Introduction

Although arsenic compounds are known as poisons, they have been used in traditional Chinese medicine for centuries. Interestingly, arsenic compounds, such as arsenic trioxide (As_2O_3) and arsenic disulfide, were recently shown to be effective in the treatment of acute promyelocytic leukemia (APL).[1] The mechanisms of action were shown to be associated with the induction of apoptosis and differentiation.[2] Moreover, *in vitro* studies revealed that clinically achievable concentrations of As_2O_3 could trigger apoptosis of leukemia[3] and lymphoma[4] cells as well as some solid tumor cells, including esophageal cancer,[5] neuroblastoma,[6] prostate cancer,[7] ovarian cancer,[7] etc. This suggests that As_2O_3-induced apoptosis may also be seen in a variety of tumor models. Although As_2O_3-mediated apoptosis has been explored in many tissue systems, little is known about the cytotoxic effects of As_2O_3 on human transitional carcinoma cells.

About 30–50% of advanced transitional cell carcinomas do not respond to cisplatin-based chemotherapy. Treatment failure is not uncommon and an effective salvage therapy for patients who failed cisplatin-based regimens is urgently needed. If As_2O_3 is to be used as a second-line agent against transitional carcinoma, apoptosis should be seen in arsenic-treated cisplatin-resistant cells. Data of this kind are also lacking.

We have previously shown that intracellular glutathione (GSH) content has a decisive effect on As_2O_3-induced apoptosis.[8] Cells that have a low GSH

content are highly sensitive to As_2O_3 and experimental up-modulation of GSH content may decrease the sensitivity to As_2O_3.[4] It was also demonstrated that ascorbic acid or buthionine sulfoximine (BSO) may sensitize cells to As_2O_3 by depleting the GSH content.[4] It will be of clinical significance if modulators like BSO are proved capable of potentiating As_2O_3 cytotoxicity in human transitional carcinomas.

This study was therefore designed to explore cytotoxic effects, typically those in the apoptotic pathway, of As_2O_3 on transitional carcinoma cells *in vitro*. By doing this, we hope this study can be of help in substantiating the clinical use of arsenic compounds in the treatment of human transitional carcinoma.

Materials and methods

Cell lines and chemicals

Three bladder transitional carcinoma cell lines were used: NTUB1, NTUB1/P (cisplatin-resistant subline)[9] and NTUB1/As (As_2O_3-resistant subline). NTUB1/P and NTUB1/As were generated by culturing NTUB1 in progressively increasing concentrations of each drug, and could thrive at 14 μM cisplatin and 0.4 μM As_2O_3, respectively. The cisplatin IC_{50} of NTUB1/P and As_2O_3 IC_{50} of NTUB1/As were 36.6 and 5.0 μM, respectively, being 15.3- and 4.2-fold higher than those of NTUB1. All cells were maintained in an RPMI 1640 medium (Gibco/BRL, Gaithersburg, MD) containing 10% heat-inactivated fetal calf serum (Gibco/BRL) at 37°C in humidified air with 5% CO_2. As_2O_3 was purchased from Sigma (St Louis, MO), and was initially dissolved in hot distilled water as a high-concentration stock and then in culture medium immediately before use.

Morphological study and sub-G_1 fraction analysis by DNA flow cytometry

The sub-G_1 fraction represents the proportion of a cell population that is undergoing apoptosis. NTUB1 (8×10^4 cells), NTUB1/P (1.4×10^5 cells) and NTUB1/As (1×10^5 cells) were treated with As_2O_3 at concentrations comparable to their respective IC_{20}s (drug concentrations inhibiting 20% of cell growth) with or without BSO at concentrations of 3 (NTUB1) and 10 (NTUB1/P and NTUB1/As) μM for up to 72 h in six-well plates. The As_2O_3 IC_{20}s for NTUB1, NTUB1/P and NTUB1/As were 0.6, 1 and 3 μM, respectively. Morphological changes were recorded every 12 h for up to 72 h. Cells were then harvested by trypsinization, washed with $1 \times$ PBS, resuspended in 200 μl PBS and fixed in 800 μl of ice-cold 100% ethanol at −20°C. After overnight incubation, the cell pellets were collected by centrifugation, resuspended in 1 ml of the hypotonic buffer (0.1% Triton X-100 and 50 μg/ml RNase A) and incubated at 37°C for 30 min. Then, 1 ml of propidium iodide solution (50 μg/ml) was added and the mixture was allowed to stand on ice for 30 min. The DNA contents of the nuclei were analyzed with a flow cytometer (FACScan; Becton Dickinson, San Jose, CA).

Induction of internucleosomal DNA fragmentation

The three cell lines were cultivated in 10-cm Petri dishes with the same treatment conditions as described in the sub-G_1 experiments, harvested after varied culture intervals (24, 48 and 72 h), resuspended in 100 μl of the lysis buffer (10 mM EDTA, 50 mM Tris–HCl, pH 8.0, 0.5% sarcosyl and 0.5 μg/ml proteinase K) and incubated at 50°C for 3 h. The mixture was then incubated with RNase A (500 μg/ml) at 50°C for 1 h. DNA fragments were extracted with phenol:chloroform:isoamyl alcohol (25:24:1) and the supernatant was collected by centrifugation for 30 min at 14 000 *g*. DNA fragments were separated by electrophoresis in 1.8% agarose gels and stained with ethidium bromide.

Determination of reactive oxygen species (ROS)

Production of ROS has been shown to be a critical step in apoptotic cell death. ROS production was studied by flow cytometric analysis using a non-polar dye, dichlorofluorescein diacetate (DCFH-DA; Molecular Probes, Eugene, OR) that readily diffuses into cells and is hydrolyzed by intracellular esterase to yield DCFH that is then trapped in the cells. Hydrogen peroxide or low-molecular-weight peroxides present in the cells oxidize DCFH to the highly fluorescent compound 2′,7′-dichlorofluorescein (DCF).[10] The fluorescence intensity is proportional to the amount of peroxide present in the cells. By quantifying the intracellular capability to oxidize DCFH and release the fluorescent compound by flow cytometry, we determined the amount of ROS production in As_2O_3-treated cells. The three cell lines were treated with As_2O_3 with or without BSO at concentrations identical to those in the sub-G_1 experiments for different time intervals and incubated with 100 μM DCFH-DA for 1 h. The green fluorescence of intracellular DCF was detected by a

flow cytometer (FACScan) with a 525-nm band pass filter. Fold induction of ROS was determined by the ratio of mean fluorescence intensity of treated cells over that of control cells.

Mitochondrial membrane potential by flow cytometry

Several studies have shown that cellular apoptosis is accompanied by loss of mitochondrial membrane potential following production of ROS.[6] Relative mitochondrial membrane potential was determined by flow cytometric analysis. Briefly, the three cell lines were treated with As_2O_3 with or without BSO at concentrations identical to those in the sub-G_1 experiments for different time intervals and then 40 nM 3,3′-dihexyloxacarbocyanine ($DiOC_6(3)$; Molecular Probes) was added to stain the cells for 15 min at 37°C. $DiOC_6(3)$, a lipophilic cationic fluorescent dye, is known to be able to anchor on the inner surface of the mitochondrial membrane and the amount of dye anchorage is positively proportional to the membrane potential. Loss of the mitochondrial membrane potential is associated with the reduction of dye anchorage and hence the reduction of green fluorescence that can be detected by flow cytometry (FACScan) with a 525-nm band pass filter. The magnitude of reduction of mitochondrial membrane potential was calculated by [1−(mean fluorescence intensity of treated cells/mean fluorescence intensity of control cells)] × 100%.

Caspase-3 activity assay

Apoptotic pathways are drug and cell type-specific and are associated with the activation of specific caspases that lead to cell death. In this study, we examined the role of the caspase-3 activation pathway in As_2O_3-induced apoptosis in the three transitional carcinoma cells. After concurrent treatment with As_2O_3 and BSO at concentrations identical to those in the sub-G_1 experiments for different time intervals, cells were collected, washed with 1 × PBS and resuspended in 25 mM HEPES (pH 7.5), 5 mM $MgCl_2$, 5 mM EDTA, 5 mM dithiothreitol, 2 mM phenylmethlysulfonyl fluoride, 10 μg/ml pepstatin A and 10 μg/ml leupeptin. Concentrations used for each cell were titrated to induce 50% cell death in the chemosensitivity assay. The caspase-3 activity assay was done using the CaspACE Assay System kit (Promega, Madison, WI). Cell lysates were centrifuged at 12 000 r.p.m. for 5 min and aliquots of clear lysate containing 50 μg of protein were incubated with 50 μM acetyl-Asp-Glu-Val-Asp-7-amino-4 methyl coumarin (Ac-DEVD-AMC) as the substrate at 30°C for 1 h. Upon cleavage by activated caspase-3, the substrate releases a yellow-green fluorescent compound, 7-amino-4 methyl coumarin (AMC) which can be detected by a spectrofluorometer (F-4500; Hitachi, Hitachinaka-Shi, Japan) with excitation and emission at 360 and 460 nm, respectively. The amount of fluorescence produced is proportional to the amount of caspase-3 activity present in the sample.[11]

Statistical methods

All symmetrical numeric data were presented as mean ± SEM and compared with the Student's *t*-test.

Results

Morphological study

Cellular death with formation of apoptotic bodies and micronuclei was clearly seen in cells treated with both As_2O_3 and BSO (Figure 1). Those treated with

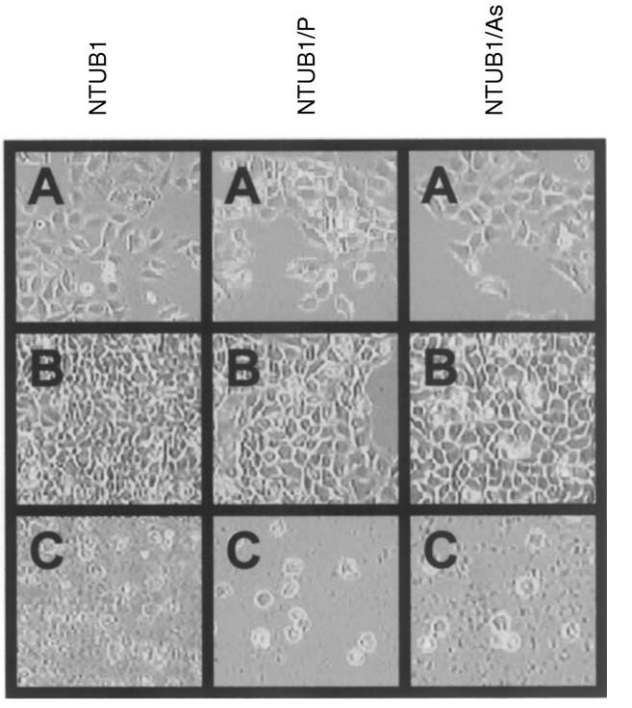

Figure 1. Morphological evaluation of transitional carcinoma cells treated with As_2O_3 and BSO (× 380). (A) Control cells at time 0. (B) Control cells at 72 h without treatment. (C) Treatment with As_2O_3 and BSO for 72 h. Apoptotic bodies and micronuclei can be seen in the combined treatments for all three cell lines.

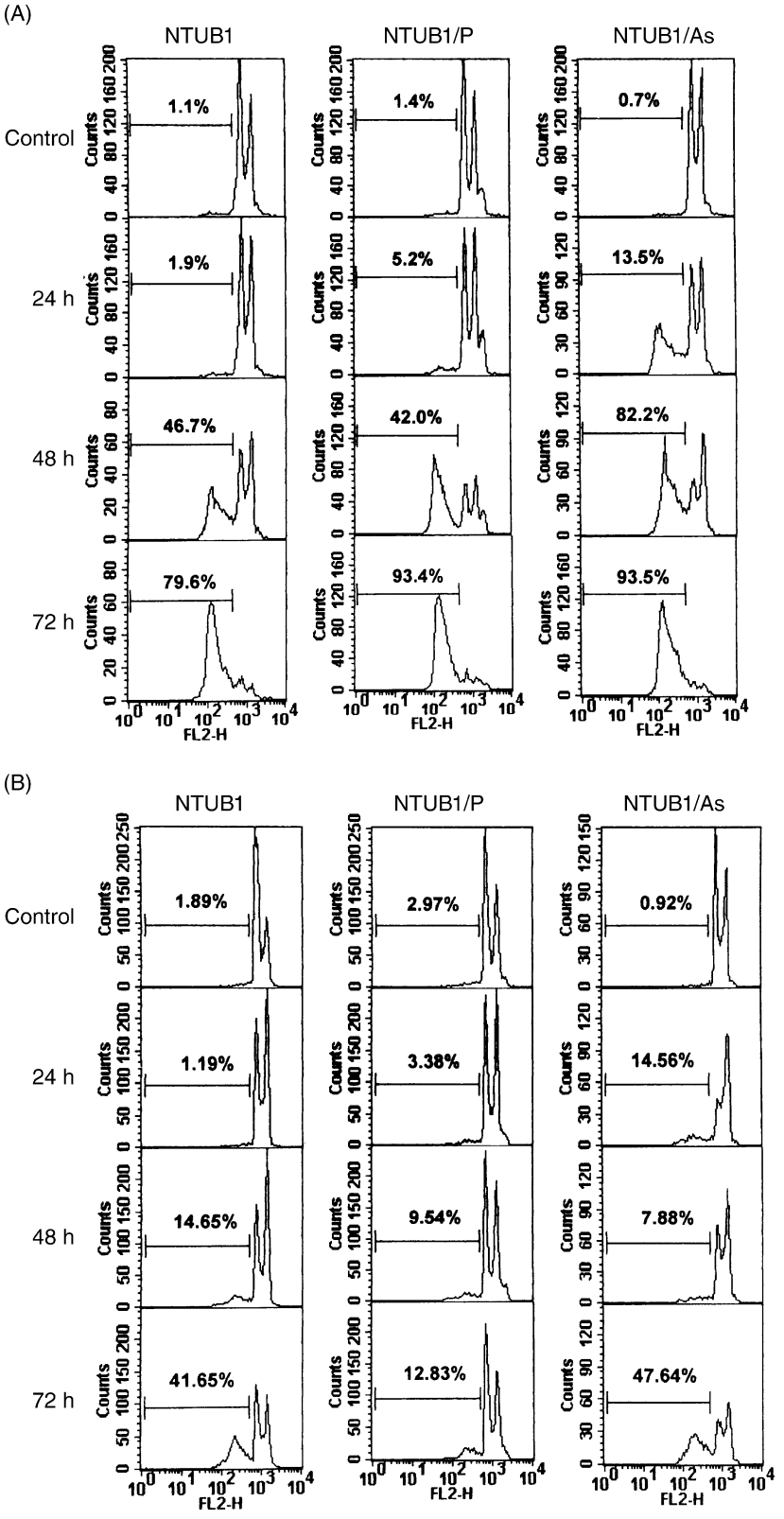

Figure 2. Sub-G_1 fraction analyses of NTUB1, NTUB1/P and NTUB1/As treated with As_2O_3 with (A) or without (B) BSO by using DNA flow cytometry. The sub-G_1 fractions that represent the apoptotic populations (given in percentages) increased dramatically over time in all three cell lines, which indicates that As_2O_3 exerted its toxic effect through the apoptotic pathway. Moreover, treatments with BSO induced more significant apoptosis than those without.

As_2O_3 alone at the respective IC_{20}s showed much less cytotoxicity than the combined treatment. BSO was non-toxic to the three cell lines at concentrations up to 100 μM (data not shown).

Sub-G_1 fraction analysis

With the combination of BSO and As_2O_3, the sub-G_1 fractions in flow cytometric analyses increased dramatically in all three cell lines, which indicates that combined treatments induced significant apoptosis in both the sensitive and resistant cells (Figure 2A). The apoptotic fractions increased over time (from 24 to 72 h) after As_2O_3 exposure. Among the three cell lines, NTUB1/As appeared to be more sensitive to the combined treatments than the others as shown by higher sub-G_1 fractions. In contrast, although evident sub-G_1 fractions were seen in all three cell lines treated with As_2O_3 alone at 72 h, these fractions remained smaller at 48 h of exposure to As_2O_3 alone than the combined treatment (Figure 2B).

Induction of the internucleosomal DNA fragmentation

Combined treatments with As_2O_3 and BSO induced evident apoptosis in the three cell lines as shown by the internucleosomal DNA fragmentation or DNA laddering (Figure 3). Combined treatments (Figure 3A) induced significant DNA fragmentation in NTUB1/As at as early as 24 h and in the other two cells at 48 h. The intensity of the DNA laddering appeared to be much weaker with As_2O_3 alone (Figure 3B) than that with combined treatments at 48 h. At 72 h, significant DNA laddering can also be seen in the three cell lines treated with As_2O_3 alone (data not shown).

Production of ROS and loss of mitochondrial membrane potential

The relative amount of ROS and mitochondrial membrane potential was determined by flow cytometric analysis. While As_2O_3 alone generated only minimal ROS in the three cell lines, the combination of As_2O_3 and BSO induced a significant amount of ROS at as early as 18 h (Figure 4). The ROS inductions by the combined treatments were 3.9-, 17.9- and 2.8-fold higher in NTUB1, NTUB1/P and NTUB1/As, respectively, as compared to the controls.

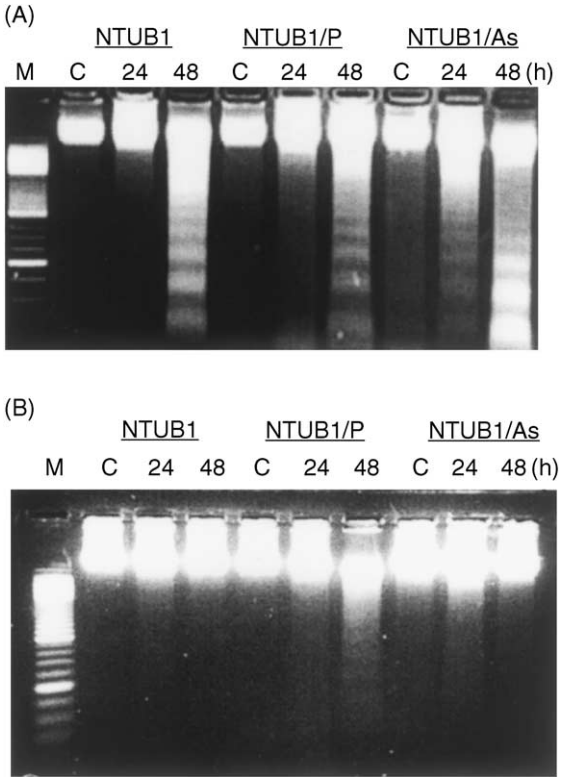

Figure 3. Induction of the internucleosomal DNA fragmentation in transitional carcinoma cells by As_2O_3 with (A) or without (B) BSO. Concurrent treatment of As_2O_3 and BSO for 48 h induced evident apoptotic DNA fragmentation in NTUB1/As at 24 h and in all three cell lines at 48 h, while treatment with As_2O_3 alone brought on only minimal DNA fragmentation. M: marker (at 100 bp increments). C: control.

As_2O_3 alone was able to reduce the mitochondrial membrane potential at 48 h or more of treatment in the two resistant cells. The reduction of the membrane potential was greater with the combination of As_2O_3 and BSO than with As_2O_3 alone. The magnitudes of reduction with the combined treatments were 53, 45 and 49% in NTUB1, NTUB1/P and NTUB1/As, respectively, as compared to 1, 22 and 38%, respectively, with As_2O_3 alone at 48 h (Figure 5).

Cellular caspase-3 activation

In the presence of BSO, As_2O_3 induced significant caspase-3 activation in all three cell lines in a time-dependent manner (Figure 6). At 48 h, the caspase-3 activity was increased 9.7-, 4.4- and 11.8-fold for NTUB1, NTUB1/P and NTUB1/As, respectively, as compared to the controls (all $p < 0.001$). Among the three cell lines, caspase-3 levels were significantly higher in NTUB1/As than in the other two cells after

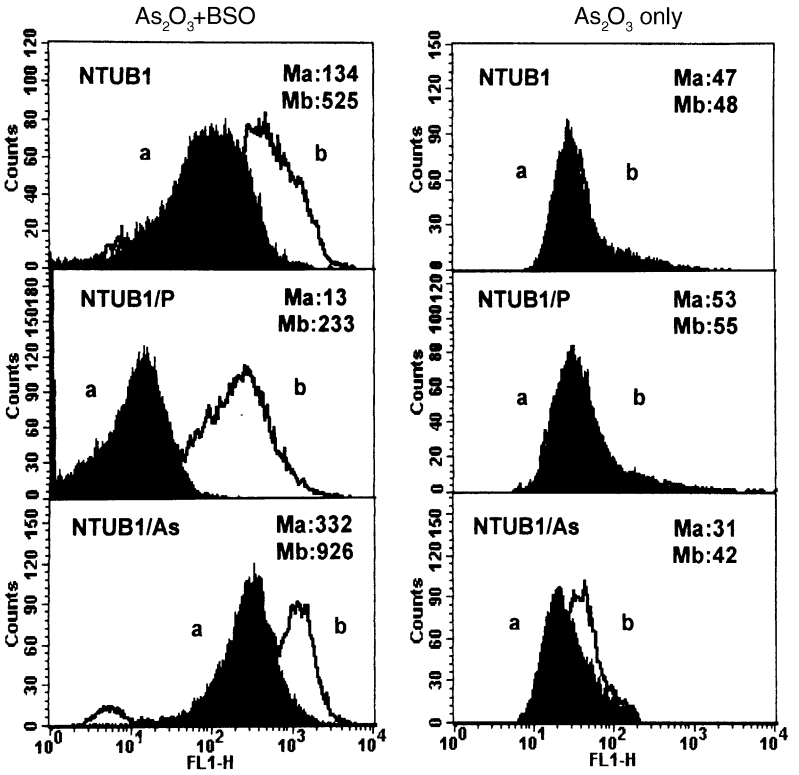

Figure 4. Flow cytometric analyses of relative amounts of ROS induced in three transitional carcinoma cell lines by As_2O_3 with or without BSO. Solid histograms (a) indicate the controls (treatment with drug-free medium for 18 h) and open histograms indicate treatment with As_2O_3 for 18 h. While As_2O_3 alone brought on little ROS induction, combined treatments with As_2O_3 and BSO induced greater amounts of ROS in all three cell lines. Ma and Mb: the mean fluorescence intensity of histograms a and b, respectively.

activation at 24 and 48 h. These data indicate that As_2O_3-mediated apoptosis in the presence of BSO was associated with the activation of the caspase-3 cascade in transitional carcinoma cells.

Discussion

Although arsenic compounds have been applied clinically in the treatment of APL, little is known about its potential use in transitional carcinomas. Cells exposed to arsenic compounds *in vitro*, typically As_2O_3, go through conventional apoptotic pathways that can be found in many tissue systems. Our data showed that As_2O_3 also induced apoptosis in transitional carcinoma cells.

Since most regimens of first-line systemic chemotherapy for advanced or metastatic transitional tumors are cisplatin-based, the possible cross-resistance between cisplatin and any second-line chemotherapeutic agents should be taken into consideration before the initiation of salvage treatment. Our data indicated that As_2O_3, especially in the presence of BSO, showed significant activity against not only sensitive transitional carcinoma cells but also those resistant to cisplatin. Evident apoptotic events can be readily induced in these resistant cells by the combined treatment of As_2O_3 plus BSO. This may warrant further investigations on its role in the salvage therapy for cisplatin-refractory transitional carcinomas.

Accumulating evidence showed that As_2O_3-induced apoptosis involves classical pathways that are associated with ROS inductive signals.[12] In brief, As_2O_3 elicits ROS production, rapid collapse in mitochondrial membrane potential, release of cytochrome *c*, caspase-3 activation, DNA fragmentation and, finally, morphologic evidence of apoptosis. However, in prostate and ovarian cancer cell models, it was shown that As_2O_3-mediated cytotoxicity did not involve superoxide generation.[7] As_2O_3-mediated apoptotic pathways have never been explored in transitional carcinoma before. We have shown that the As_2O_3-induced apoptosis in transitional carcinoma cells also went through the classical pathway as shown by the appearance of the sub-G_1 fraction and

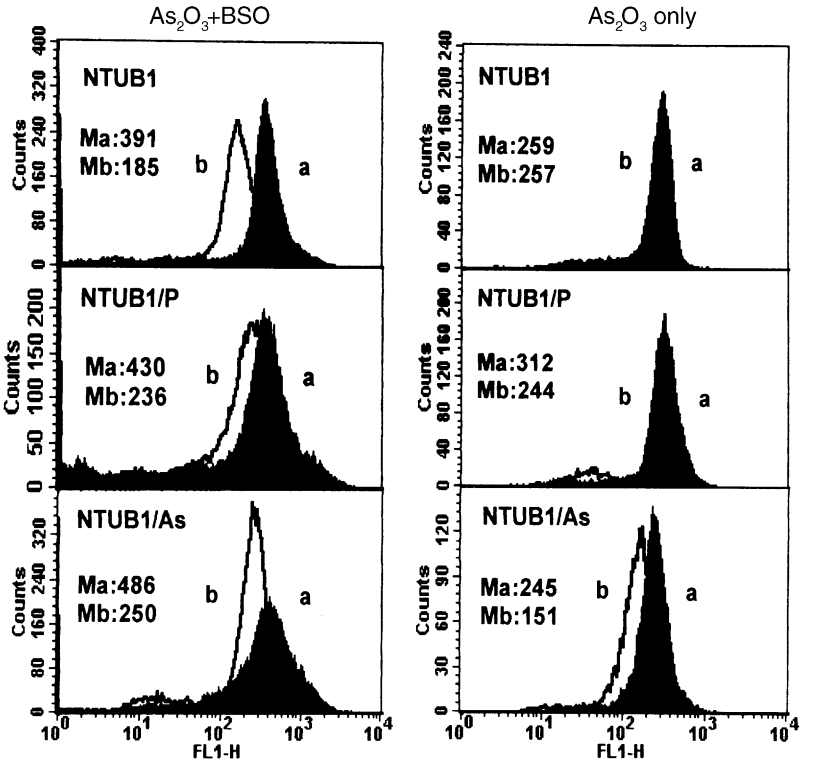

Figure 5. Flow cytometric analyses of relative levels of the mitochondrial membrane potential in three transitional carcinoma cells treated with As_2O_3 with or without BSO. Solid histograms (a) indicate the controls (treatment with drug-free medium for 48 h) while open histograms indicate treatment with As_2O_3 for 48 h. Reduction of the membrane potential was greater with the combined treatments than with As_2O_3 alone. Ma and Mb: the mean fluorescence intensity of the histograms a and b, respectively.

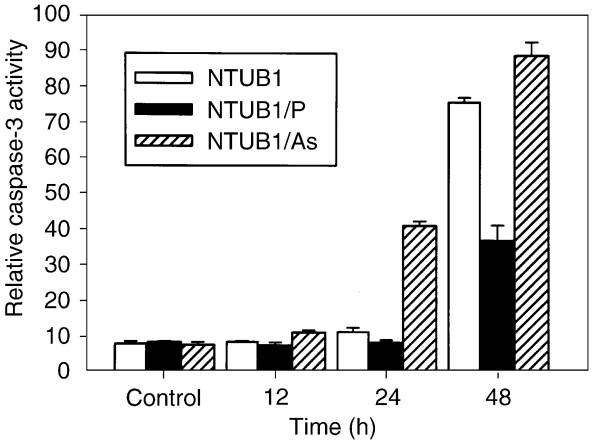

Figure 6. Relative caspase-3 activity induced by As_2O_3 in the presence of BSO. At 48 h, the caspase-3 activity was increased 9.7-, 4.4- and 11.8-fold for NTUB1, NTUB1/P and NTUB1/As, respectively, as compared to the controls (all $p < 0.001$). Data are presented as mean $\pm$ SEM of three separate experiments.

internucleosomal DNA fragmentation upon exposure to As_2O_3. The upstream events included the production of ROS, loss of mitochondrial membrane potential and activation of caspase-3. These events may take place in a sequence as shown here since arsenic-mediated ROS production occurred at as early as 18–24 h, yet the caspase-3 activity was not seen in NTUB1 and NTUB1/P until 48 h, and in NTUB1/As until 24 h after As_2O_3 exposure. The apoptotic events can be demonstrated not only in parental cells, but also in cells that are resistant to cisplatin or arsenic. Of note, cells treated with As_2O_3 and BSO showed a significantly greater extent of apoptosis than those with As_2O_3 alone within the same treatment duration. Since As_2O_3-mediated apoptosis is time dependent, all three cell lines would show evident apoptosis with longer exposure to As_2O_3 alone. We only used one parental cell line in the present study. Additional studies using more transitional carcinoma cell lines are needed to generalize the notion that transitional carcinoma is sensitive to As_2O_3.

In conclusion, As_2O_3 may serve as an active agent against human transitional carcinoma. As_2O_3 exerts its cytotoxic effect via the conventional apoptotic pathway that involves ROS production, loss of mitochondrial membrane potential, activation of

caspase-3 and internucleosomal DNA breakdown. Our results have clinical implications and represent one of the few efforts to substantiate the clinical use of arsenic compounds in the treatment of human transitional carcinomas.

References

1. Shen ZX, Chen GQ, Ni JH, *et al*. Use of arsenic trioxide (As_2O_3) in the treatment of acute promyelocytic leukemia (APL): II. Clinical efficacy and pharmacokinetics in relapsed patients. *Blood* 1997; **89**: 3354–60.
2. Chen GQ, Zhu J, Shi XG, *et al*. *In vitro* studies on cellular and molecular mechanisms of arsenic trioxide (As_2O_3) in the treatment of acute promyelocytic leukemia: As_2O_3 induces NB4 cell apoptosis with downregulation of Bcl-2 expression and modulation of PML-RAR alpha/PML proteins. *Blood* 1996; **88**: 1052–61.
3. Zhu XH, Shen YL, Jing YK, *et al*. Apoptosis and growth inhibition in malignant lymphocytes after treatment with arsenic trioxide at clinically achievable concentrations. *J Natl Cancer Inst* 1999; **91**: 772–8.
4. Dai J, Weinberg RS, Waxman S, Jing Y. Malignant cells can be sensitized to undergo growth inhibition and apoptosis by arsenic trioxide through modulation of the glutathione redox system. *Blood* 1999; **93**: 268–77.
5. Shen ZY, Tan LJ, Cai WJ, *et al*. Arsenic trioxide induces apoptosis of oesophageal carcinoma *in vitro*. *Int J Mol Med* 1999; **4**: 33–7.
6. Akao Y, Nakagawa Y, Akiyama K. Arsenic trioxide induces apoptosis in neuroblastoma cell lines through the activation of caspase 3 *in vitro*. *FEBS Lett* 1999; **455**: 59–62.
7. Uslu R, Sanli UA, Sezgin C, *et al*. Arsenic trioxide-mediated cytotoxicity and apoptosis in prostate and ovarian carcinoma cell lines. *Clin Cancer Res* 2000; **6**: 4957–64.
8. Yang CH, Kuo ML, Chen JC, Chen YC. Arsenic trioxide sensitivity is associated with low level of glutathione in cancer cells. *Br J Cancer* 1999; **81**: 796–9.
9. Hour TC, Chen J, Huang CY, *et al*. Characterization of chemoresistance mechanisms in a series of cisplatin-resistant transitional carcinoma cell lines. *Anticancer Res* 2000; **20**: 3221–5.
10. LeBel CP, Ali SF, McKee M, Bondy SC. Organometal-induced increases in oxygen reactive species: the potential of 2′,7′-dichlorofluorescin diacetate as an index of neurotoxic damage. *Toxicol Appl Pharmacol* 1990; **104**: 17–24.
11. Thornberry NA. Interleukin-1 beta converting enzyme. *Methods Enzymol* 1994; **244**: 615–31.
12. Hei TK, Liu SX, Waldren C. Mutagenicity of arsenic in mammalian cells: role of reactive oxygen species. *Proc Natl Acad Sci USA* 1998; **95**: 8103–7.

(Received 27 November 2001; accepted 10 December 2001)

Resistance to Paclitaxel Is Proportional to Cellular Total Antioxidant Capacity

Balakrishnan Ramanathan,[1] Kun-Yan Jan,[1] Chien-Hung Chen,[1] Tzyh-Chyuan Hour,[3] Hong-Jen Yu,[2] and Yeong-Shiau Pu[2]

[1]Institute of Cellular and Organismic Biology, Academia Sinica; [2]Department of Urology, National Taiwan University College of Medicine, Taipei, Taiwan; and [3]Institute of Biochemistry, Kaohsiung Medical University, Kaohsiung, Taiwan

Abstract

Paclitaxel, one of the most commonly prescribed chemotherapeutic agents, is active against a wide spectrum of human cancer. The mechanism of its cytotoxicity, however, remains controversial. Our results indicate that paclitaxel treatment increases levels of superoxide, hydrogen peroxide, nitric oxide (NO), oxidative DNA adducts, G_2-M arrest, and cells with fragmented nuclei. Antioxidants pyruvate and selenium, the NO synthase inhibitor N^{ω}-nitro-L-arginine methyl ester, and the NO scavenger manganese (III) 2-(4-carboxyphenyl)-4,4,5,5-tetramethyl-imidazoline-1-oxyl-3-oxide all decreased paclitaxel-mediated DNA damage and sub-G_1 cells. In contrast, the glutamylcysteine synthase inhibitor buthionine sulfoximine (BSO) and the superoxide dismutase (SOD) inhibitor 2-methoxyestradiol (2-ME) increased the sub-G_1 fraction in paclitaxel-treated cells. These results suggest that reactive oxygen and nitrogen species are involved in paclitaxel cytotoxicity. This notion is further supported with the observation that concentrations of paclitaxel required to inhibit cell growth by 50% correlate with total antioxidant capacity. Moreover, agents such as arsenic trioxide (As_2O_3), BSO, 2-ME, PD98059, U0126 [mitogen-activated protein/extracellular signal-regulated kinase inhibitors], and LY294002 (phosphatidylinositol 3-kinase/Akt inhibitor), all of which decrease clonogenic survival, also decrease the total antioxidant capacity of paclitaxel-treated cells, regardless whether they are paclitaxel sensitive or paclitaxel resistant. These results suggest that paclitaxel chemosensitivity may be predicted by taking total antioxidant capacity measurements from clinical tumor samples. This, in turn, may then improve treatment outcomes by selecting out potentially responsive patients. (Cancer Res 2005; 65(18): 8455-60)

Introduction

Paclitaxel, originally isolated from *Taxus brevifolia* (pacific yew), is one of the most active chemotherapeutic agents against a wide panel of solid tumors including urothelial, breast, lung, and ovarian cancers (1, 2). The mechanism of paclitaxel cytotoxicity, however, remains controversial. Paclitaxel promotes the stable assembly of microtubules from α- and β-tubulin heterodimers and inhibits their de-polymerization (3). Thus, the antitumor effects of this drug may result from interference with the normal function of microtubules and from blocking of cell cycle progression in late G_2-M phases (4). Paclitaxel-induced apoptosis in hepatoma cells is mediated through G_2-M arrest and DNA fragmentation (5). Cells with a defective G_1 checkpoint and with an increased percentage of G_2-M fractions were found to have increased sensitivity to paclitaxel (6–8). However, the observation that in some cell lines, pulsed paclitaxel exposures causes apoptosis but not G_2-M arrest suggests that paclitaxel-induced apoptosis may occur without a prior G_2-M arrest (9). Moreover, paclitaxel has been shown to induce apoptosis in G_1 and S stages, but induce both apoptosis and necrosis in G_2-M phase (10).

Paclitaxel has been reported to induce the formation of reactive oxygen species (ROS) and alter mitochondrial membrane permeability (11). Reduction of ROS by catalase or ascorbic acid treatment, however, does not correlate with the reduction of cytotoxicity in the human herpes virus 8–related tumor cell line BCBL-1, suggesting that oxidative stress is only partially involved in paclitaxel cytotoxicity (12). Moreover, treatment of the human T-cell lymphoblastic leukemia cell line CCRF-HSB-2 with the antioxidant *N*-acetyl-L-cysteine showed inhibition of paclitaxel-induced ROS production but did not prevent paclitaxel-induced apoptosis, indicating that paclitaxel-induced apoptosis in these cells is ROS independent (13). In murine bladder tumor MBT-2 cells, paclitaxel has also been shown to activate a macrophage-mediated antitumor mechanism through a nitric oxide (NO)–dependent pathway (14). Cotreating the human myeloid leukemia cell line HL-60 with paclitaxel and the NO-generating agent *S*-nitrosoglutathione decreases the accumulation of G_2-M fractions, suggesting that NO prevents paclitaxel-treated cells from entering the G_2-M phase (15).

The current study reveals our investigation into the role(s) of ROS and reactive nitrogen species in paclitaxel toxicity. Results support our hypothesis that ROS and reactive nitrogen species are involved in paclitaxel-induced apoptosis. We further show that in a wide panel of human cancer cell lines, cellular total antioxidant capacity is a critical determinant of cellular sensitivity to paclitaxel.

Materials and Methods

Cells. Cell lines MCF-7 and HCC1937 were cultured in DMEM. H460, H1299, H1355, SC-M1, HR, NTUB1 (16), and BFTC905 (17) were cultured in RPMI 1640. SV-HUC-1, 293, and T24 were cultured in F-12 medium; BEAS-2B was cultured in LHC-9 medium (BioSource International, Inc., Camarillo, CA); T24/A (18) was cultured in RPMI 1640 containing 0.4 μmol/L doxorubicin. NTUB1/P and NTUB1/T were maintained in RPMI 1640 containing 14 μmol/L cisplatin and 5 nmol/L paclitaxel, respectively (19). All growth media were supplemented with 10% FCS, penicillin (100 units/mL), streptomycin (100 μg/mL), and 0.03% glutamine. Cultures were maintained at 37°C in a water-saturated atmosphere containing 5% CO_2.

Requests for reprints: Yeong-Shiau Pu, Department of Urology, National Taiwan University Hospital, 7 Chung-Shan South Road, Taipei, Taiwan. Phone: 886-2-23123456 ext. 5249; Fax: 886-2-23219145; E-mail: yspu@ha.mc.ntu.edu.tw.

doi:10.1158/0008-5472.CAN-05-1162

BEAS-2B is an immortalized human bronchial epithelial cell line and MCF-7 and HCC1937 are breast cancer cell lines. H460, H1299, and H1355 are lung cancer cell lines; SC-M1 and HR are gastric cancer cell lines. The 293 cell line is derived from adenovirus-transformed human embryonic kidney epithelial cells. T24, BFTC905, and NTUB1 are human bladder urothelial carcinoma cell lines; SV-HUC-1 is an SV40 large T–transformed human urothelial cell line; T24/A is a doxorubicin-resistant subline to T24. NTUB1/P and NTUB1/T are cisplatin- and paclitaxel-resistant sublines to NTUB1, respectively.

Measurement of O_2^-, H_2O_2, nitric oxide, and total antioxidant capacity. Superoxide production was measured using the chemiluminescence probe L-012 as previously described (20). Cellular levels of H_2O_2 were measured with the aid of the fluorogenic probe Amplex Red (21). NO production was measured by detecting nitrite released in culture medium using 2,3-diaminonaphthalene (22). For determining cellular total antioxidant capacity, posttreatment cells (1×10^6) were washed with PBS and suspended in 200 μL of ice-cold lysis buffer [10 mmol/L Tris-HCl (pH 7.4), 1 mmol/L EDTA, 0.5 mmol/L phenylmethylsulfonyl fluoride, 0.5 μg/mL leupeptin, 0.5 μg/mL pepstatin] and sonicated for 3 minutes with a 9-second pulse and 1 second off. The lysate was centrifuged at 10,000 rpm for 10 minutes, and protein concentration of the supernatant fraction was determined with a Bio-Rad Protein Assay Kit (Hercules, CA). Bovine serum albumin was used as a standard. The Trolox equivalent antioxidant activity was measured by assessing the ability of hydrogen-donating antioxidants to scavenge the radical cation generated by 2,2′-azinobis(3-ethylbenzothiazoline)-6-sulfonic acid (23).

Measurement of DNA damage. The comet assay, involving an incubation with endonuclease III and formamidopyrimidine-DNA glycosylase, was carried out as described (24). Migration of DNA from the nucleus in each cell was measured with Comet Assay III software.[4]

Measurement of G_2-M and sub-G_1 fractions. Cells seeded for overnight incubation were treated with paclitaxel for 12 hours to measure G_2-M fractions. For sub-G_1 fraction measurements, cells were treated with paclitaxel for 48 hours. The DNA histogram was measured by an EPICS XL-MCL flow cytometer (Beckman-Coulter) with excitation at 488 nm and emission at 620 nm, as previously described (25).

Measurement of nuclear fragmentation. Cells seeded for overnight incubation were treated with paclitaxel for 48 hours. The nuclear integrity of 500 cells was examined for each treatment as previously described (25).

Measurement of cell growth inhibition. The cytotoxic effect of paclitaxel was measured using standard 3-(4,5-dimethylthiazol-2-yl)-2,5-diphenyl tetrazolium bromide (MTT) assay.

Colony formation assay. Cells were seeded into 60 mm Petri dishes and left in the incubator for 6 hours to allow cell attachment. The number of cells seeded per dish was varied so that about 100 colonies were counted after a 12-day incubation period. For each treatment, three dishes of cells were plated. The cells were treated with different drugs, with or without paclitaxel, for 12 days. After 12 days, colonies were fixed for 10 minutes in 100% methanol and stained with a 10% Giemsa solution for 10 minutes. Colonies containing over 50 cells were counted. Percent colony formation was calculated by assigning untreated cultures as 100%. The percent colony formation of treated cells was calculated by using the following formula: percent colony formation of treated cells = (colony formation of treated cells / colony formation of untreated cells) × 100.

Statistical methods. All experiments were done independently at least thrice. The mean of each independent experiment was collected and data are expressed as mean ± SD. Statistical comparisons were made using Student's *t* test. Pearson's correlation tests were carried out to measure the relationship between cellular IC_{50} and total antioxidant capacity. All tests were two sided with $P < 0.001$ as statistically significant.

Results

Paclitaxel induces reactive oxygen species in T24 cells. Treating T24 cells with paclitaxel significantly increased fluorescence intensity of Amplex Red. This effect is reduced by antioxidants, superoxide dismutase (SOD), catalase, pyruvate, and selenium (Fig. 1*A*). These results indicate that paclitaxel treatment increases intracellular H_2O_2 levels. Paclitaxel treatment also increases chemiluminescent intensity of L-012, a probe used for measuring O_2^- (Fig. 1*B*). Production of O_2^- is decreased in the presence of SOD. Treating T24 cells with paclitaxel did not induce any DNA strand break, as analyzed by the standard comet assay. However, large amounts of DNA strand breaks are generated by incubating paclitaxel-treated T24 cells with endonuclease III or formamidopyrimidine-DNA glycosylase because endonuclease III removes oxidized pyrimidines and formamidopyrimidine-DNA glycosylase removes oxidized purines (26). These results suggest paclitaxel induces oxidative DNA damages (Fig. 1*C*). Similarly, the extent of oxidative base–specific DNA strand breaks is significantly reduced in the presence of antioxidants pyruvate and/or selenium (Fig. 2*A*).

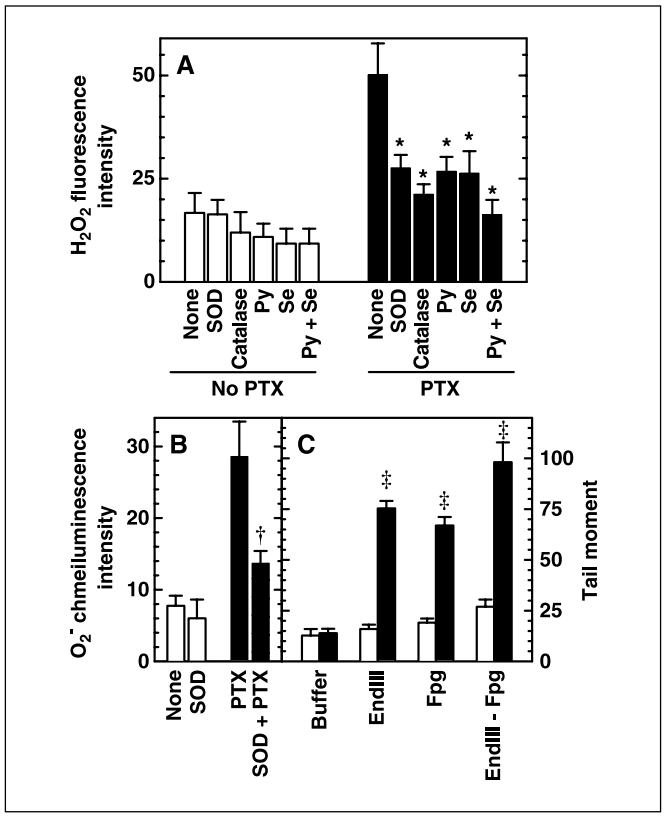

Figure 1. Treatment with paclitaxel increased levels of ROS and oxidative DNA damage in T24 cells. *A,* cells were treated for 2 hours with 100 milliunits SOD, 200 milliunits catalase, 2 μmol/L pyruvate (*Py*), and 2 μmol/L selenium (*Se*) with or without 0.04 μmol/L paclitaxel (*PTX*). Cellular levels of H_2O_2 were measured with the fluorescence probe Amplex Red. *, $P < 0.001$, paclitaxel versus paclitaxel plus antioxidant. *B,* cells were treated for 2 hours with 100 milliunits SOD and/or 0.04 μmol/L paclitaxel. The chemiluminescent intensity of L-012, reflecting the superoxide level, was then measured. †, $P < 0.001$, paclitaxel versus paclitaxel plus SOD. *C,* cells were treated (*solid columns*) or untreated (*open columns*) with 0.02 μmol/L paclitaxel for 6 hours and the level of DNA strand breaks was measured using the comet assay with or without endonuclease III (*EndIII*) and/or formamidopyrimidine-DNA glycosylase (*Fpg*) digestion. ‡, $P < 0.001$, paclitaxel without versus paclitaxel with enzyme digestion. *Columns,* mean of three experiments; *bars,* SD.

Paclitaxel induces G_2-M arrest, nuclear fragmentation, and cell growth inhibition. Paclitaxel treatment induces significant accumulation of cells in the G_2-M phase (Fig. 2*B*), increases the proportion of cells with fragmented nuclei (Fig. 2*C*), and inhibits cell

[4] http://www.perceptive.co.uk.

growth (Fig. 2*D*). All of these paclitaxel-mediated cytotoxic effects are partially suppressed by pyruvate and/or selenium.

Paclitaxel induces nitric oxide production in T24 cells. Treating T24 cells with paclitaxel increased NO production as evidenced by the increase of nitrite levels in the culture medium (Fig. 3*A*). NO production was also suppressed by the NO synthase inhibitor N^{ω}-nitro-L-arginine methyl ester (NAME) and the NO scavenger manganese (III) 2-(4-carboxyphenyl)-4,4,5,5-tetramethyl-imidazoline-1-oxyl-3-oxide (c-PTIO). These NO modulators also partially salvaged the paclitaxel-mediated oxidative DNA damage as shown by the comet assay (Fig. 3*B*).

Antioxidants and nitric oxide modulators suppress paclitaxel toxicity in various cell lines. Results thus far suggest that H_2O_2, O_2^-, and NO may all be involved in paclitaxel-induced cytotoxicity observed in T24 cells. To investigate whether or not this is a cell-specific phenomenon, we next examined the effect of antioxidants (pyruvate plus selenium) and NO modulators (NAME or c-PTIO), using DNA flow cytometry, on paclitaxel-induced sub-G_1 fraction accumulation in cell lines other than T24 cells, including two other human urothelial carcinoma cell lines (BFTC905 and NTUB1), one SV40-transformed human urothelial cell line (SV-HUC-1), one human lung epidermoid carcinoma cell line (H1355), and one human breast cancer cell line (MCF-7; Fig. 4). Results indicate that pyruvate plus selenium, NAME, and c-PTIO significantly decrease paclitaxel-induced sub-G_1 fraction accumulation in these cell types (Fig. 4*A* and *B*). Moreover, blocking glutathione synthesis with buthionine sulfoximine (BSO) or inhibiting SOD activity with 2-methoxyestradiol (2-ME) enhances paclitaxel cytotoxicity as evidenced by a significant enhancement in accumulation of sub-G_1 fractions

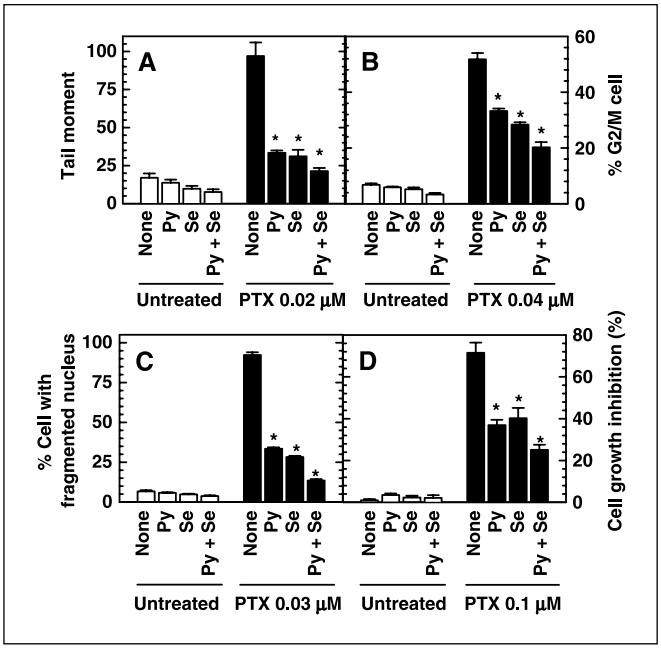

Figure 2. Antioxidants pyruvate and selenium suppressed paclitaxel-induced oxidative base–specific DNA strand breaks (*A*), G_2-M arrest (*B*), nuclear fragmentation (*C*), and cell growth inhibition (*D*) in T24 cells. Cells were treated for 6 hours (*A*), 12 hours (*B*), 48 hours (*C*), or 72 hours (*D*) with paclitaxel alone or in combination with 2 μmol/L pyruvate and/or 2 μmol/L selenium. The use of different concentrations of paclitaxel and different exposure time was intended to show substantial changes in each variable by antioxidants. *, $P < 0.001$, paclitaxel versus paclitaxel plus antioxidant(s). *Columns,* mean of three experiments; *bars,* SD.

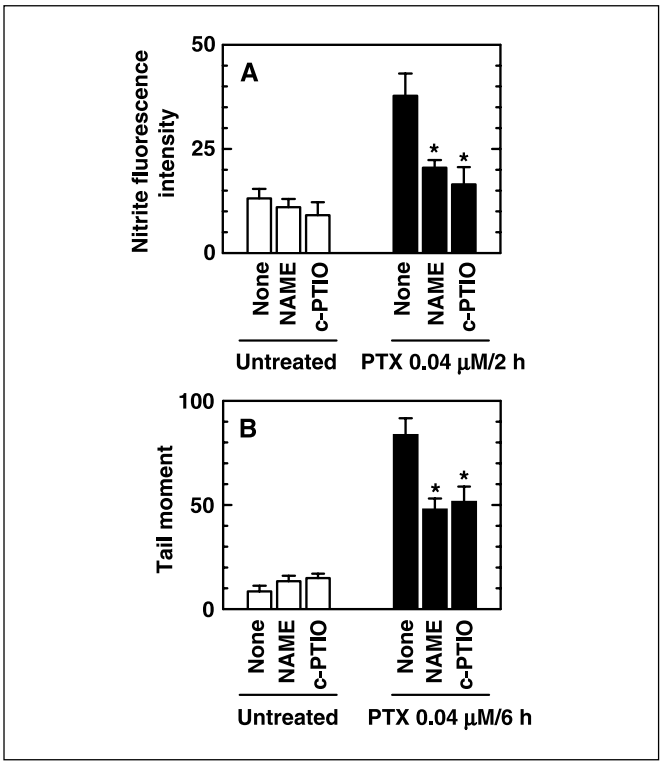

Figure 3. *A,* treatment with paclitaxel increased NO levels in T24 cells. Cells were treated for 2 hours with 100 μmol/L NAME and 100 μmol/L c-PTIO, with or without 0.04 μmol/L paclitaxel. Nitrite fluorescence intensity in the medium was then measured. *B,* NO modulators, NAME, and c-PTIO decreased paclitaxel-induced DNA damage. Cells were treated with NO modulators, with or without paclitaxel, for 6 hours. DNA damage was then measured by the comet assay with nuclear extract incubation. *, $P < 0.001$, paclitaxel versus paclitaxel plus NO modulator.

(Fig. 4*C* and *D*). These data indicate that in a wide spectrum of cell lines, ROS and NO are both involved in paclitaxel-induced cytotoxicity.

Total antioxidant capacity correlates to paclitaxel resistance. Because H_2O_2, O_2^-, and NO were found to be involved in paclitaxel-induced cytotoxicity, we hypothesized that tumor cells with higher total antioxidant capacity would be more resistant to paclitaxel than those with lower total antioxidant capacity. To test this hypothesis, we measured total antioxidant capacity (Fig. 5*A*) and paclitaxel IC_{50} (Fig. 5*B*) of 16 different cell lines. Results showed that total antioxidant capacity had a positive correlation with the paclitaxel IC_{50} measured by the MTT assay (Pearson's correlation coefficient $r = 0.90$, $P < 0.0001$; Fig. 5*D*). We further confirmed these results by next performing a colony formation assay (Fig. 5*D*). Cell lines selected for the colony formation assay included MCF-7 (a highly paclitaxel-sensitive line), T24 (a paclitaxel-sensitive line), T24/A (a doxorubicin-resistant subline to T24), and NTUB1/P and NTUB1/T (cisplatin- and paclitaxel-resistant sublines to NTUB1, respectively). Data from the colony formation assay confirmed our previous results, indicating that total antioxidant capacity correlates very well with the paclitaxel IC_{50} (Pearson's correlation coefficient $r = 0.93$, $P = 0.024$; Fig. 5*D*).

Agents that reduce paclitaxel resistance also decrease total antioxidant capacity. The above results suggest that the higher the paclitaxel IC_{50} of tumor cells, the higher the total antioxidant capacity. We tested this hypothesis by examining whether the

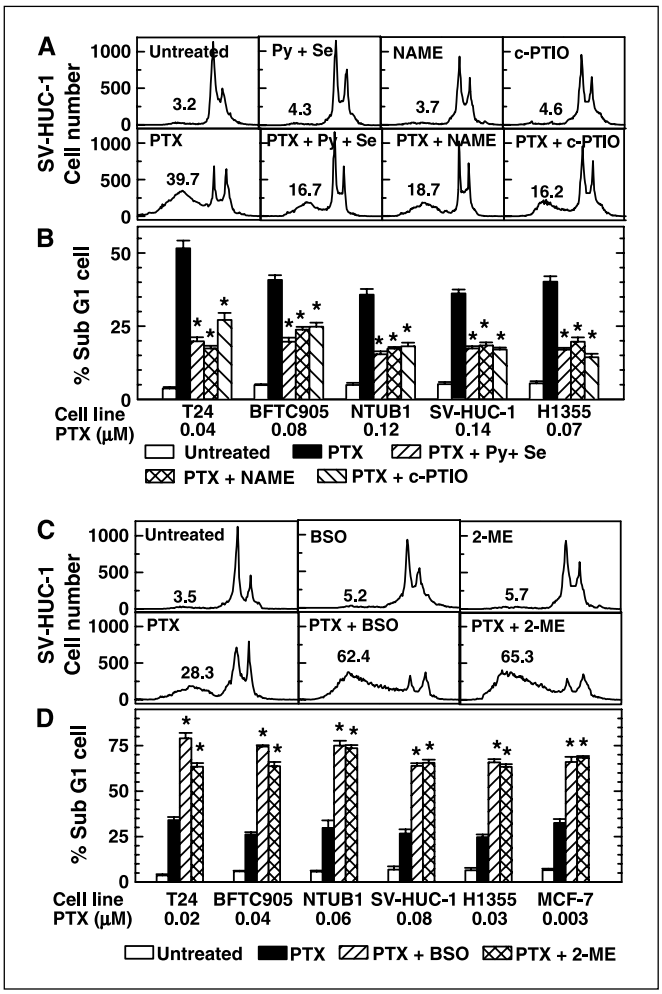

Figure 4. *A* and *B*, antioxidants and nitric oxide modulators decreased paclitaxel-induced apoptosis. *C* and *D*, BSO and 2-ME increased the apoptosis. Cells were treated with drugs for 48 hours. *A* and *C,* the percentage of cells with sub-G_1 DNA content is indicated. *A* and *B,* cells were treated with higher concentrations of paclitaxel than in *C* and *D*. This design was intended to give more room for demonstrating decreasing and increasing effects of the modulators. The sub-G_1 fractions were very low (<6%) in untreated cultures or cells treated with 2 μmol/L pyruvate plus 2 μmol/L selenium, 100 μmol/L NAME, 100 μmol/L c-PTIO, 50 μmol/L BSO, or 10 μmol/L 2-ME. *, $P < 0.001$, paclitaxel alone versus paclitaxel plus modulator.

agents that reduce paclitaxel resistance would also reduce cellular total antioxidant capacity. Results indicate that in MCF-7 (the most sensitive cell line) and NTUB1/T cells (the most resistant cell line), PD98059 [a mitogen-activated protein/extracellular signal-regulated kinase (MEK/ERK) inhibitor], U0126 (a MEK/ERK inhibitor), LY294002 (a phosphatidylinositol 3-kinase/Akt inhibitor), BSO, 2-ME, and As_2O_3 (an ROS-generating agent) all significantly reduce clonogenic survival (Fig. 6*A* and *B*) and decrease total cellular antioxidant capacity (Fig. 6*C* and *D*). Similar results were observed for other cell lines, including T24, T24/A, and NTUB1/P cells (data not shown).

Discussion

In this study, evidence has been collected that supports the notion that paclitaxel may exert its toxicity via elevation of intracellular O_2^-, H_2O_2, and NO levels. This theory is confirmed by our data showing that (*a*) paclitaxel induced the production of O_2^-, H_2O_2 and NO; (*b*) paclitaxel induced oxidative DNA damage; (*c*) agents that decreased H_2O_2 and NO production suppressed paclitaxel-induced DNA damage, G_2-M arrest, apoptosis, and cell growth inhibition; (*d*) inhibition of SOD or glutamylcysteine synthase increased paclitaxel-induced apoptosis; (*e*) cell lines with higher total antioxidant capacity were more resistant to paclitaxel cytotoxicity; and (*f*) agents that decreased clonogenic survival in paclitaxel-treated cells also decreased cellular total antioxidant capacity. Thus, paclitaxel chemoresistance correlates very well to intracellular antioxidant capacity.

Kong et al. (27) speculated that many chemotherapeutic agents exert their toxic effects on cancer cells by producing free radicals, leading to irreversible cell injury, and that overproduction of ROS in cancer cells may exhaust the capacity of SOD and other adaptive antioxidant defenses. This concept is consistent with our results showing that depletion of cellular antioxidant

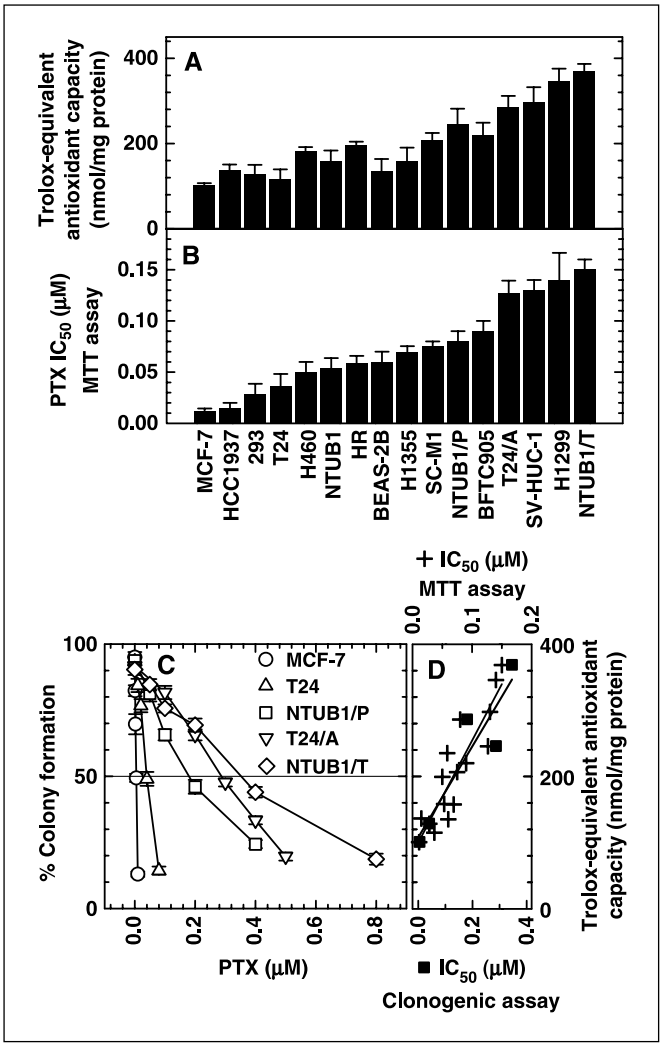

Figure 5. Resistance to paclitaxel positively correlated with cellular total antioxidant capacity. *A,* cells were seeded and incubated overnight; total antioxidant capacity was then measured. *B,* cells were treated with paclitaxel for 72 hours. The paclitaxel IC_{50}s were determined by the MTT method. *C,* cell growth inhibition was determined with the colony formation assay in five selected cells. Cultures were treated with various concentrations of paclitaxel for 12 days; colony numbers were then counted. *D,* total antioxidant capacities were plotted against the paclitaxel IC_{50}s from MTT assay (Pearson's correlation $r = 0.90$, $P < 0.0001$) and from the clonogenic assay (Pearson's correlation $r = 0.93$, $P < 0.024$).

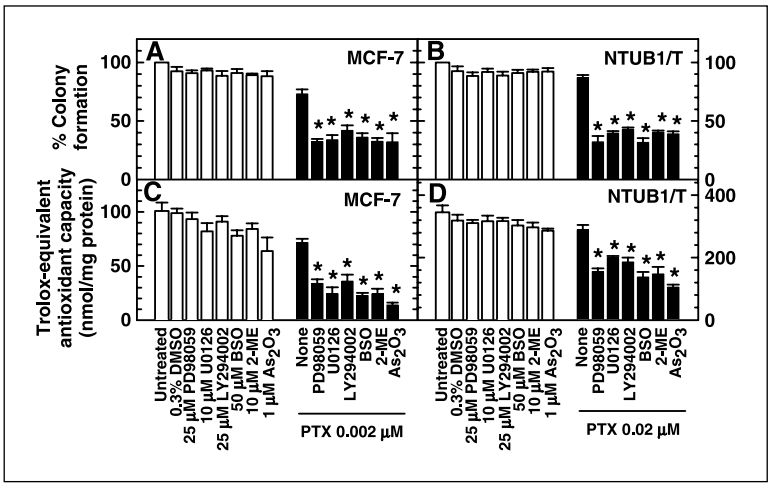

Figure 6. PD98059, U0126, LY294002, BSO, 2-ME, and As_2O_3 decreased the cellular total antioxidant capacity and the clonogenic survival in paclitaxel-treated MCF-7 (paclitaxel-sensitive) and NTUB1/T (paclitaxel-resistant) cells. For total antioxidant capacity and the clonogenic assay, cells were treated with drugs for 24 hours and 12 days, respectively. *, $P < 0.001$, paclitaxel versus paclitaxel plus modulator.

capacity enhanced paclitaxel toxicity. Recently, it was reported that paclitaxel treatment activates the MEK/ERK and phosphatidylinositol 3-kinase/Akt signaling pathways (28). Inhibiting these pathways with PD98059, U0126, or LY294002 down-regulated paclitaxel-mediated survivin induction and enhanced cell death in MCF-7 cells. Our data further showed that inhibition of these pathways also enhanced paclitaxel-induced cell death in NTUB1/P, T24/A, and NTUB1/T cells, which was respectively about 25, 42, and 53 times more resistant to paclitaxel than the MCF-7 cells. Neither MEK inhibitors PD98059 and U0126 nor phosphatidylinositol 3-kinase inhibitor LY294002 alone decreased the intracellular total antioxidant capacity. However, these inhibitors decreased the intracellular total antioxidant capacity of paclitaxel-treated cells. The reason for the decrease in total antioxidant capacity of paclitaxel-treated cells caused by these inhibitors is not clear at this moment. Our results showed that paclitaxel treatment increased O_2^- levels and SOD decreased production of H_2O_2 in paclitaxel-treated cells. The inhibition of SOD by 2-ME increased paclitaxel-induced apoptosis. These results suggest that paclitaxel may increase intracellular H_2O_2 levels by elevating O_2^- levels. Interference in microtubule dynamics is known to disrupt redox signaling. Cytoskeletal disruption can lead to activation of NADPH oxidase and the production of intracellular ROS (29). More research is needed to elucidate the mechanisms of how paclitaxel induces the generation of H_2O_2, O_2^-, and NO.

H_2O_2 is known to produce the $^{\bullet}OH$ radical in the presence of Fenton metals. O_2^- can also react rapidly with $NO^{\bullet}$ to form peroxynitrite, a highly reactive species. There are many antioxidants that exist within the extracellular space, cell membrane, and cytosol. Cooperation among the different antioxidants provides greater protection against oxidant attacks than any one compound alone. Thus, measuring the overall antioxidant capacity seems to give more biologically relevant information than that obtained from measuring individual antioxidant content. To quantify total antioxidant capacity, the capacity of hydrogen-donating molecules that can reduce cation radicals generated by oxidation of 2,2′-azinobis-(3-ethylbenzothiazoline-6-sulfonic acid) was measured in cell extracts. This measurement presumably covers most radicals produced by O_2^-, H_2O_2, and NO. Our results imply that tumor sensitivity to paclitaxel chemotherapy in a clinical setting might be predictable if total antioxidant capacity measurements can be determined from tumor specimens, thus providing a way of tailoring cytotoxic therapy to each individual patient.

It has been reported that paclitaxel can induce DNA single-strand breaks (30–32). Our data indicate that paclitaxel may induce oxidative DNA damage by generating increased levels of H_2O_2 and NO. On DNA damage, cells may halt their progression in the cell cycle to repair damage. They may also initiate programmed cell death or allow the cell cycle to proceed without repairing damages even in the presence of profuse mutations or molecular alterations. The causal relationship between DNA damage and G_2-M arrest, or between DNA damage and subsequent apoptosis in paclitaxel-treated cells, remains largely unknown. Here, we showed that in T24 cells, paclitaxel induced oxidative DNA adducts at a concentration as low as 0.02 μmol/L. This level of paclitaxel is lower than the required concentration needed for inducing nuclear fragmentation, sub-G_1 accumulation, and G_2-M arrest. Indeed, this finding may explain why gene mutation accumulation from minor DNA insults may facilitate the occurrence of drug-resistant cell clones rather than cell death.

Our results have a number of clinical implications. Because paclitaxel cytotoxicity can be significantly reduced by an antioxidant such as selenium, it is imperative to determine whether concurrent administration of antioxidants from over-the-counter food supplements may attenuate the efficacy of paclitaxel chemotherapy in clinical settings. It is feasible, however, to enhance the effects of paclitaxel treatment in clinical practice by applying agents that reduce intracellular antioxidant capacity, such as PD98059, U0126, LY294002, BSO, 2-ME, and As_2O_3. More importantly, chemosensitivity to paclitaxel may be determined by taking total antioxidant capacity measurements from clinical tumor samples. This, in turn, may then improve treatment outcomes by selecting out potentially responsive patients.

Acknowledgments

Received 4/5/2005; revised 6/7/2005; accepted 7/1/2005.

Grant support: National Science Council and Academia Sinica, ROC.

The costs of publication of this article were defrayed in part by the payment of page charges. This article must therefore be hereby marked *advertisement* in accordance with 18 U.S.C. Section 1734 solely to indicate this fact.

We thank Drs. Y.C. Liu, J.R. Gurr, and L.H. Yih for valuable comments.

References

1. Bokemeyer C, Hartmann JT, Kuczyk MA, et al. The role of paclitaxel in chemosensitive urological malignancies: current strategies in bladder cancer and testicular germ-cell tumors. World J Urol 1996;14:354–9.
2. Rowinsky EK. Paclitaxel pharmacology and other tumor types. Semin Oncol 1997;24:11–2.
3. Schiff PB, Horwitz SB. Taxol stabilizes microtubules in mouse fibroblast cells. Proc Natl Acad Sci U S A 1980;77: 1561–5.
4. Fuchs DA, Johnson RK. Cytologic evidence that taxol, an antineoplastic agent from *Taxus brevifolia*, acts as a mitotic spindle poison. Cancer Treat Rep 1978;62: 1219–22.
5. Lin HL, Liu TY, Chau GY, Lui WY, Chi CW. Comparison of 2-methoxyestradiol-induced, docetaxel-induced, and paclitaxel-induced apoptosis in hepatoma cells and its correlation with reactive oxygen species. Cancer 2000;89:983–94.
6. DiPaola RS. To arrest or not to G(2)-M Cell-cycle arrest. Clin Cancer Res 2002;8:3311–4. Commentary to: Tyagi AK et al. Clin Cancer Res 2002;8:3512–9.
7. Lanzi C, Cassinelli G, Cuccuru G, et al. Cell cycle checkpoint efficiency and cellular response to paclitaxel in prostate cancer cells. Prostate 2001;48:254–64.
8. Ioffe ML, White E, Nelson DA, Dvorzhinski D, DiPaola RS. Epothilone induced cytotoxicity is dependent on p53 status in prostate cells. Prostate 2004;61:243–7.
9. Dziadyk JM, Sui M, Zhu X, Fan W. Paclitaxel-induced apoptosis may occur without a prior G2/M-phase arrest. Anticancer Res 2004;24:27–36.
10. Liao PC, Lieu CH. Cell cycle specific induction of apoptosis and necrosis by paclitaxel in the leukemic U937 cells. Life Sci 2005;76:1623–39.
11. Varbiro G, Veres B, Gallyas F, Jr., Sumegi B. Direct effect of Taxol on free radical formation and mitochondrial permeability transition. Free Radic Biol Med 2001; 31:548–58.
12. Wang YF, Chen CY, Chung SF, Chiou YH, Lo HR. Involvement of oxidative stress and caspase activation in paclitaxel-induced apoptosis of primary effusion lymphoma cells. Cancer Chemother Pharmacol 2004; 54:322–30.
13. Park SJ, Wu CH, Gordon JD, Zhong X, Emami A, Safa AR. Taxol induces caspase-10-dependent apoptosis. J Biol Chem 2004;279:51057–67.
14. Choi SC, Oh HM, Park JS, et al. Soluble factor from murine bladder tumor-2 cell elevates nitric oxide production in macrophages and enhances the taxol-mediated macrophage cytotoxicity on tumor cells. Cancer Invest 2003;21:708–9.
15. Pae HO, Yoo JC, Choi BM, Kang CL, Kim JD, Chung HT. Apoptotic cell death induced by taxol is inhibited by nitric oxide in human leukemia HL-60 cells. Immunopharmacol Immunotoxicol 1999;21:667–82.
16. Yu HJ, Tsai TC, Hsieh TS, Chiu TY. Characterization of a newly established human bladder carcinoma cell line, NTUB1. J Formos Med Assoc 1992;91:608–13.
17. Tzeng CC, Liu HS, Li C, et al. Characterization of two urothelium cancer cell lines derived from a blackfoot disease endemic area in Taiwan. Anticancer Res 1996;16: 1797–804.
18. Pu YS, Hsieh TS, Tsai TC, et al. Tamoxifen enhances the chemosensitivity of bladder carcinoma cells. J Urol 1995;154:601–5.
19. Pu YS, Chen J, Huang CY, Guan JY, Lu SH, Hour TC. Cross-resistance and combined cytotoxic effects of paclitaxel and cisplatin in bladder cancer cells. J Urol 2001;165:2082–5.
20. Sohn HY, Gloe T, Keller M, Schoenafinger K, Pohl U. Sensitive superoxide detection in vascular cells by the new chemiluminescence dye L-012. J Vasc Res 1999;36: 456–64.
21. Zhou M, Diwu Z, Panchuk-Voloshina N, Haugland RP. A stable nonfluorescent derivative of resorufin for the fluorometric determination of trace hydrogen peroxide: applications in detecting the activity of phagocyte NADPH oxidase and other oxidases. Anal Biochem 1997;253:162–8.
22. Eu JP, Liu L, Zeng M, Stamler JS. An apoptotic model for nitrosative stress. Biochemistry 2000;39:1040–7.
23. Miller NJ, Rice-Evans C, Davies MJ, Gopinathan V, Milner A. A novel method for measuring antioxidant capacity and its application to monitoring the antioxidant status in premature neonates. Clin Sci (Lond) 1993;84:407–12.
24. Wang TS, Chung CH, Wang AS, et al. Endonuclease III, formamidopyrimidine-DNA glycosylase, and proteinase K additively enhance arsenic-induced DNA strand breaks in human cells. Chem Res Toxicol 2002;15:1254–8.
25. Gurr JR, Bau DT, Liu F, Lynn S, Jan KY. Dithiothreitol enhances arsenic trioxide-induced apoptosis in NB4 cells. Mol Pharmacol 1999;56:102–9.
26. Ide H. DNA substrates containing defined oxidative base lesions and their application to study substrate specificities of base excision repair enzymes. Prog Nucleic Acid Res Mol Biol 2001;68:207–21.
27. Kong Q, Beel JA, Lillehei KO. A threshold concept for cancer therapy. Med Hypotheses 2000;55:29–35.
28. Ling X, Bernacki RJ, Brattain MG, Li F. Induction of survivin expression by taxol (paclitaxel) is an early event, which is independent of taxol-mediated G2/M arrest. J Biol Chem 2004;279:15196–203.
29. Kustermans G, El Benna J, Piette J, Legrand-Poels S. Perturbation of actin dynamics induces NF-κB activation in myelomonocytic cells via a NADPH oxidase-dependent pathway. Biochem J 2004;387:531–40.
30. Ollikainen T, Knuuttila A, Suhonen S, et al. *In vitro* sensitivity of normal human mesothelial and malignant mesothelioma cell lines to four new chemotherapeutic agents. Anticancer Drugs 2000;11:93–9.
31. Digue L, Orsiere T, De Meo M, et al. Evaluation of the genotoxic activity of paclitaxel by the *in vitro* micronucleus test in combination with fluorescent *in situ* hybridization of a DNA centromeric probe and the alkaline single cell gel electrophoresis technique (comet assay) in human T-lymphocytes. Environ Mol Mutagen 1999;34:269–78.
32. Branham MT, Nadin SB, Vargas-Roig LM, Ciocca DR. DNA damage induced by paclitaxel and DNA repair capability of peripheral blood lymphocytes as evaluated by the alkaline comet assay. Mutat Res 2004;560:11–7.

Differential Expression of Molecular Markers in Arsenic and Non-arsenic-related Urothelial Cancer

TZYH-CHYUAN HOUR[1], YEONG-SHIAU PU[2], CHIA-CHI LIN[3], SHI-WEI HUANG[2], JUN CHEN[2], ALLEN W. CHIU[4], CHIEN-JEN CHEN[5], and CHAO-YUAN HUANG[2*]

[1]Department of Biochemistry, Kaohsiung Medical University College of Medicine, Kaohsiung, Taiwan
[2]Department of Urology, National Taiwan University College of Medicine, Taipei, Taiwan
[3]Department of Oncology, National Taiwan University College of Medicine Taipei, Taiwan,
[4]Department of Urology, Chi-Mei Foundation Hospital Tainan, Taiwan
[5]Graduate Institute of Epidemiology, National Taiwan University College of Public Health, Taipei, Taiwan
Running title: Markers in arsenic urothelial carcinoma

* Correspondence to:
Chao-Yuan Huang, MD
Department of Urology, National Taiwan University Hospital,
7 Chung-Shan South Road,
Taipei, Taiwan 100, Taiwan
TEL: 886-2-23123456 ext. 5238
FAX: 886-2-23219145
E-mail: cyh0909@ha.mc.ntu.edu.tw

Key Words: arseniasis, bladder cancer, glutathione, Bcl-2, P53, glutathione-*S*-transferase-π

Indication: Experimental study
Submitted date: 8/24/2005
Grand supported by: NSC 91-2314-B-002-019, NSC91-3112-B-002-010, NSC92-3112-B-002-024, NSC93-3112-B-002-008 and from the National Science Council, Executive Yuan, Taiwan, ROC.

Abstract

Background: Little is known about the mechanisms of arsenic-related UC (AsUC). This study is to reveal differential expression of molecular markers between AsUC and non-arsenic related UC (non-AsUC)

Materials and Methods: Tissues of AsUC (n=33), non-AsUC (n=20) and normal bladder urothelia from patients with benign diseases (n=4) were examined for multiple selected molecular markers responsible for various cellular functions, including glutathione, GST-π, Bcl-2, P53 and c-Fos.

Results: Mean cellular glutathione contents of normal mucosal samples (33.4±7.2 μM/μg protein) were significantly higher than either non-AsUC (22.8±1.8, p=0.04) or AsUC (16.4±1.6, p=0.002). The glutathione content of non-AsUC was higher than AsUC (p=0.012). Expressions of Bcl-2 and c-Fos in AsUC were significantly higher than in non-AsUC (p=0.004 and p=0.02, respectively).

Conclusions: The carcinogenic pathway for AsUC is partially different from non-AsUC. Cellular glutathione contents may be down-regulated during urothelial carcinogenesis. Bcl-2 and c-Fos may play important roles in arsenic-mediated carcinogenesis of the urothelium.

Introduction

It has been well known that chronic arseniasis is considered responsible for the endemicity of urothelial carcinoma (UC) in southwest Taiwan (1). UC may arise from the renal pelvis, ureter, urinary bladder and urethra. Long-term efforts have been devoted to explore the epidemiology and pathophysiology of these arsenic-related UCs (AsUC) (2). Previous reports from other countries, such as Chile, America, and Argentina, also indicated that contamination of drinking water with arsenic is strongly associated with the occurrence of UCs in those areas (3-5). The molecular mechanisms underlying arsenic-related carcinogenesis pathway, however, remain largely unknown. Most data were obtained from artificial models of either *in vitro* or animal studies (6).

There were only a few reports in the literature that addressed the cellular or molecular changes secondary to arsenic exposure in the UC model. Dr. Shibata et al. reported that 62% of AsUC had p53 gene mutations (7). Dr. Warner demonstrated that there were increased micronuclei in exfoliated bladder cells of individuals who chronically ingest arsenic-contaminated water in Nevada, USA (8). Dr. Smith et al. showed that after reducing the intake of arsenic-contaminated water, exfoliated bladder cell micronuclei could be significantly decreased and this could serve as a potential biomarker for arsenic genotoxicity (9). Dr. Byrd revealed that inorganic arseniasis was associated with a deregulated cell cycle control (10). However, more detailed or in-depth studies on arsenic-mediated carcinogenesis are still awaited.

This is one of the few studies that sought to reveal differential expressions of molecular markers between AsUC and non-AsUC. Tissues of AsUC, non-AsUC, and normal-appearing bladder mucosa from non-cancer patients were examined and compared for expressions of multiple selected molecular factors that may be involved in arsenic-related carcinogenesis of the urothelium.

Material and Methods

Tissue samples. UC tumor samples and normal-appearing bladder mucosa were used to examine selected cellular and molecular factors that had been reported to be involved in carcinogenesis of the urothelium. All UCs were confirmed by histopathology. Samples contained snap frozen tissues (at -135℃) and paraffin-embedded archival tissues. Tissue collection was approved by the institutional review board of National Taiwan University Hospital.

In total, tumor tissues of 33 AsUCs and 25 non-AsUCs as well as four normal-appearing bladder mucosal samples from non-cancer patients were studied. Tissues were harvested in a way that neoplastic parts were separated from adjacent normal parts. All 33 patients with AsUC had lived or been living in the arseniasis endemic area in southwest Taiwan where people drank the arsenic-contaminated artesian well water for at least 10 years (2).

Glutathione contents. GSH is the major antioxidant in cells and functions as a free radical scavenger, which may detoxify toxins or chemotherapeutic agents. Thus, the intracellular GSH content may be altered in urothelial carcinogenesis. Tissue extracts were prepared from frozen tissues by a standard extraction protocol. Briefly, about 0.5 cm^3 tumor chip was used. Total protein was extracted by solubilizing with the Laemmli buffer (PIERCE Life Science Co., Rockford, IL). Protein contents of tissue extracts were determined using a commercial BCA kit (PIERCE Life Science Co., Rockford, IL). Cells (3×10^6) were resuspended in 0.5 ml 5% metaphosphoric acid (Sigma Chemical Co., St. Louis, MO) on ice for 20 min. Cells were then lysed by three cycles of freeze-and-thaw. The supernatant was collected by centrifugation. Cellular GSH content was examined using the GSH-400 kit (Oxis International, Portland, OR). Briefly, 50 ml supernatant were incubated with 0.4 ml reaction buffer (200 mM potassium phosphate, 0.2 mM diethylene-triamine pentaacetic acid and 0.025% lubrol, pH 7.8). Then 25 ml chromogenic reagent in 0.2 N HCl and 25 ml 30% NaOH were sequentially added and mixed thoroughly. The mixture was reacted in the dark at room temperature for at least 10 min. The colorimetric density of the target chromogen was determined by a spectrophotometer (DU640i; Beckman, Fullerton, CA) at 400 nm.

Western blotting. Protein extracts (50 mg) were separated on 10%

SDS-PAGEs and transferred to microporous polyvinylidene difluoride membranes (Millipore, Bedford, MA). After blocking with the TBST buffer (10 mM Tris-base; pH=7.5, 100 mM NaCl, 0.1 % Tween 20) plus 1% bovine serum albumin (BSA), the membranes were incubated with human specific anti-P53 (Santa Cruz Biotechnology, Santa Cruz, CA), anti-Bcl-2 (Santa Cruz Biotechnology), anti-c-Fos (Santa Cruz Biotechnology) and anti-GST-π (Signet Laboratories Inc., Dedham, MA) antibodies at 4°C for 12 hrs. The membranes were then washed three times with the TBST buffer (20 min each) and incubated with horseradish peroxidase-conjugated goat anti-mouse or anti-rabbit immunoglobulin (Santa Cruz Biotechnology) for 1 hr at room temperature, respectively. After 3 washes, these proteins were detected by Western Blotting Luminol Reagent (Santa Cruz Biotechnology). The protein band intensities were digitalized and quantified using the Imagemaster VDS version 3.0 software (ImagemasterVDS; AmershamPharmacia). The band intensities of proteins were normalized to that of β-actin, which was run in parallel blots.

Statistical methods. Glutathione levels between the two groups were compared with the Student's t-test. Three separate experiments with triplicate data were performed and data was presented as mean $\pm$ standard error of the means (SEM). Fisher's exact test or Chi-square test was used to compare protein expressions determined by Western blotting analysis. All tests were two-sided with $p<0.05$ as being statistically significant.

Results

The mean glutathione (GSH) concentrations in both non-AsUC (22.8±1.8 μM/μg protein) and AsUC tissues (16.4±1.6 μM/μg protein) were significantly lower than that of normal mucosal tissues (33.4±7.2 μM/μg protein; p=0.04 and 0.002, respectively) by using the Student's t-test (Fig. 1). Further, GSH levels were significantly higher in non-AsUC than in AsUC (p=0.012). These results demonstrated cellular GSH contents may be down-regulated in urothelial carcinogenesis.

Protein levels of GST-π, Bcl-2, P53 and c-Fos were determined by Western blotting. All AsUC expressed GST-π and P53 proteins. A few cases of non-AsUC did not express the two proteins. The expressions of Bcl-2 and c-Fos were significantly higher in AsUC than in non-AsUC by using the Fisher's exact test (p=0.004 and p=0.02, respectively)(Table I). However, there were no significant differences in GST-π (p=0.18) or P53 (p=0.29) levels between the two groups.

Discussion

It has been shown that AsUC and non-AsUC may be different from each other in clinicopathological parameters (11), which suggests that carcinogenic processes of the two may also be different. In this study, we showed that reduction of intracellular GSH levels may be an important feature in urothelial carcinogenesis. The reasons why the GSH levels of non-AsUC were significantly higher than in AsUC, however, are unclear. The glutathione/glutathion-*S*-transferase (GSH/GST) system in normal and tumor tissues plays a role in the susceptibility to endogenous and/or exogenous toxic compounds. GSH contents and GST-π activity have been analyzed in several tissues including human bladder tumors (12). These results revealed the reduced glutathione levels of bladder carcinoma were significantly lower in patients as compared with the control group (12;13). Interestingly, similar results have also been found in this study. The low GSH concentration of the urothelia may be responsible for the vulnerability of UC to chemical carcinogenesis. Previous studies have reported overexpression of GST-π and elevations of GSH in some arsenic-resistant cancer cell lines (14). The same features were also detected in arsenic-resistant UC cell lines in our previous report (15). There were no significant differences in the GST-π protein levels between AsUC and non-AsUC in this study. However, some studies have suggested it is the GST-π activity or other isoforms of GST (such as α, μ and θ isoforms), not GST-π total protein levels, that is involved in arsenic-mediated carcinogenesis (12;16;17). Further study is necessary to clarify the issue.

The expressions of oncoproteins Bcl-2 and c-Fos were significantly up-regulated in AsUC compared to non-AsUC. Hu, et al., (2002) have suggested that protein level of Bcl-2 was one of practical biomarkers to screen arseniasis-mediated skin carcinoma (18). In our series, all 33 cases of AsUC expressed Bcl-2 detected by Western blotting. In contrast, 6 of the 25 non-AsUC (24%) did not express Bcl-2 protein, which appears compatible to the findings of Hu, et al. Recent studies showed that Bcl-2 protein was positive expression in UC by immunochemical staining (19;20). However, since up to 75% of non-AsUC expresses Bcl-2 in this study. Therefore, Bcl-2 may be a sensitive marker but not a marker with good specificity for arseniasis. AP-1, a heterodimeric transcription factor of c-Fos and c-Jun, can mediate many biological effects of tumor promoters and was an important regulator of cell growth. Arsenic has been shown to modulate the mitogen-activated protein kinase cascade in several cell systems, resulting in the activation of

transcription factors, including AP-1 (21). Recently, many studies have demonstrated the same results that arsenic induction of AP-1 DNA binding activity was accompanied by up-regulation of c-Fos and c-Jun nuclear proteins in bladder epithelial cells (22). We have also observed that more AsUC than non-AsUC expressed c-Fos. Of particular relevance to the present studies was a report that c-Fos expression was as a concomitant factor associated with arsenic-mediated carcinogenesis (23). However, a larger sample size is needed to validate the hypothesis that c-Fos up-regulation is closed associated with AsUC.

We did not find a statistic difference in the expression of wild-type P53 protein levels between the two groups of tumors. Tchounwou et al., (2003) have also shown that the level of P53 protein did not significantly differ between arsenic trioxide-treated and control liver carcinoma cells (24). Contrarily, many studies have shown that high protein levels of mutant-type P53 were detected in AsUC (7;18). It is thus possible that arsenic-mediated urothelial carcinogenesis involves P53 mutation but not transcriptional or translational modification of P53 protein levels. Further studies were needed to determine if mutant-type P53 involved in arsenic-mediated urothelial carcinogenesis.

In summary, our results suggest that cellular GSH contents are down-regulated in urothelial carcinogenesis, especially in arsenic-related tumors. The Bcl-2 and c-Fos oncoproteins may play important roles in arsenic-mediated urothelial carcinogenesis. Carcinogenic pathway of AsUC is at least partly different from that of non-AsUC.

Reference

1 Chen CJ, Chen CW, Wu MM, and Kuo TL: Cancer potential in liver, lung, bladder and kidney due to ingested inorganic arsenic in drinking water. Br J Cancer *66*: 888-892, 1992.

2 Chiou HY, Hsueh YM, Liaw KF, Horng SF, Chiang MH, Pu YS, Lin JS, Huang CH, and Chen CJ: Incidence of internal cancers and ingested inorganic arsenic: a seven-year follow-up study in Taiwan. Cancer Res *55*: 1296-1300, 1995.

3 Karagas MR, Tosteson TD, Blum J, Morris JS, Baron JA, and Klaue B: Design of an epidemiologic study of drinking water arsenic exposure and skin and bladder cancer risk in a U.S. population. Environ Health Perspect *106*: 1047-1050, 1998.

4 Hopenhayn-Rich C, Biggs ML, Fuchs A, Bergoglio R, Tello EE, Nicolli H, and Smith AH: Bladder cancer mortality associated with arsenic in drinking water in Argentina. Epidemiology *7*: 117-124, 1996.

5 Smith AH, Goycolea M, Haque R, and Biggs ML: Marked increase in bladder and lung cancer mortality in a region of Northern Chile due to arsenic in drinking water. Am J Epidemiol *147*: 660-669, 1998.

6 Miller WH, Jr., Schipper HM, Lee JS, Singer J, and Waxman S: Mechanisms of action of arsenic trioxide. Cancer Res *62*: 3893-3903, 2002.

7 Shibata A, Ohneseit PF, Tsai YC, Spruck CH, III, Nichols PW, Chiang HS, Lai MK, and Jones PA: Mutational spectrum in the p53 gene in bladder tumors from the endemic area of black foot disease in Taiwan. Carcinogenesis *15*: 1085-1087, 1994.

8 Warner ML, Moore LE, Smith MT, Kalman DA, Fanning E, and Smith AH: Increased micronuclei in exfoliated bladder cells of individuals who chronically ingest arsenic-contaminated water in Nevada. Cancer Epidemiol Biomarkers Prev *3*: 583-590, 1994.

9 Smith AH, Hopenhayn-Rich C, Warner M, Biggs ML, Moore L, and Smith MT: Rationale for selecting exfoliated bladder cell micronuclei as potential biomarkers for arsenic genotoxicity. J Toxicol Environ Health *40*: 223-234, 1993.

10 Byrd DM, Roegner ML, Griffiths JC, Lamm SH, Grumski KS, Wilson R, and Lai S: Carcinogenic risks of inorganic arsenic in perspective. Int Arch Occup Environ Health *68*: 484-494, 1996.

11 Chow NH, Guo YL, Lin JS, Su JH, Tzai TS, Guo HR, and Su IJ: Clinicopathological features of bladder cancer associated with chronic exposure to arsenic. Br J Cancer *75*: 1708-1710, 1997.

12 Hassan AA, Tagliabue G, Codegoni AM, D'Incalci M, el Sewedy SM, and Airoldi L: Glutathione S-transferase activity and glutathione content in human bladder carcinoma associated with schistosomiasis: comparison with uninvolved surrounding tissues. Cancer Lett *121*: 19-23, 1997.

13 Lafuente A, Giralt M, Cervello I, Pujol F, and Mallol J: Glutathione-S-transferase activity in human superficial transitional cell carcinoma of the bladder. Comparison with healthy controls. Cancer *65*: 2064-2068, 1990.

14 Liu J, Chen H, Miller DS, Saavedra JE, Keefer LK, Johnson DR, Klaassen CD, and Waalkes MP: Overexpression of glutathione S-transferase II and multidrug resistance transport proteins is associated with acquired tolerance to inorganic arsenic. Mol Pharmacol *60*: 302-309, 2001.

15 Hour TC, Huang CY, Lin CC, Chen J, Guan JY, Lee JM, and Pu YS: Characterization of molecular events in a series of bladder urothelial carcinoma cell lines with progressive resistance to arsenic trioxide. Anticancer Drugs *15*: 779-785, 2004.

16 Schuliga M, Chouchane S, and Snow ET: Upregulation of glutathione-related genes and enzyme activities in cultured human cells by sublethal concentrations of inorganic arsenic. Toxicol Sci *70*: 183-192, 2002.

17 Lee TC, Wei ML, Chang WJ, Ho IC, Lo JF, Jan KY, and Huang H: Elevation of glutathione levels and glutathione S-transferase activity in arsenic-resistant Chinese hamster ovary cells. In Vitro Cell Dev Biol *25*: 442-448, 1989.

18 Hu C, Zhang A, and Huang X: Value of BCL-2 and P53mt proteins in screening skin carcinoma caused by arseniasis. Zhonghua Liu Xing Bing Xue Za Zhi *23*: 206-208, 2002.

19 Ong F, Moonen LM, Gallee MP, ten BC, Zerp SF, Hart AA, Bartelink H, and Verheij M: Prognostic factors in transitional cell cancer of the bladder: an emerging role for Bcl-2 and p53. Radiother Oncol *61*: 169-175, 2001.

20 Bilim VN, Tomita Y, Kawasaki T, Takeda M, and Takahashi K: Variable Bcl-2 phenotype in benign and malignant lesions of urothelium. Cancer Lett *128*: 87-92, 1998.

21 Gubits RM and Fairhurst JL: c-fos mRNA levels are increased by the cellular stressors, heat shock and sodium arsenite. Oncogene *3*: 163-168, 1988.

22 Simeonova PP, Wang S, Toriuma W, Kommineni V, Matheson J, Unimye N, Kayama F, Harki D, Ding M, Vallyathan V, and Luster MI: Arsenic mediates cell proliferation and gene expression in the bladder epithelium: association with activating protein-1 transactivation. Cancer Res *60*: 3445-3453, 2000.

23 Drobna Z, Jaspers I, Thomas DJ, and Styblo M: Differential activation of AP-1 in human bladder epithelial cells by inorganic and methylated arsenicals. FASEB J *17*: 67-69, 2003.

24 Tchounwou PB, Yedjou CG, and Dorsey WC: Arsenic trioxide-induced transcriptional activation of stress genes and expression of related proteins in human liver carcinoma cells (HepG2). Cell Mol Biol (Noisy -le-grand) *49*: 1071-1079, 2003.

Legends

Figure 1. *Cellular GSH contents were down-regulated in urothelial carcinogenesis. The mean GSH concentrations in both non-AsUC (22.8±1.8 μM/μg. protein; p=0.04) and AsUC tumors (16.4±1.6 μM/μg protein; p=0.002) were significantly lower than normal mucosal tissues (33.4±7.2 μM/μg. protein) by using the Student's t-test. Of note, GSH levels of AsUC were significant lower than that of non-AsUC (p=0.012).*

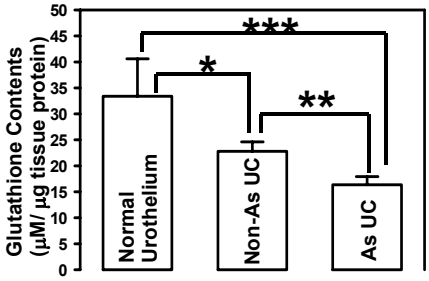

Fig. 1

Table I. Comparison of protein expressions of GST-π, P53, Bcl-2 and c-Fos in two groups of tumors by Western blotting

Molecular markers	GST-π		P53		Bcl-2		c-Fos	
Expression	**+**[d]	**–**[e]	**+**	**–**	**+**	**–**	**+**	**–**
AsUC[a] **(n=33)**	**33**	**0**	**19**	**14**	**33**	**0**	**30**	**3**
Non-AsUC[b] **(n=25)**	**23**	**2**	**10**	**15**	**19**	**6**	**16**	**9**
Total	**56**	**2**	**29**	**29**	**52**	**6**	**46**	**12**
***p* value**[c]	**0.18**		**0.29**		**0.004****		**0.02***	

[a]AsUC = arsenic-related urothelial carcinoma
[b]Non-AsUC = non-arsenic related urothelial carcinoma
[c]Fisher's exact test (two-sided) was used to compare protein expressions in the two groups of tumors
[d]The detectable intensity of protein by Western blotting was scored as "+"
[e]The undetectable intensity of protein by Western blotting was scored as "-"